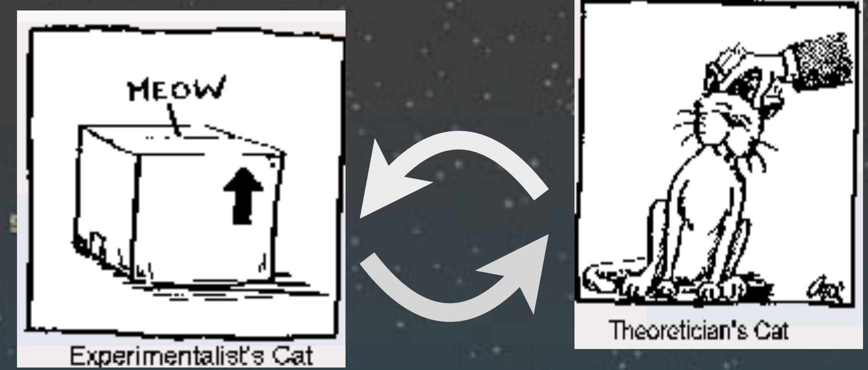

Spectrum and composition of (G+EG) cosmic rays: overview of the experimental results

Antonella Castellina
INFN & INAF, Torino, Italy

KIT Composition Workshop, 21-23 September 2015

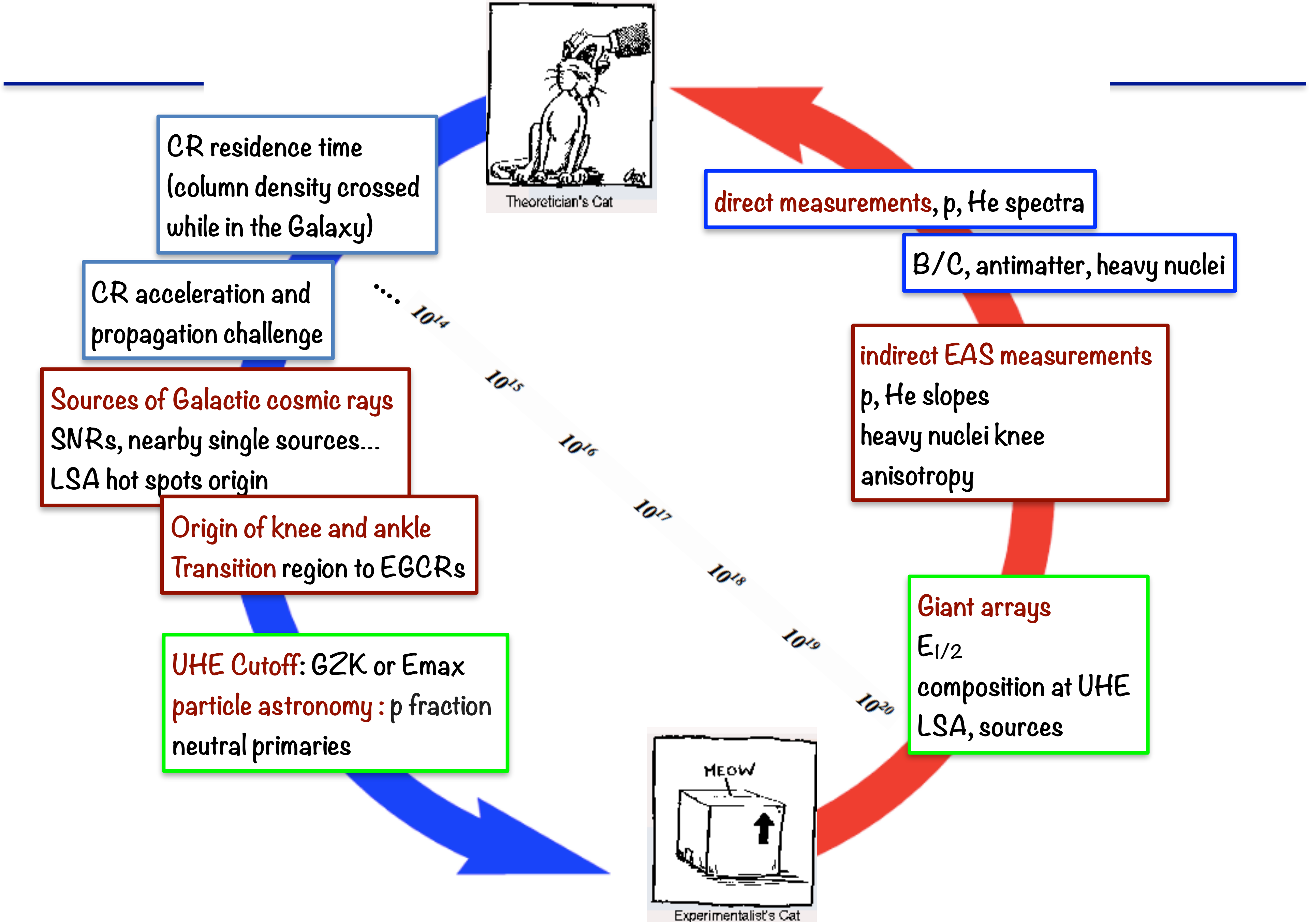
Theoretician's Cat
CR residence time (column density crossed while in the Galaxy)
CR acceleration and propagation challenge
Sources of Galactic cosmic rays
SNRs, nearby single sources...
LSA hot spots origin
Origin of knee and ankle
Transition region to EGCRs
UHE Cutoff: GZK or Emax
particle astronomy : p fraction
neutral primaries
direct measurements, p, He spectra
B/C, antimatter, heavy nuclei
indirect EAS measurements
p, He slopes
heavy nuclei knee
anisotropy
Giant arrays
$E_{1/2}$
composition at UHE
LSA, sources
...
10^{14}
10^{15}
10^{16}
10^{17}
10^{18}
10^{19}
10^{20}
MEOW
Experimentalist's Cat

All particle spectrum

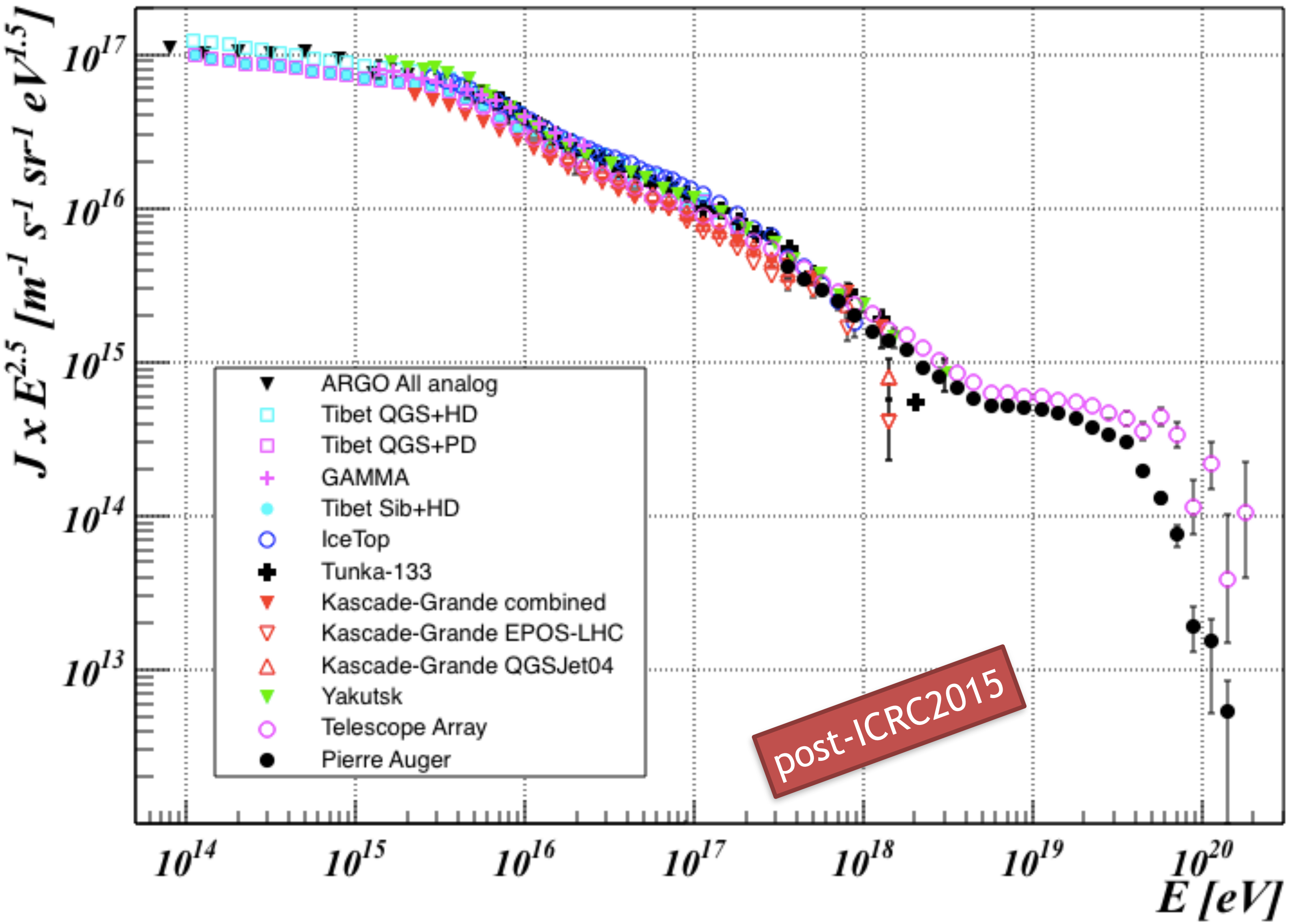

The experimental observables

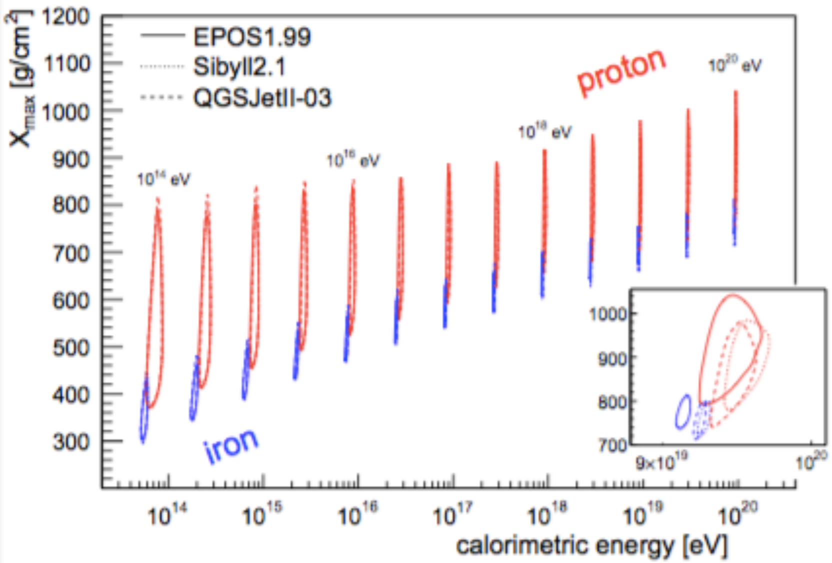

E_{calo}, Xmax from longitudinal distribution

$$\langle X^p_{max}\rangle \approx \lambda_p + X_0 \ln\left(\frac{E}{2N\varepsilon_c^{em}}\right) \qquad \langle X^A_{max}\rangle = \langle X^p_{max}\rangle - D_p\langle \ln A\rangle$$

$$\sigma_p^2 \approx \lambda_p^2 + \left(X_0\frac{\sigma(N)}{N}\right)^2 + \left(X_0\frac{\sigma(\kappa_{ela})}{\kappa_{ela}}\right)^2$$

$$\sigma(X_{max})^2 = \langle\sigma_i^2\rangle + D_p^2(\langle \ln^2 A\rangle - \langle \ln A\rangle^2)$$

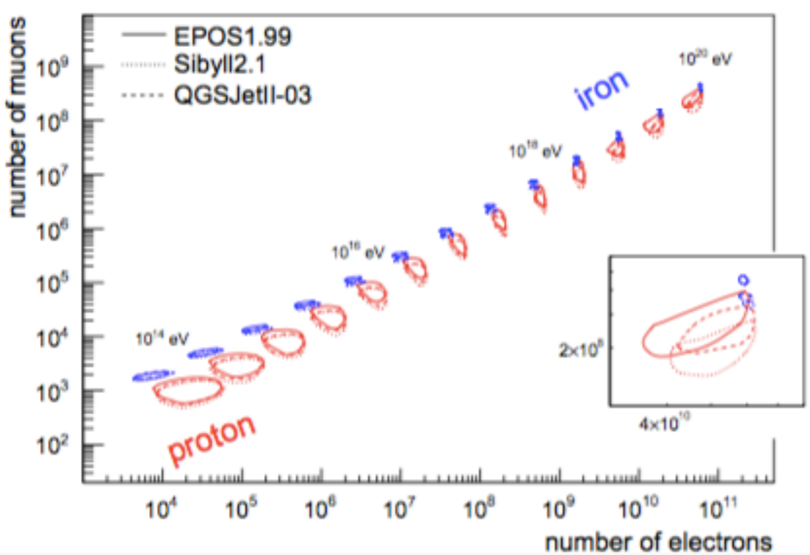

ρ_e, ρ_μ, temporal distributions; muons underground

$$N^p_{e,max} \approx \frac{E}{\varepsilon_c^{em}} = N^A_{e,max} \qquad N^p_\mu \approx \left(\frac{E}{\varepsilon_d^\pi}\right)^\beta$$

$$N_{e,ground} \approx N_{e,max}\exp\left(-\frac{\Delta X}{\Lambda}\right) \qquad N^A_\mu = N^p_{\mu,max}A^{1-\beta}$$

$$\frac{\sigma(N_{e,ground})}{N_{e,ground}} \approx \frac{\sigma(X_{max})}{\Lambda}$$

Array	g cm^{-2}	Detector	ΔE [eV]	Area [km^2]
ARGO	600	RPC hybrid (LLASHO)	0.3-5 10^{15}	0.0056
Tibet-ASγ	600	Scintillator/burst detector	1-200 10^{15}	0.0037 [0.5 phase III]
EasTop	820	scintillator/muon	1-100 10^{15}	0.01
GAMMA	700	scintillator/muon	3-200 10^{15}	0.03
KASCADE	1020	scintillator/muon	2-90 10^{15}	0.04
CASA-MIA	860	scintillator/muon	0.1-100 10^{15}	0.25
Kascade-Grande	1020	scintillator/muon	10^{16}-10^{18}	0.49
IceTop	680	ice Cher.tanks	10^{16}-10^{18}	1
Tunka	900	unshielded PMTs	10^{15}-10^{18}	3
Yakutsk	1020	scintillator/ unshielded PMTs	10^{15}-10^{19}	~40
Telescope Array +TALE	880	scintillator+ fluorescence tel.	4 10^{15}-10^{20}	700
Auger +Infill	840	water Cher.tanks fluorescence tel.	10^{17}-10^{20}	3000

High altitude experiments:

- N_{part} ~ indip of composition
- close to maximum of EAS: low fluctuations

energy resolution

Sea level experiments:

- EAS after maximum
- exploit longitudinal distribution differencies for different primaries

composition

Direct-indirect measurements... a reminder

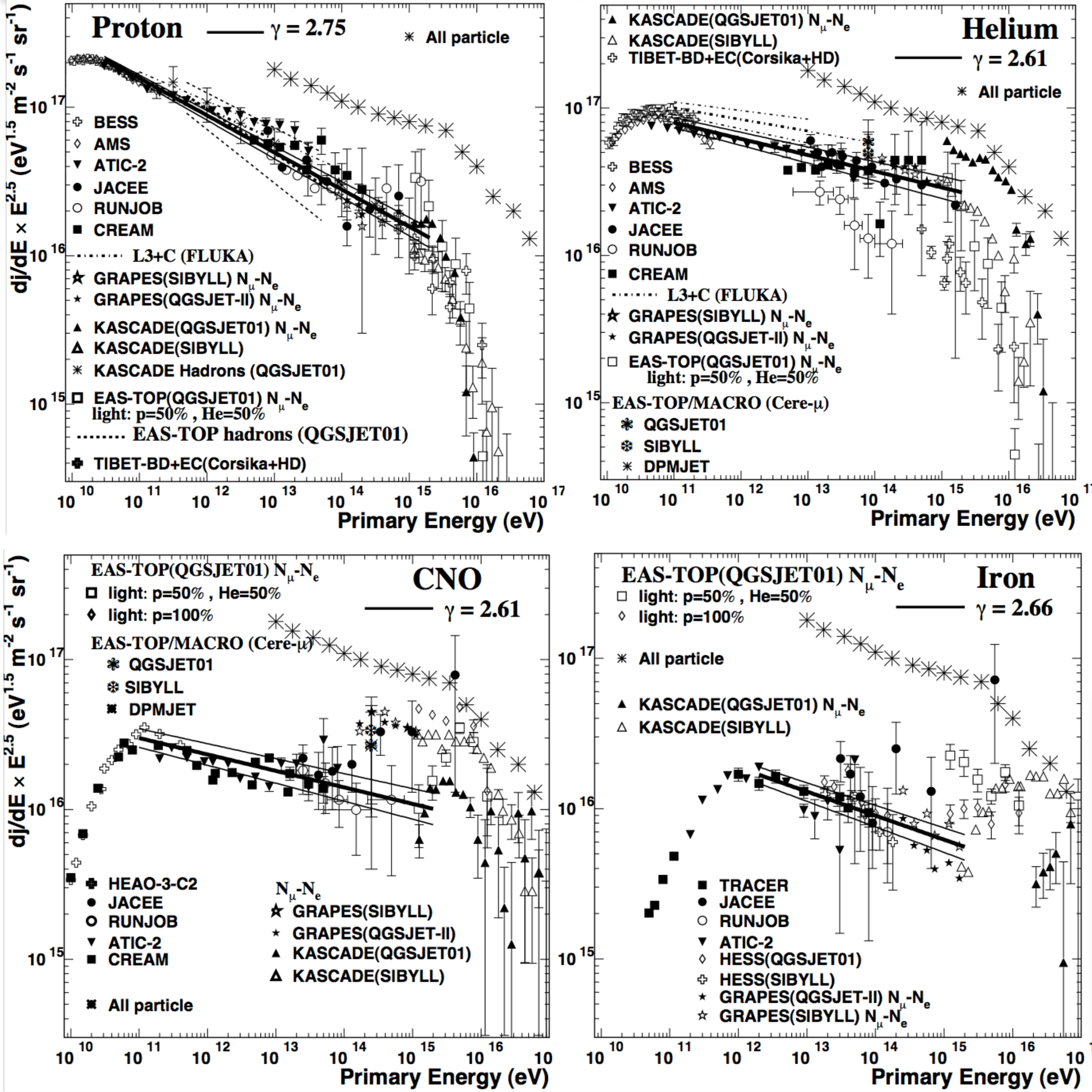

Past experiments:

- single hadrons from EasTop and Kascade,
- coincidence between EAS Cherenkov light and underground TeV muons from EasTop/MACRO
- Ne-Nμ (EasTop, Kascade, Grapes)
- burst detectors (Tibet)
- ...

- overlap with direct measurements
- Helium spectrum harder than proton one
- helium is the most abundant element below the knee
- proof of hadr. int. models below 10 PeV

The knee region : "old" results

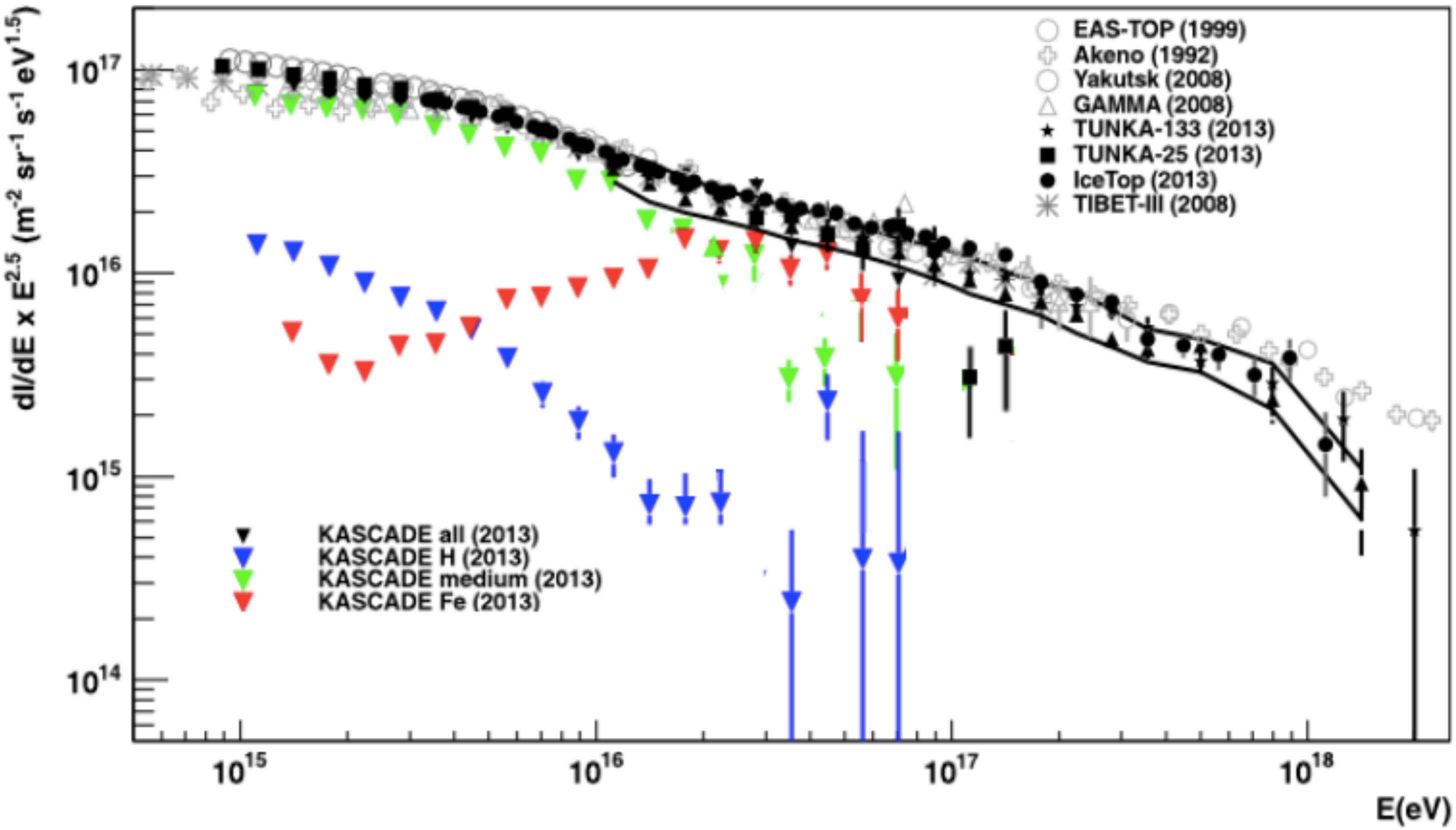

- all-particle knee ~ 4 10^{15} eV
- most experiments point to a p+He knee around few PeV, heavier knee not visible (no statistics)
- if Peters cycles, E_k(Fe) must be found at ~ 2 x E_k(p) ~ 7-10 10^{16} eV
- different indication from Tibet-ASγ, proton knee at lower energy

TIBET-II and III

- AS detector: 221 scintillator counters on a 15 m grid detectors: N_e, ϑ [upgraded to 771, surronded by 28 density counters]
- emulsion chambers (80 m^2): E, position, ϑ of γ families
- burst detectors below EC : N_b (burst size)

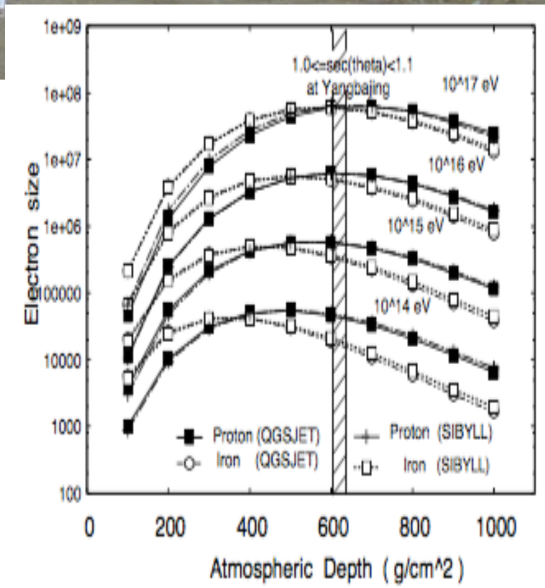

Tibet-ASγ all particle spectrum (10^{14} - 10^{17} eV)

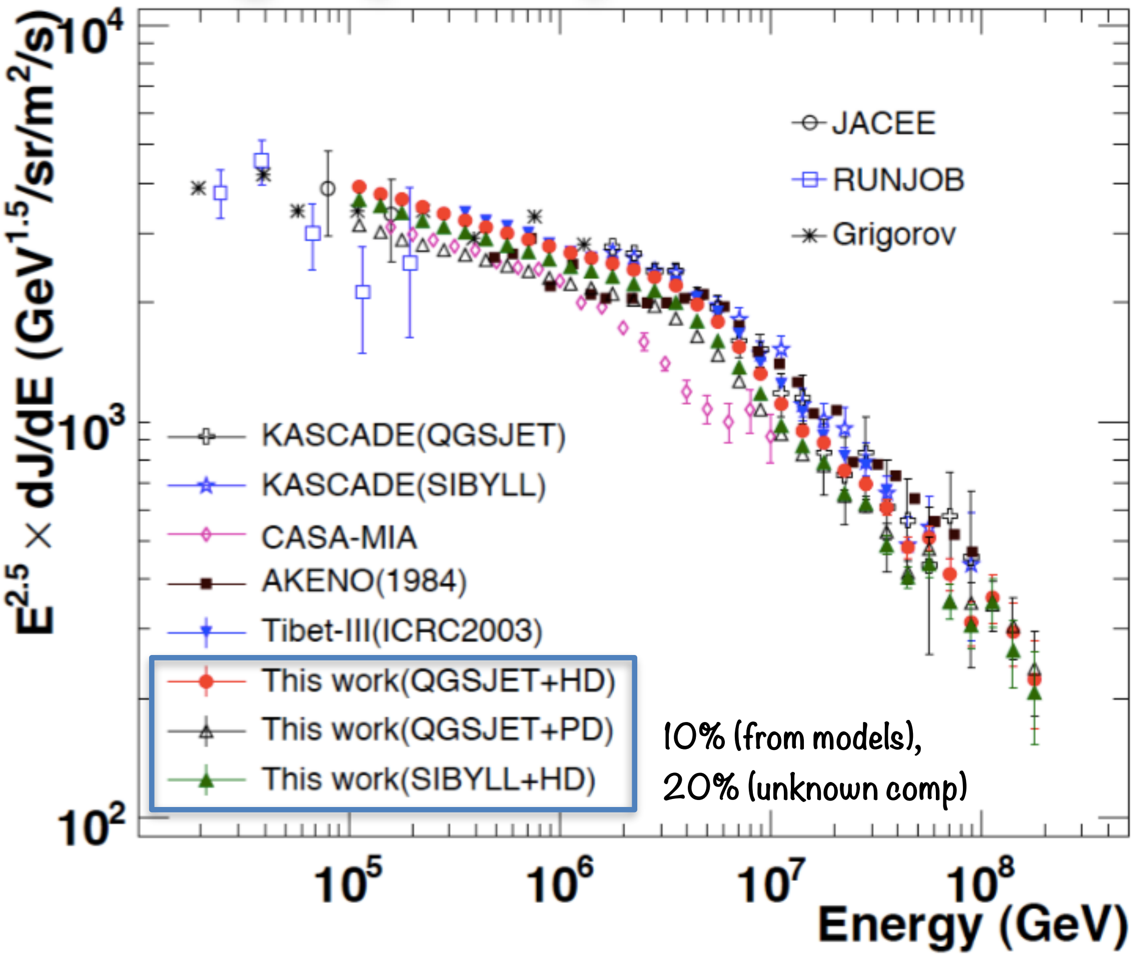

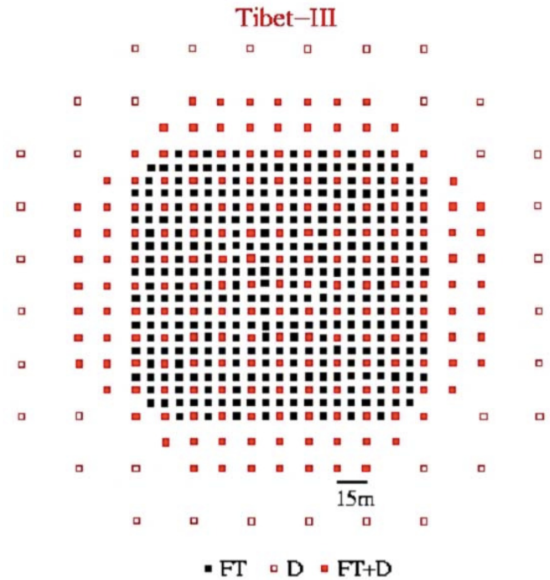

Model	Knee Position (PeV)	Index of spectrum
QGS.+HD	4.0± 0.1	R1= -2.67± 0.01 R2= -3.10± 0.01
QGS.+PD	3.8± 0.1	R1= -2.65± 0.01 R2= -3.08± 0.01
SIB.+HD	4.0± 0.1	R1= -2.67± 0.01 R2= -3.12± 0.01

A sharp knee

- single source?
- more efficient acceleration of heavy component?

Tibet-ASγ light component

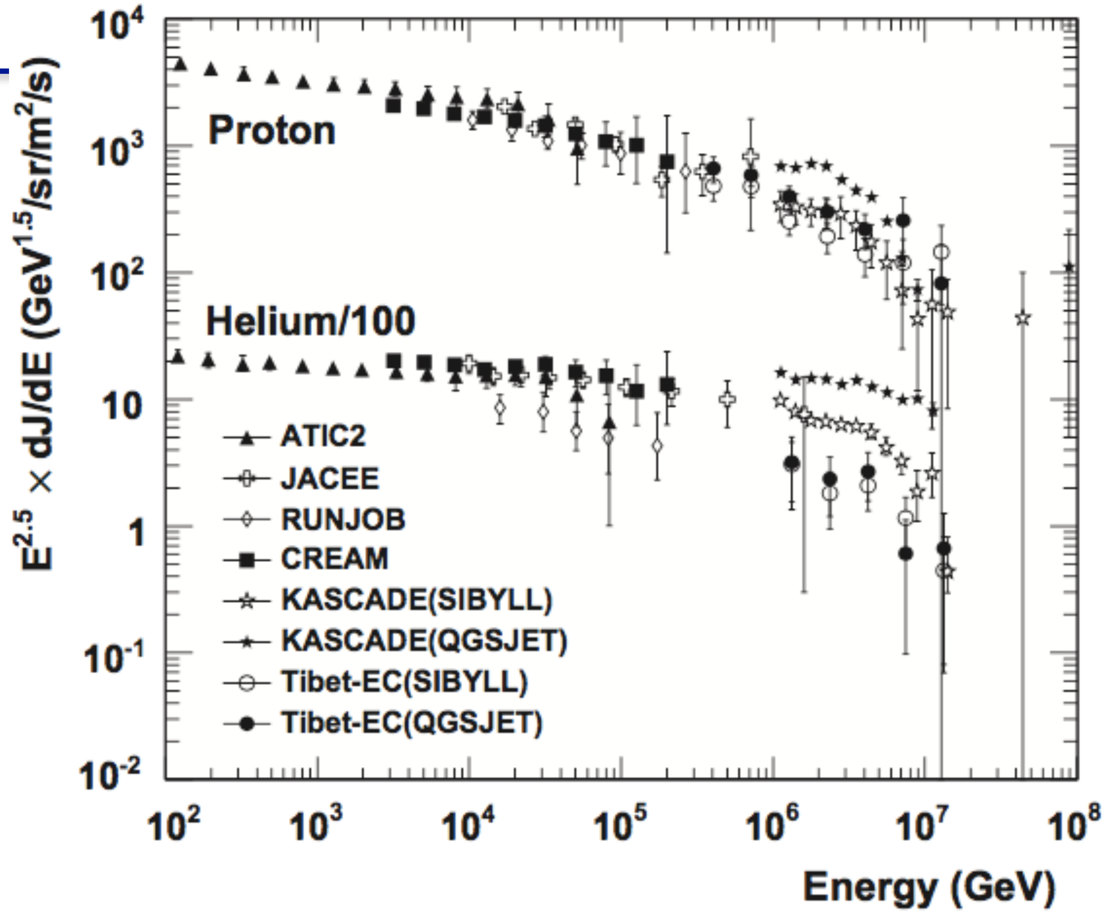

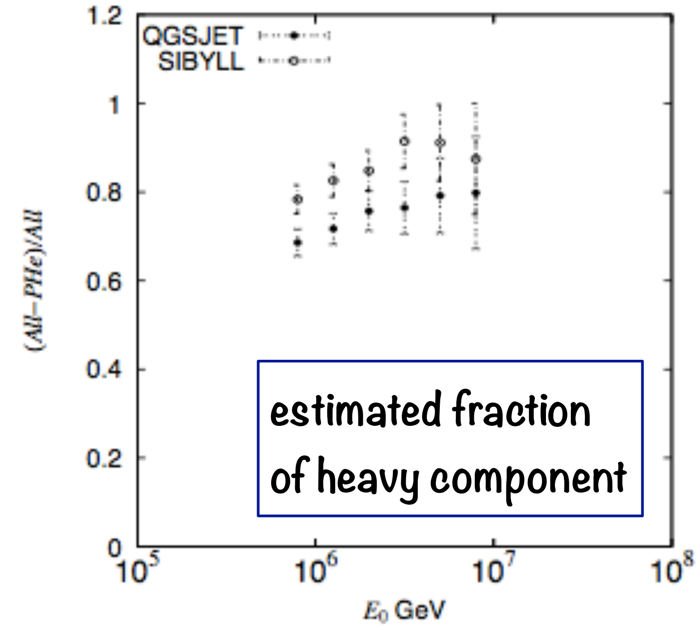

Separation based on shower core study (burst detectors)

Low statistics (1176 events)

- power index for light spectrum steeper wrt all-particle one: E_k(light) < E_k(all)
- main component at the all particle knee is heavy

TIBET [YAC-II + Tibet-III + MD]

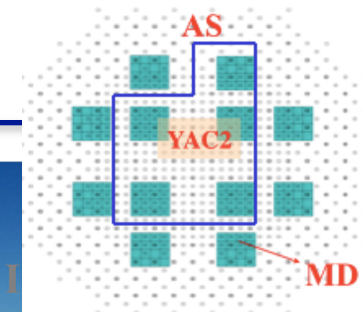

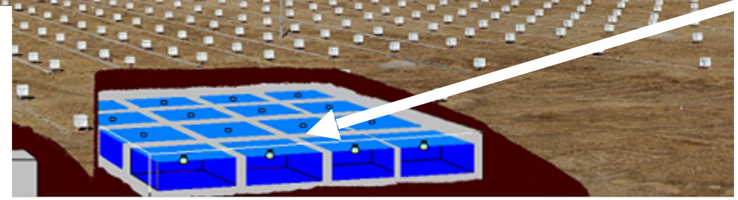

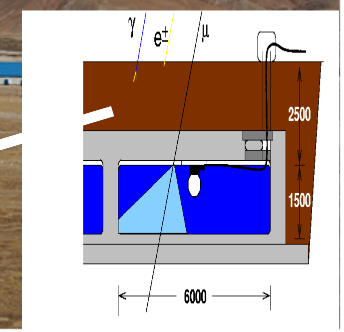

- Tibet-III (50000 m^2): fast timing counters + density counters for Primary energy and incident direction.
- YAC-II (5000 m^2): 400 High energy AS core with large dynamic range (1 to 10^6 MIP)
- Tibet-MD (4500 m^2) : underground water Cherenkov muon detector

Expected performances of the new hybrid Tibet experiment

- simultaneous observation of cores with YAC and MD: claim ability to separate p, He, medium and heavy between 50 TeV and 10 PeV accurately.
- energy resolution at 1 PeV better than 12%

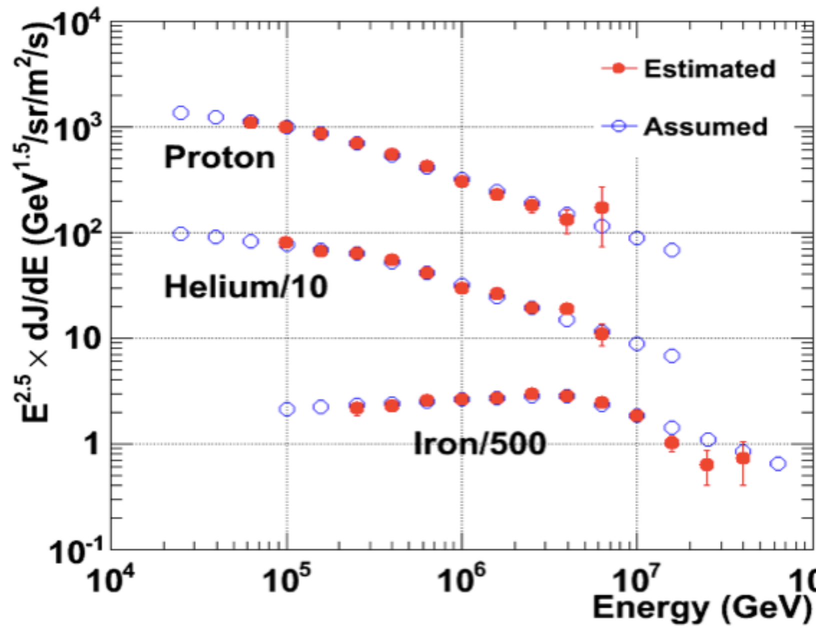

ARGO-YBJ

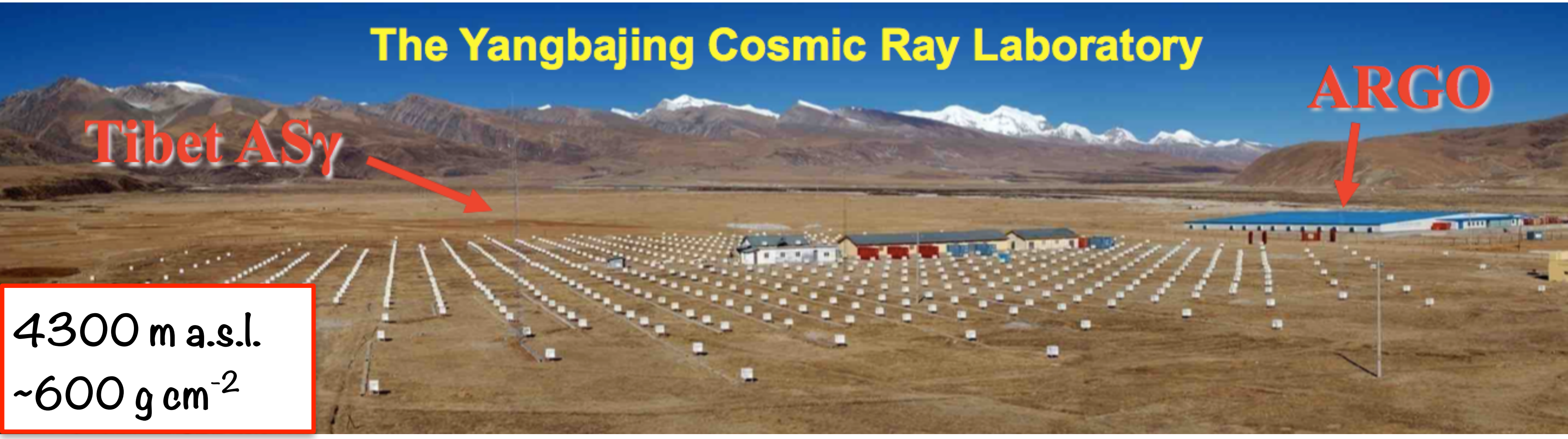
The Yangbajing Cosmic Ray Laboratory
Tibet ASγ
ARGO
4300 m a.s.l.
~600 g cm^{-2}

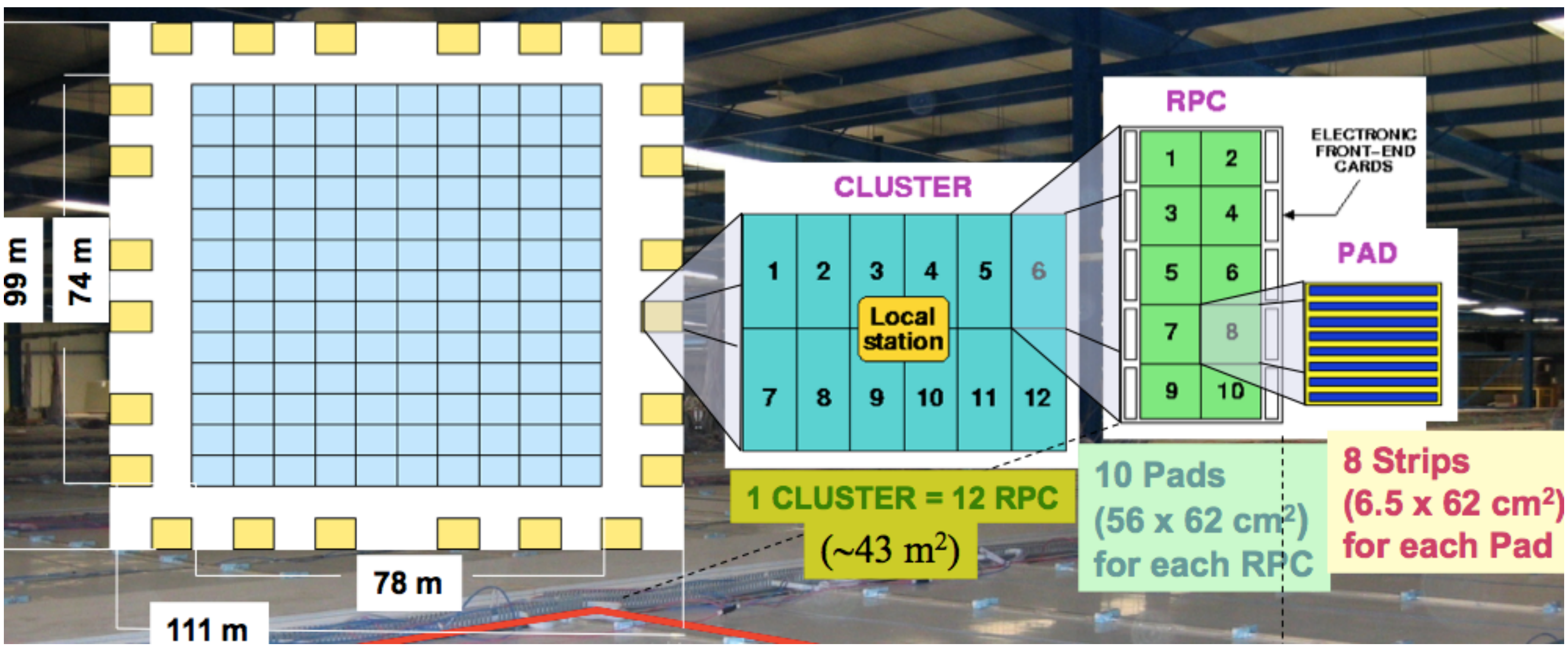
99 m
74 m
78 m
111 m
CLUSTER
1 2 3 4 5 6
Local station
7 8 9 10 11 12
1 CLUSTER = 12 RPC
(~43 m^2)
RPC
1 2 3 4 5 6 7 8 9 10
ELECTRONIC FRONT-END CARDS
PAD
10 Pads
(56 x 62 cm^2)
for each RPC
8 Strips
(6.5 x 62 cm^2)
for each Pad

Analog (ev by ev) measurement

ARGO - RPC

Energy measured by N_{p8} (<8 m) + EAS age

$$N_{p8\,max} \approx N_{p8} \cdot e^{\frac{h_0 \sec\theta - X_{max}(s')}{\lambda_{abs}}}$$

needs assumption on EAS attenuation after max (120 g cm^{-2})

Mass sensitive parameters:

correlation between age and N_{p8}

Hybrid measurement

ARGO + WFCTA (LLHASO)

Energy measured by N_{phe}^{total} (<120 m)

needs accurate determination of geometry

σ_θ<0.4°, σ_{core} ~ 2 m

Mass sensitive parameters:

Nmax(<3 m), shape of Cherenkov images

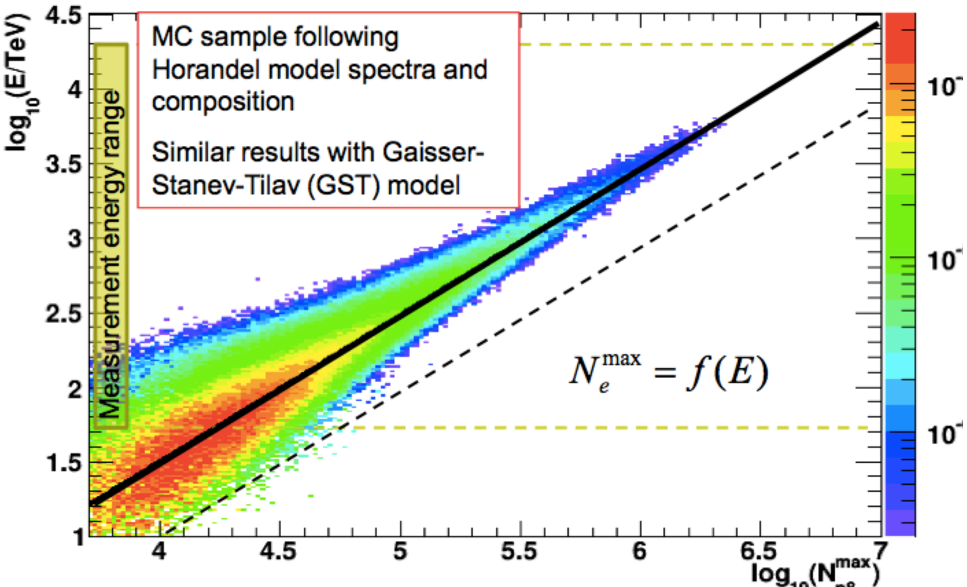

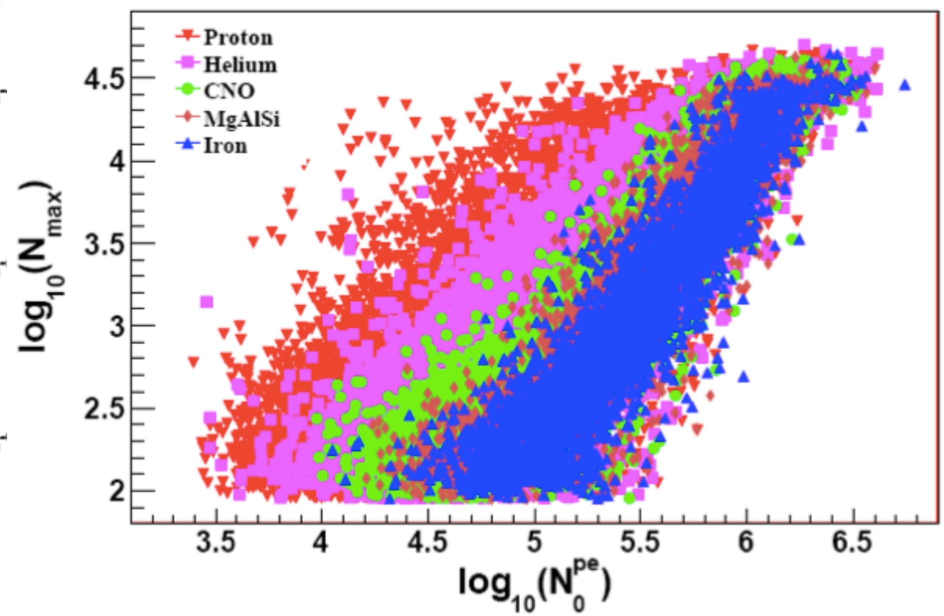

Analog measurement

For the flux:

- Geometrical Aperture : (5 % in/out contamination) ⊕ (2.5% angular contamination) =5.6 %
- Efficiency: (5% from MC samples) ⊕ (<10% efficiency estimation of the mixture) = 5.0-11.2 %
- Unfolding: 3%
- Hadronic interaction model < 5%
- **TOTAL: 8.1% - 13.8 %**
- **TOTAL: (conservative) = 14%**

Preliminary

For the energy scale:

- Gain of the analog system: 3.7 %
- Energy calibration: 0.03 in LogE = 6.9%
- Hadronic interaction model: 5%
- **TOTAL: 9.3 %**
- **TOTAL: (conservative) = 10%**

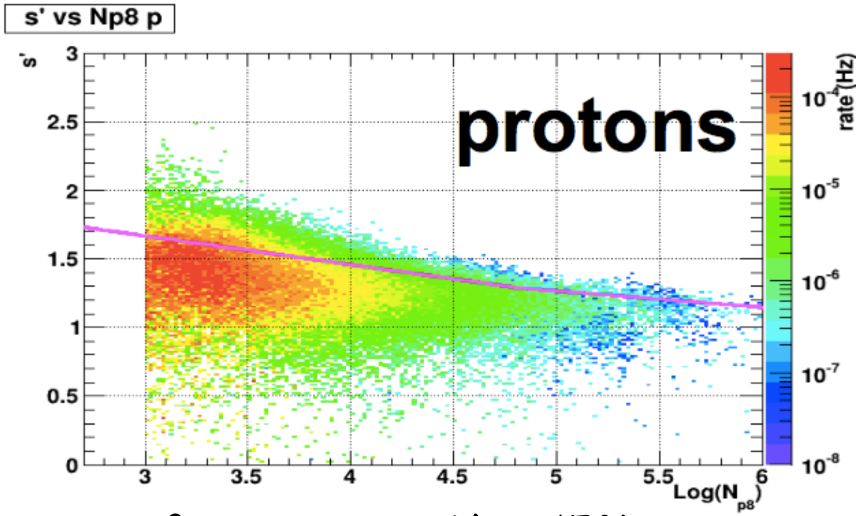

Contamination > He: ≈ 15%

Hybrid measurement

Wide Filed of View Cherenkov Telescope: a prototype of the future LHAASO telescopes

- 5 m^2 spherical mirror
- 16 x 16 PMT array
- pixel size 1°
- FOV: 14° x 14°
- Elevation angle: 60°

❖ *ARGO-YBJ:* core reconstruction & lateral distribution in the core region → mass sensitive

❖ *Cherenkov telescope:* longitudinal information Hillas parameters → mass sensitive

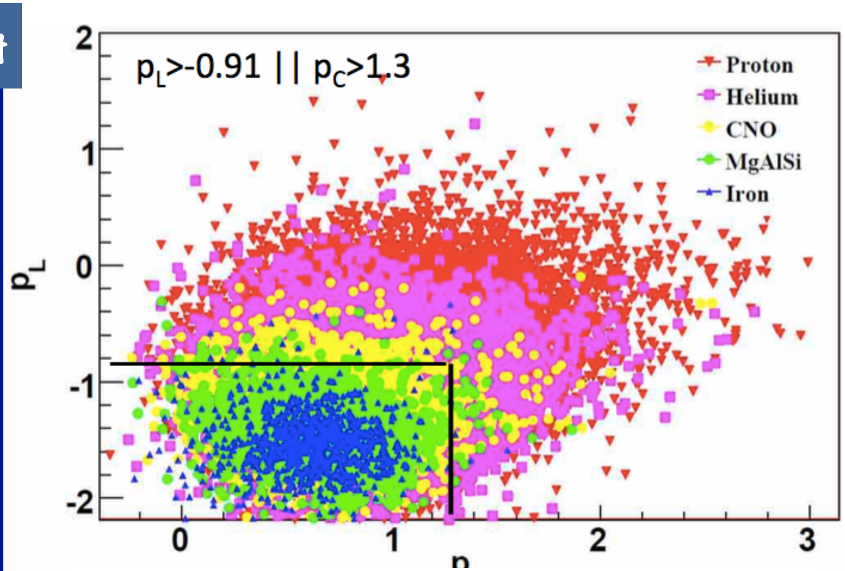

$$p_L = log_{10}(N_{max}) - 1.44 \cdot log_{10}(E_{rec}/TeV)$$

$$p_C = L/W - 0.0091(R_p/1\,m) - 0.14 \cdot log_{10}(E_{rec}/TeV)$$

ARGO-YBJ all particle spectrum

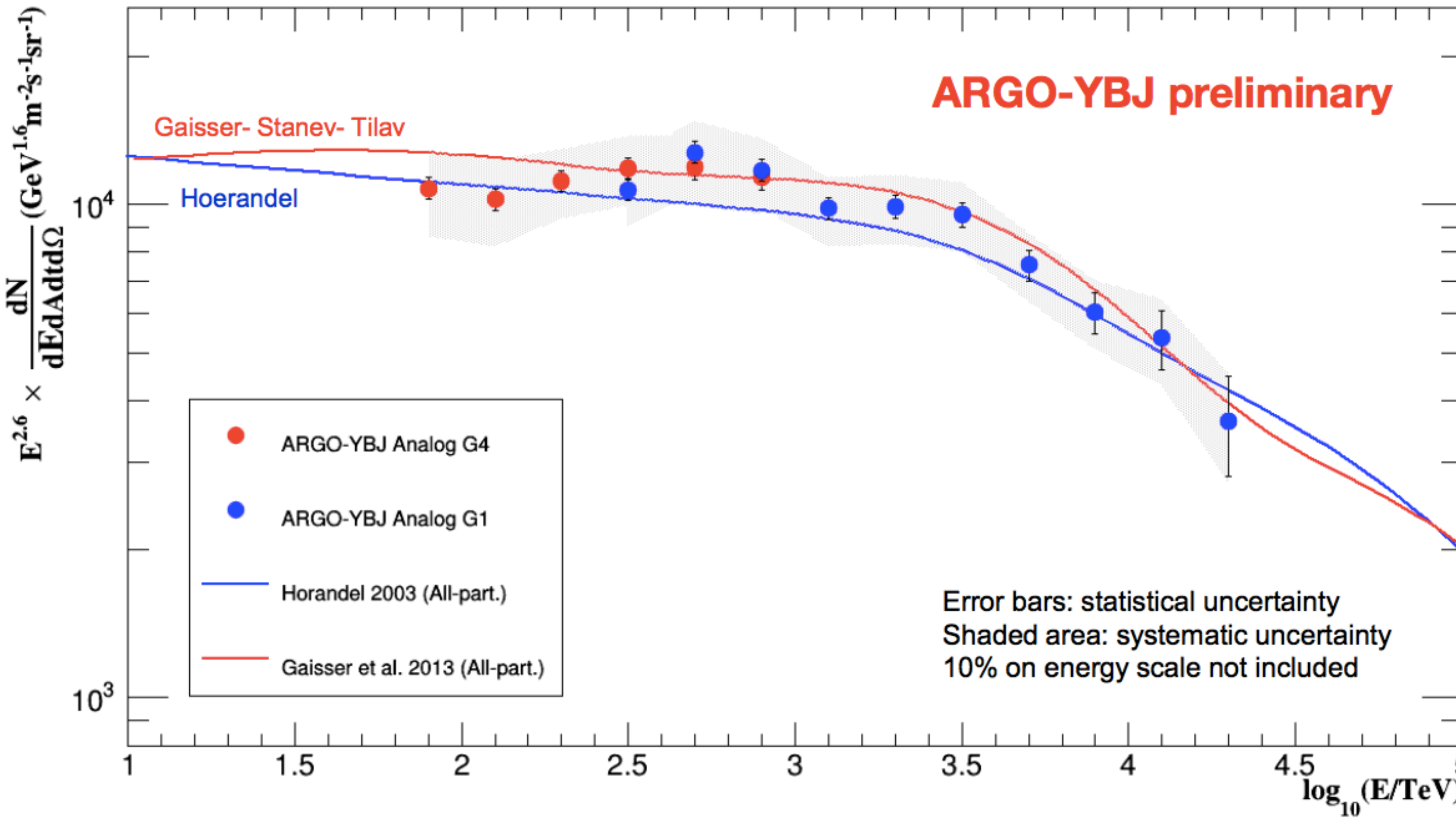

ARGO-YBJ light (p+He) spectrum

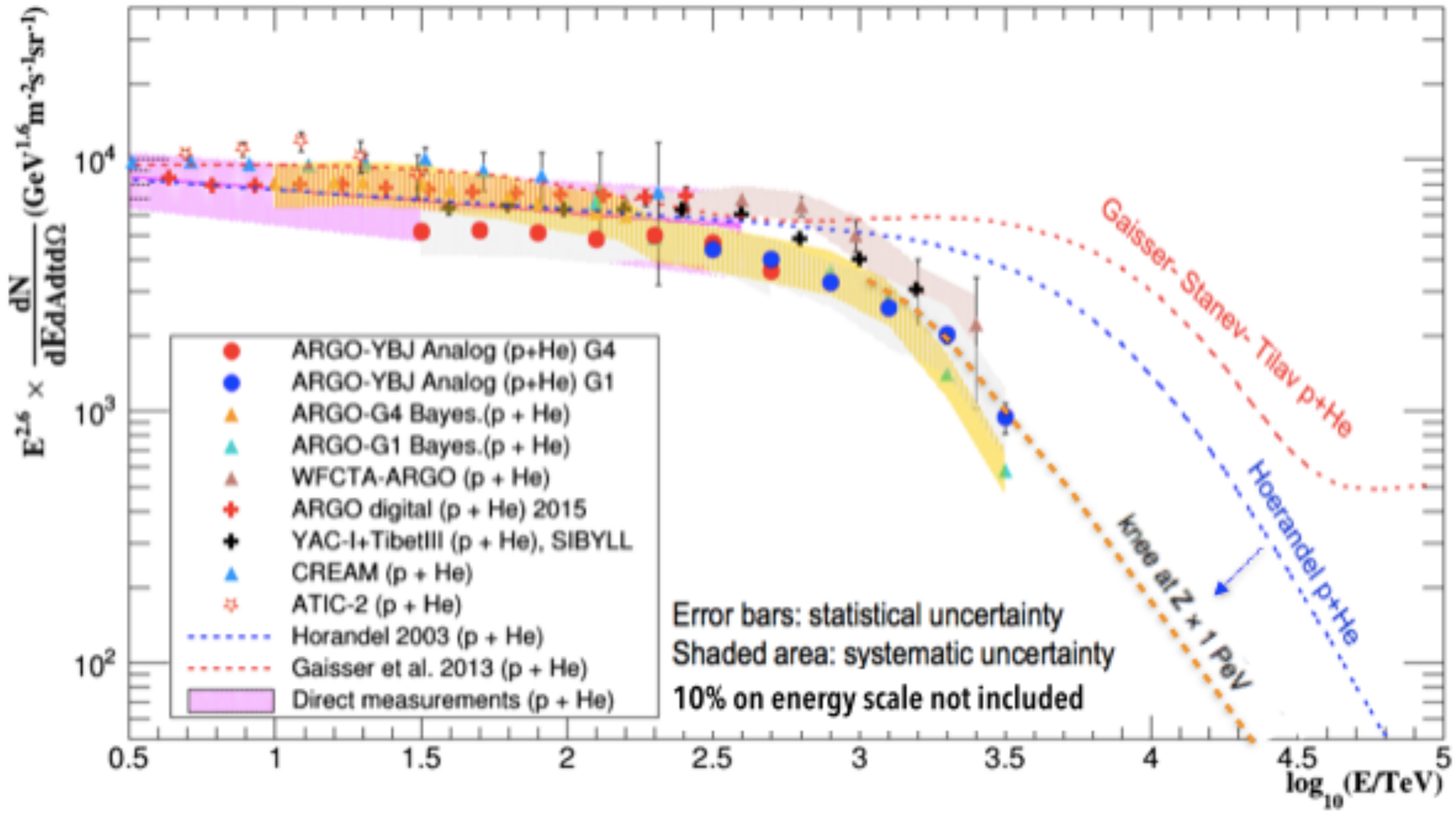

Data	σ(E)	σ^{sys} (E scale)	σ^{sys} (flux)
Hybrid	25%	~ 9.7%	~28%
Analog	15%	5%	20%

- evidence for a proton knee at E_k=(700 ±230) TeV
- γ from (-2.56±0.05) to (-3.24±0.36)
- compatible with JH spectrum with proton knee at 1 PeV

ARGO-YBJ all particle spectrum

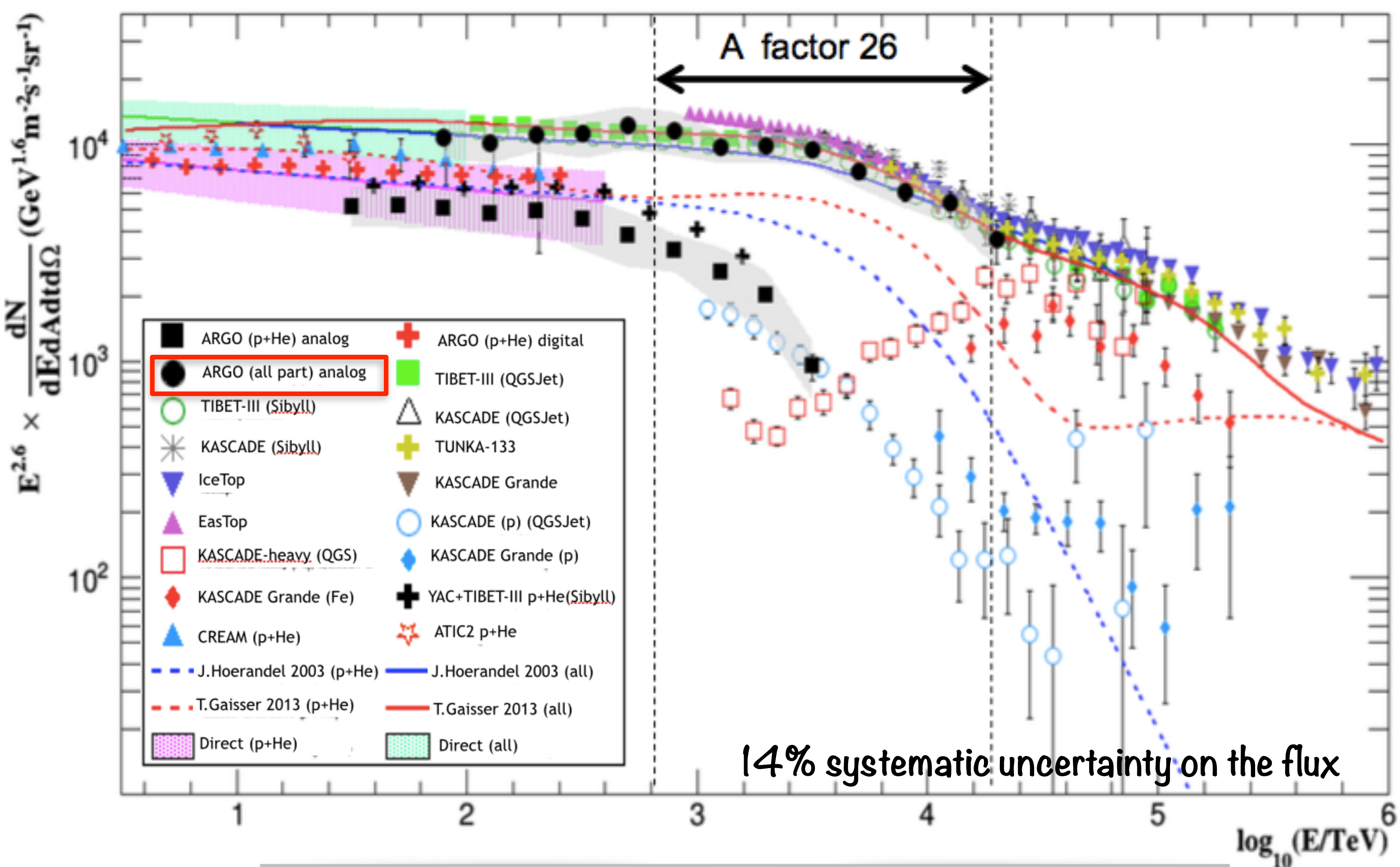

- all particle knee ~ 4 PeV
- consistent with direct and indirect measurements

Above the knee : KASCADE-Grande

2005 m a.s.l. [820 g cm^{-2}]
A ~ 10^5 m^2
10^{16} - 10^{18} eV

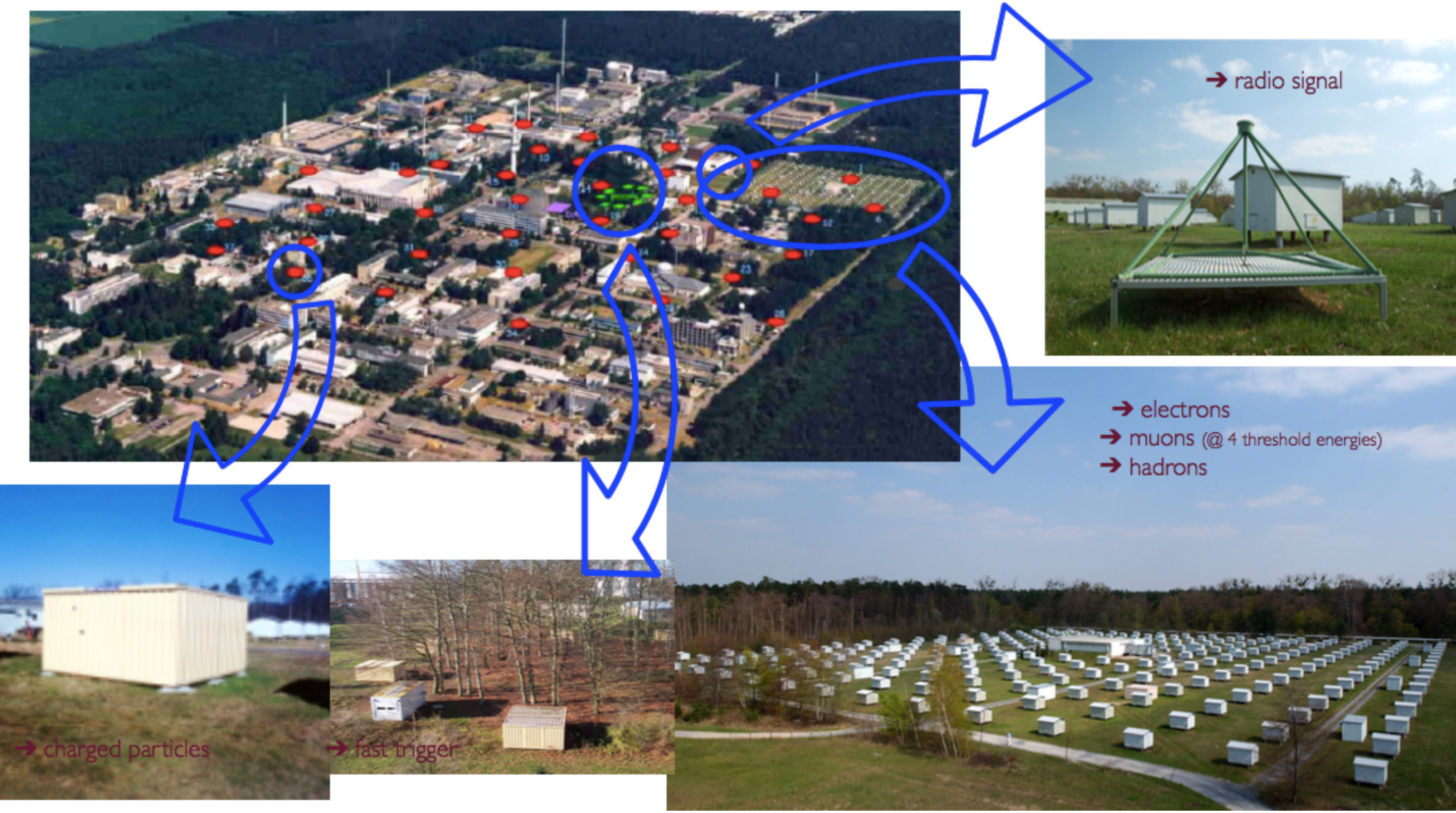

Kascade-Grande : Analysis technique

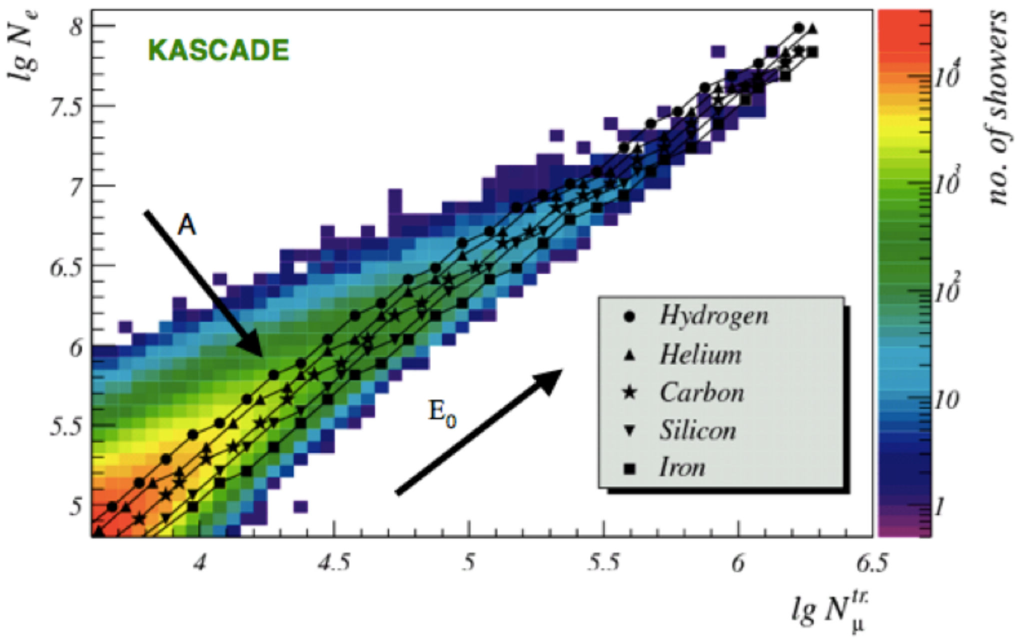

Unfolding technique

$$\frac{dJ}{d\log N_e \, d\log N_\mu} =$$

$$\Sigma_A \int_{-\infty}^{+\infty} \frac{dJ_A}{d\log E} \; p_A(\log N_e, \log N_\mu \,|\, \log E) \, d\log E$$

$$p_A = \int_{-\infty}^{+\infty}\int_{-\infty}^{+\infty} s_A \epsilon_A r_A \, d\lg N_e^{true} \, d\lg N_\mu^{tr,true}$$

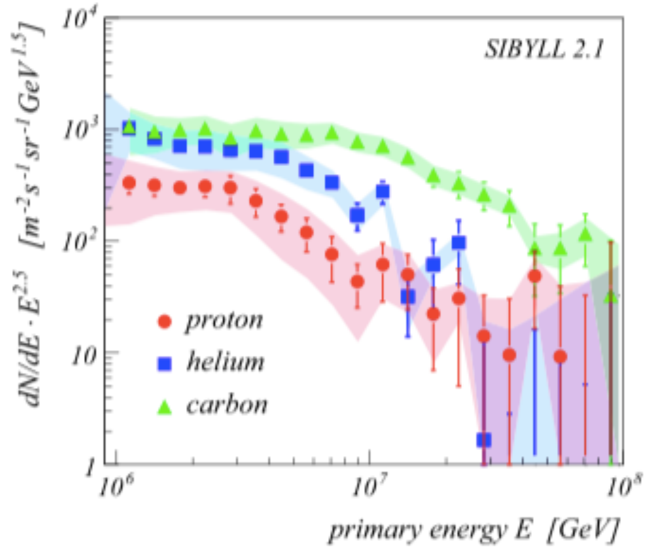

- takes into account the correlation in the fluctuations of N_e, N_μ
- relies on kernel function describing (E,A) —> (N^{obs}_e, N^{obs}_μ) —> simulations, hadronic interaction model
- systematic uncertainties increasing with energies

Kascade-Grande : Analysis technique

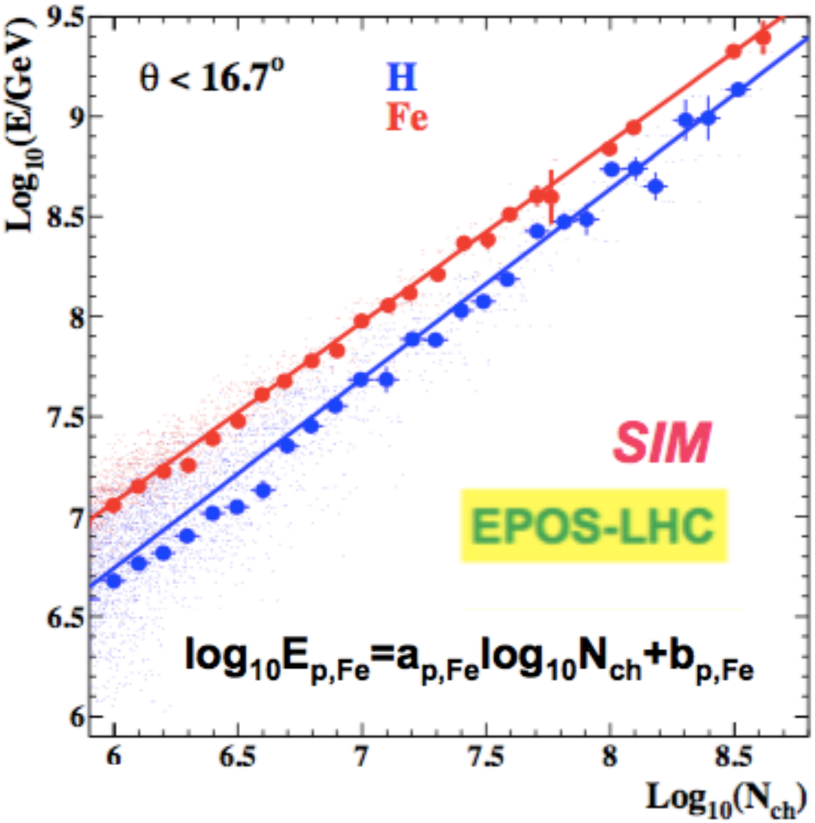

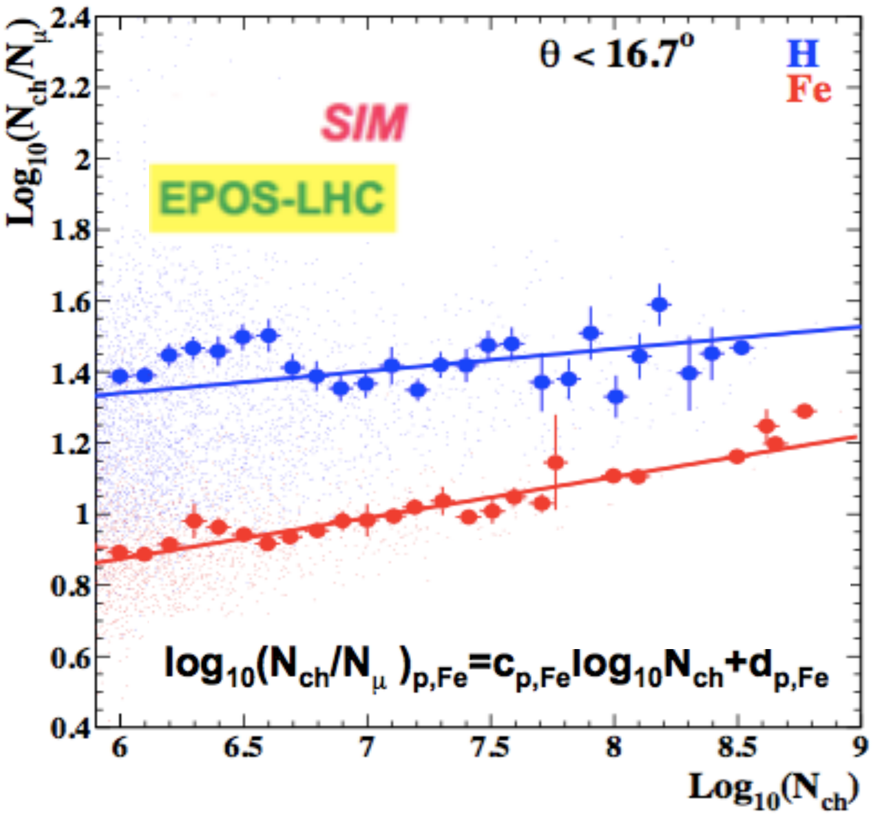

$$k = \frac{\log_{10}(N_{ch}/N_{\mu}) - \log_{10}(N_{ch}/N_{\mu})_p}{\log_{10}(N_{ch}/N_{\mu})_{Fe} - \log_{10}(N_{ch}/N_{\mu})_p}$$

$$\log_{10}E=[a_p+(a_{Fe}-a_{,p})]\cdot k\cdot \log_{10}(N_{ch})+[b_p+(b_{Fe}-b_p)\cdot k]$$

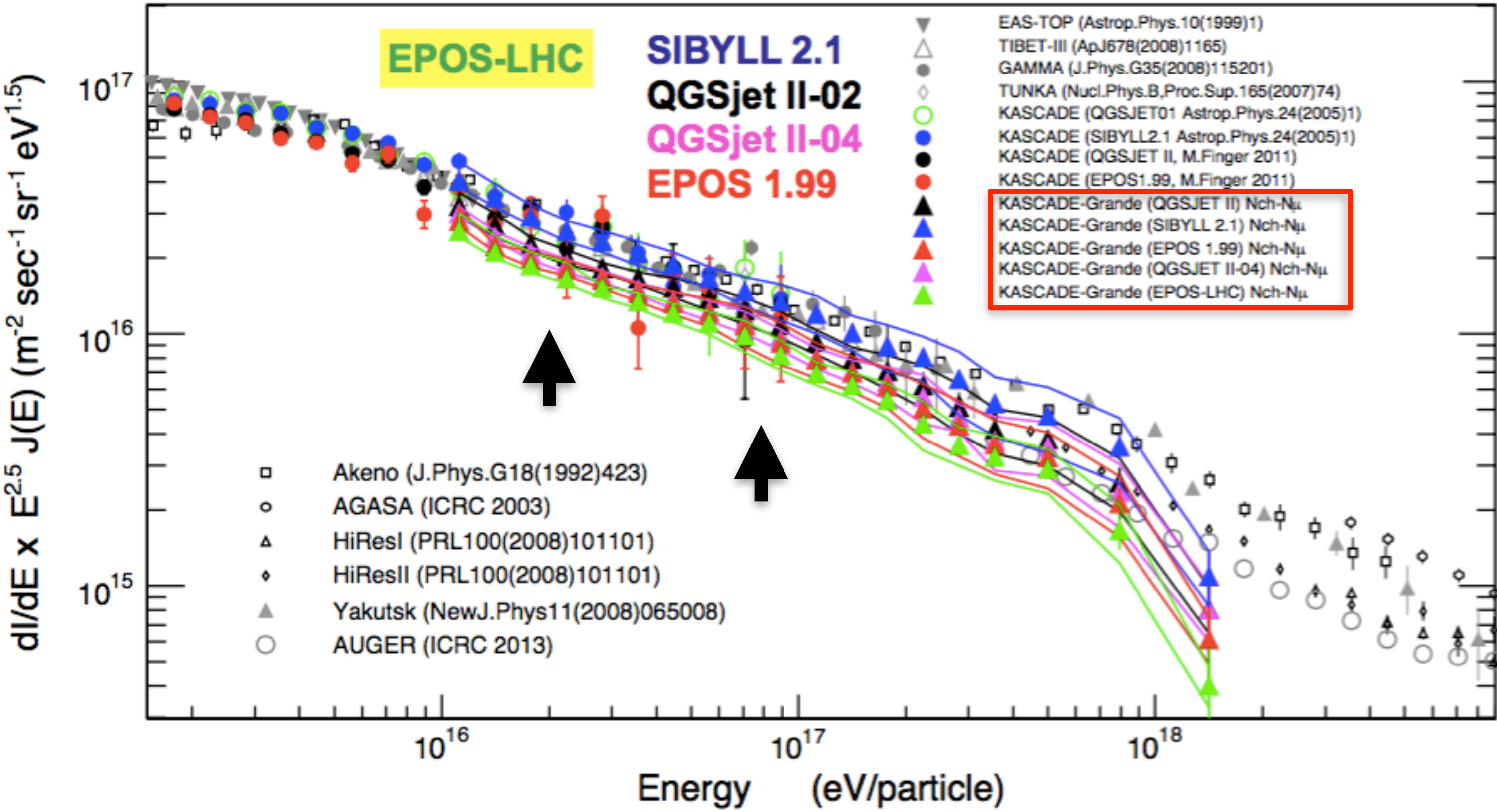

Source of uncertainty	10^{16} eV (%)	10^{17} eV (%)	10^{18} eV (%)
Intensity in different angular bins (attenuation)	−0/+6.5	10.9	21.3
Energy calibration and composition	10.3	5.8	13.4
Slope of the primary spectrum	4.0	2.0	1.9
Reconstruction (core and shower sizes)	0.1	1.4	6.5
Total	−11.1/+12.8	12.6	26.1
Artificial spectrum structures (extreme cases)		<10	
Hadronic interaction model (EPOS-QGSJet)	−5.3	−16.9	−14.6
Statistical error	0.6	2.7	17.0
Energy resolution (mixed composition)	24.7	18.6	13.6

Kascade-Grande

All particle spectrum

(10^{16}- 10^{18} eV)

Kascade-Grande

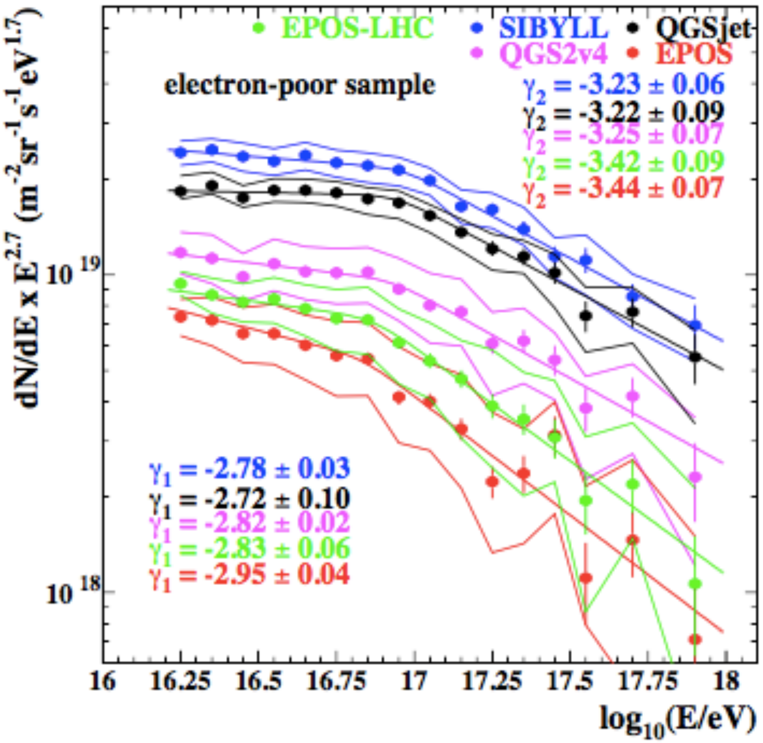

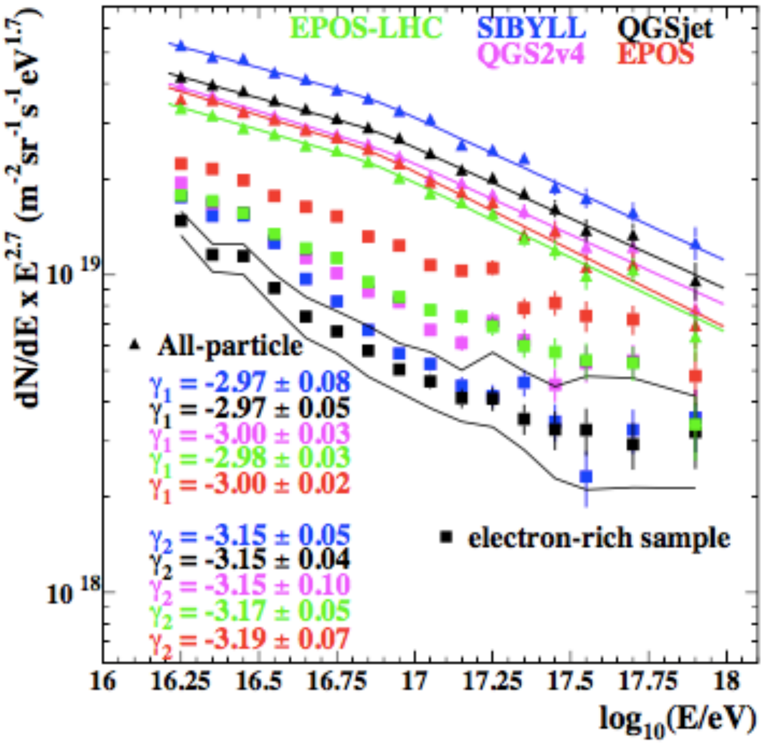

$$k(E) > k_h(E) = (k_{Si}(E) + k_C(E))/2$$

$$k(E) < k_l(E) = (k_C(E) + k_{He}(E))/2$$

- knee feature ~10^{17} eV in the spectrum of the heavy group
- a constant slope well represents the light-medium group: hardening at higher energies?
- similar behavior for all hadronic interaction models

Kascade-Grande : ankle-like feature

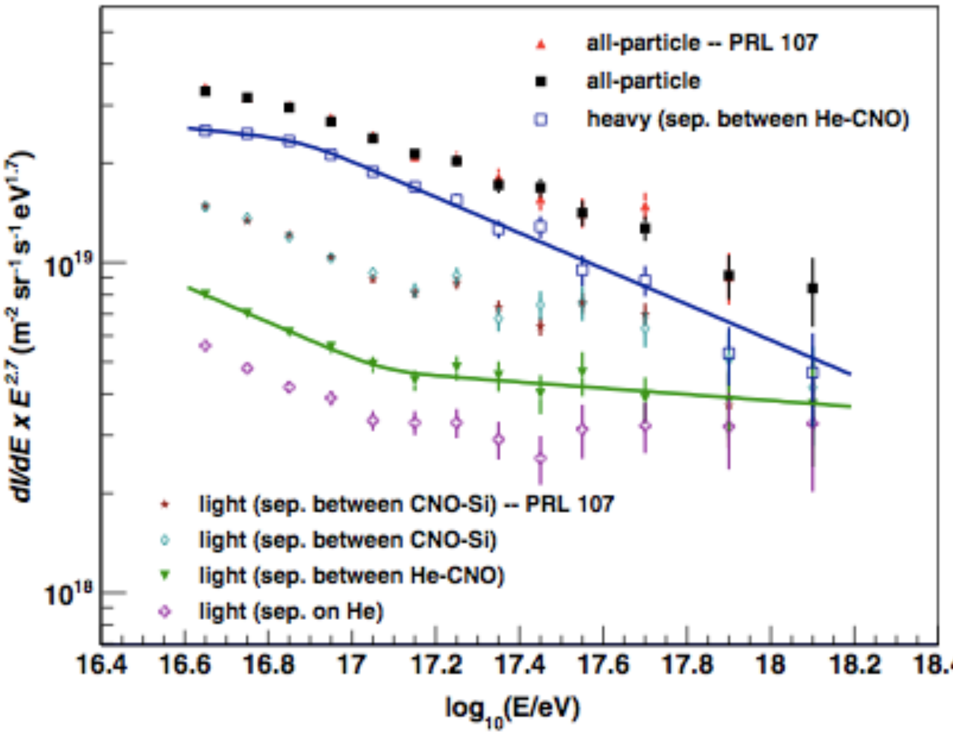

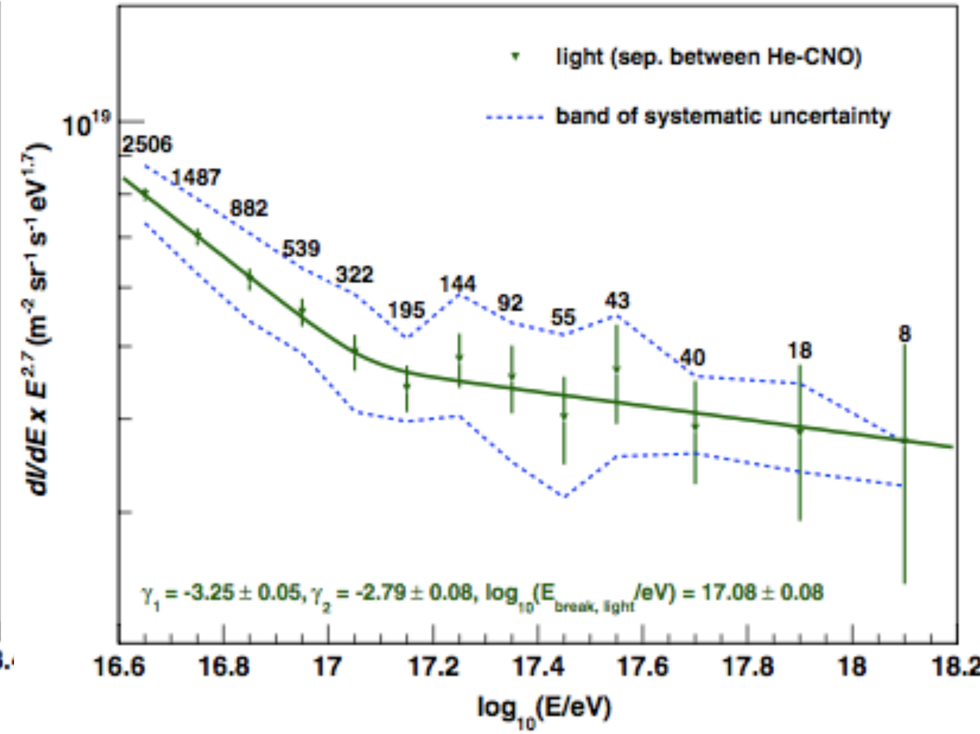

- (heavy+medium) component knee ~$10^{16.88}$ eV
- light component knee ~$10^{17.08}$ eV, $\Delta\gamma$=0.46 (from -3.25 to -2.79) —> 5.8σ : start of the transition ?
- same population for heavy above E_k(heavy) and light below E_k(light) ???

Kascade-Grande - Unfolding

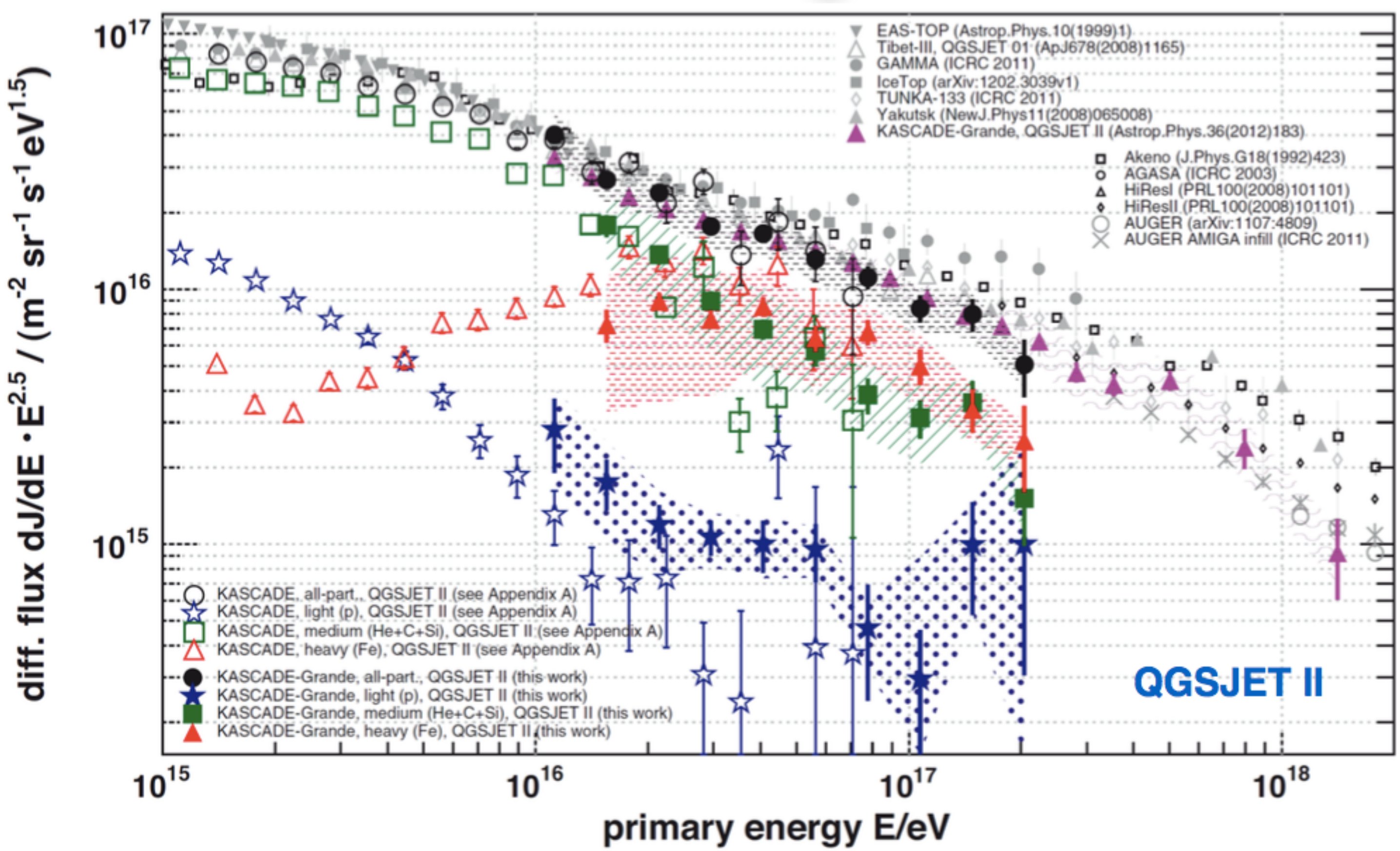

p

medium

heavy

- **all particle:** compatibility among different experimental results, lower intensity at higher E
- **elemental groups**: good agreement with Kascade(QGSJetII-02) : heavy elements knee at 80 PeV, possible recover of protons above 10^{17} eV (but lack of statistics)
- combined analysis on-going

Kascade-Grande & Kascade (10^{14}- 10^{18} eV)

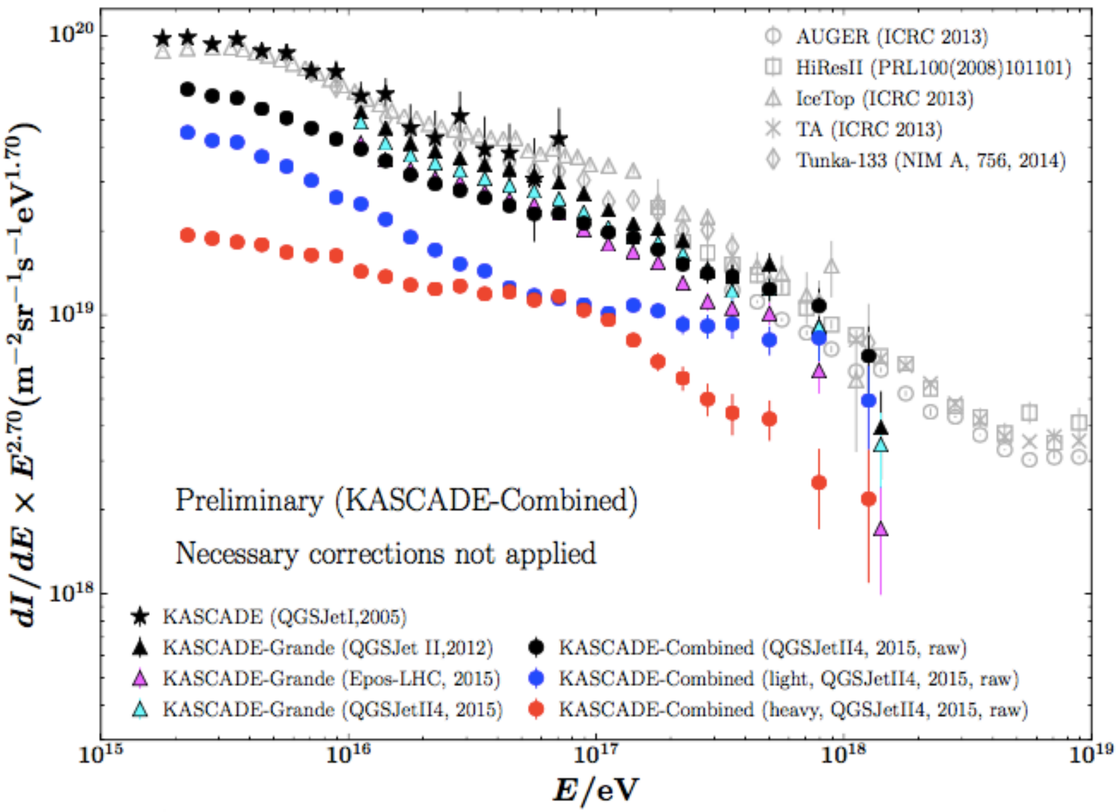

- advantages in analysis thanks to more accurate reconstruction and larger fiducial area
- can be extended to 10^{14} eV

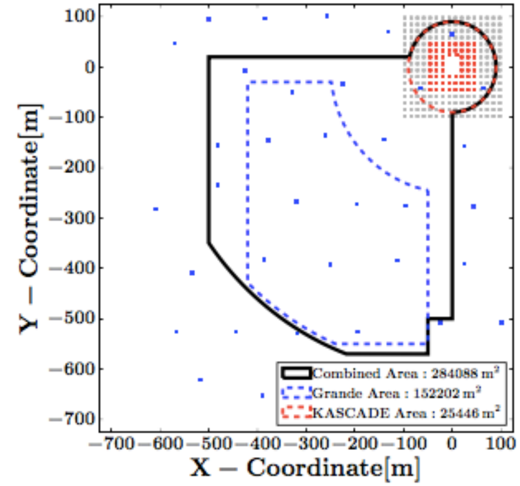

Combined-Array:

- 37 + 252 detectors
- area:
  $700 \times 700\,\mathrm{m}^2$
  used: $284088\,\mathrm{m}^2$
- measures:
  N_{ch}, N_{μ}
- energy range: $10^{14} - 10^{18}\,\mathrm{eV}$
- $\sim 87\%$ larger fid. area compared to Grande standalone
- more than 103 million events inside the selected area survive the quality cuts and arrived within 0 to 35° to the zenith.

Above the knee : IceTop

2835 m a.s.l. [680 g cm^{-2}]
A ~ 1 km^2, 125 m grid
162 ice Cherenkov tanks (2/station)

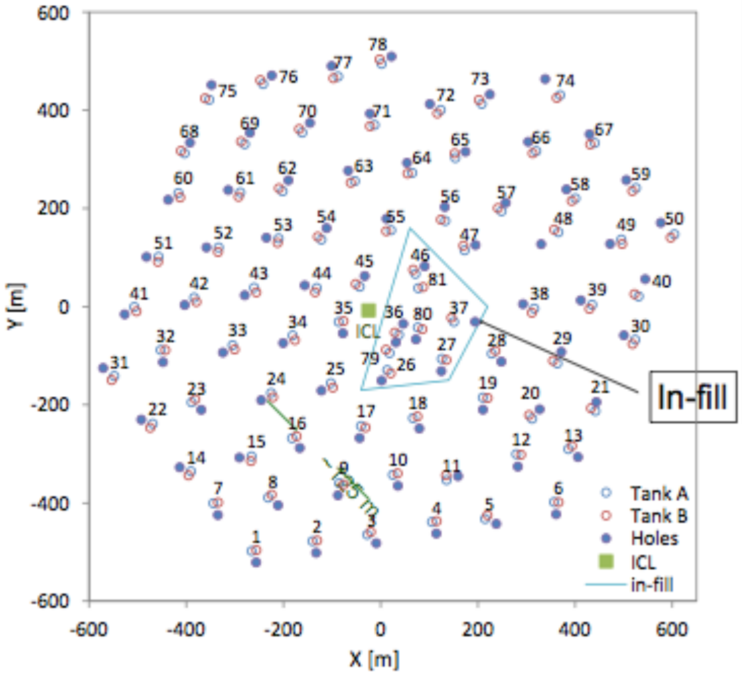

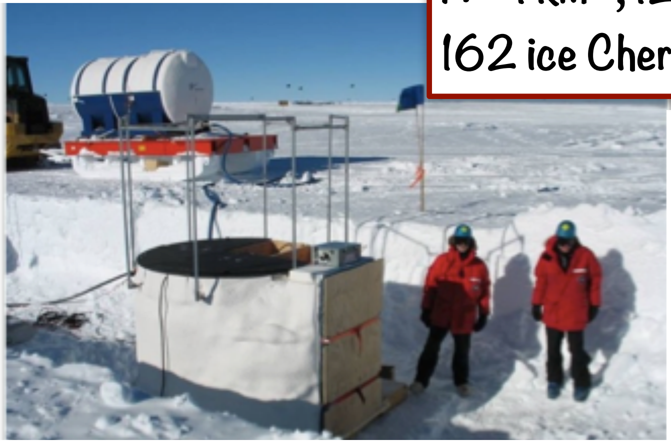

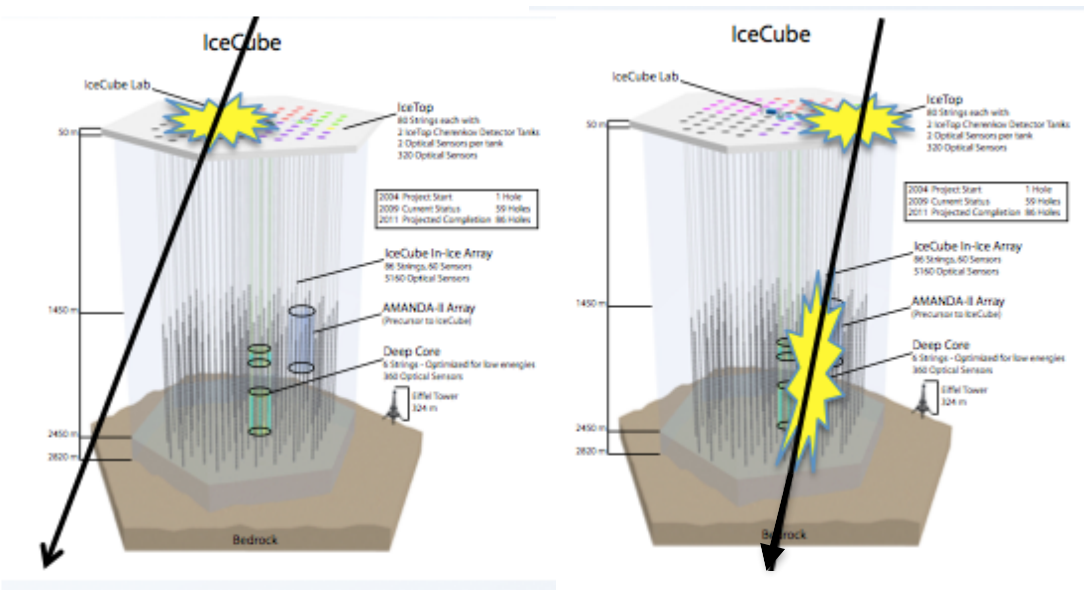

81 stations (162 tanks)

typical spacing: 125 m

fill ratio ~ 4×10^{-4}

altitude: 2835 m (X = 680 g cm^{-2})

IceTop : Analysis technique

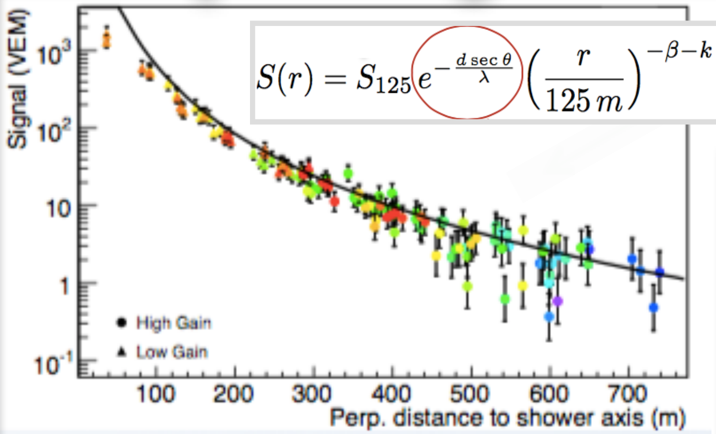

$$S(r) = S_{125} e^{-\frac{d \sec \theta}{\lambda}} \left(\frac{r}{125\,m}\right)^{-\beta - k \log\left(\frac{r}{125\,m}\right)}$$

IceTop alone

E

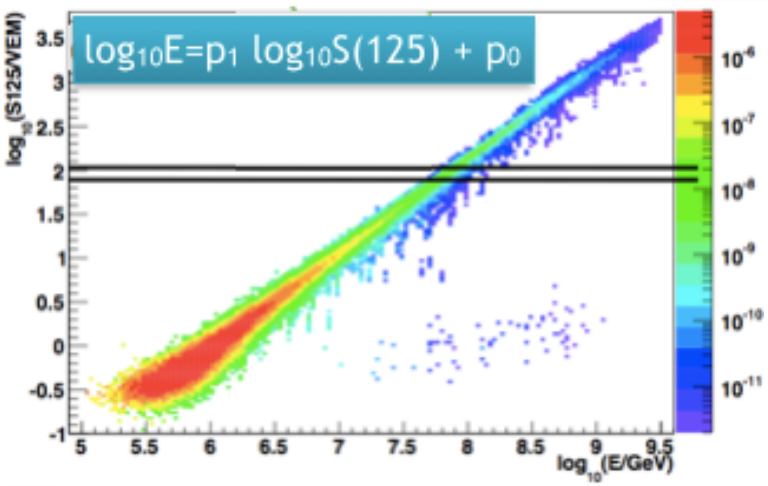

MC simulation assuming a composition

Largest syst.on the flux from snow correction

(height measured twice per year)

Attenuation different for μ and em component

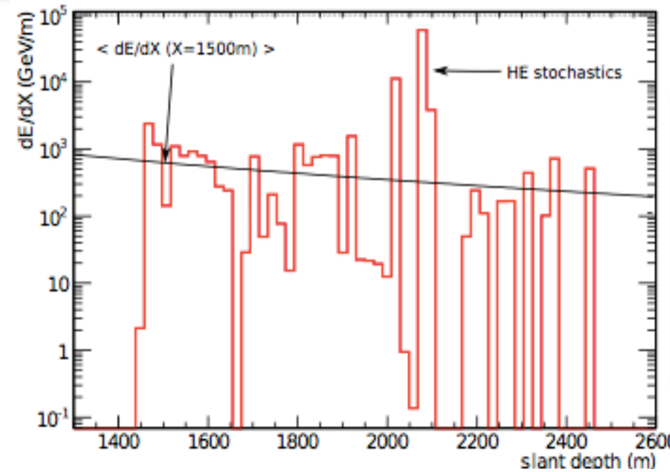

IceTop + IceCube

E,A

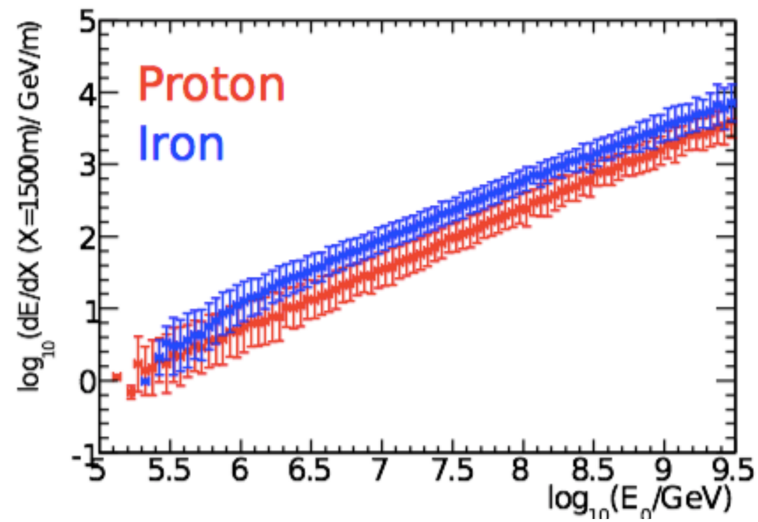

Fit energy loss profile in IceCube

Energy loss (1500 m)

NN (S125, ϑ , dE/dx(1500), stohastic losses)

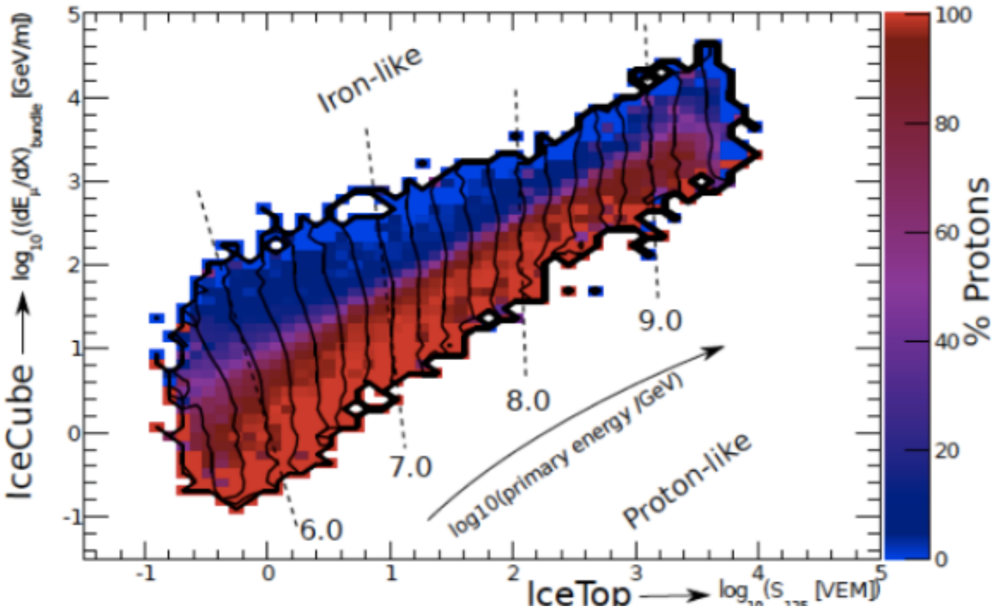

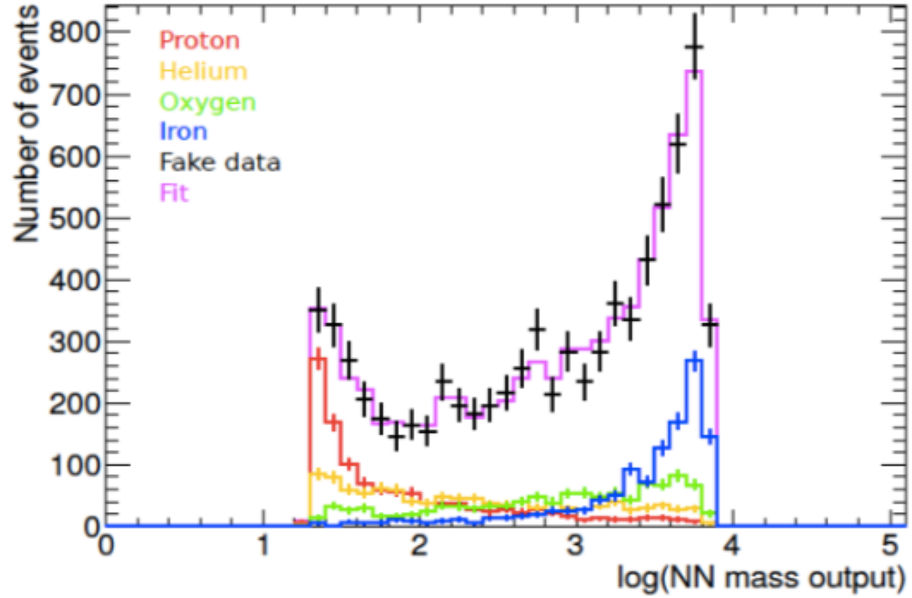

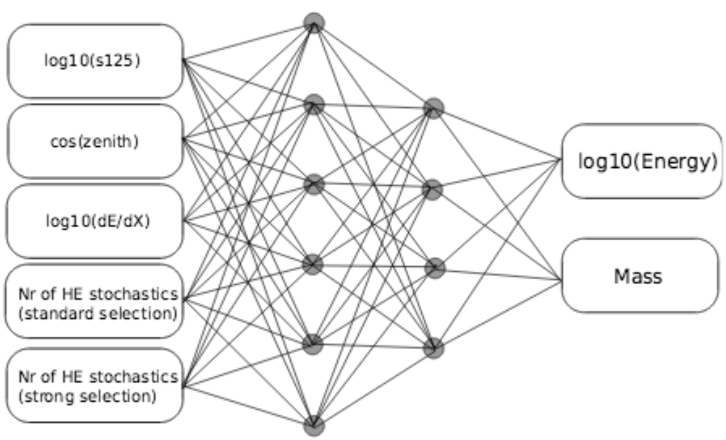

$$(\mathrm{Data})_i = f_H\, H_i + f_{He}\, He_i + f_O\, O_i + f_{Fe}\, Fe_i$$

IceTop

- hardening around 2 10^{16} eV in both standalone and coincidence analysis
- steepening at ~ 1.3 10^{17} eV

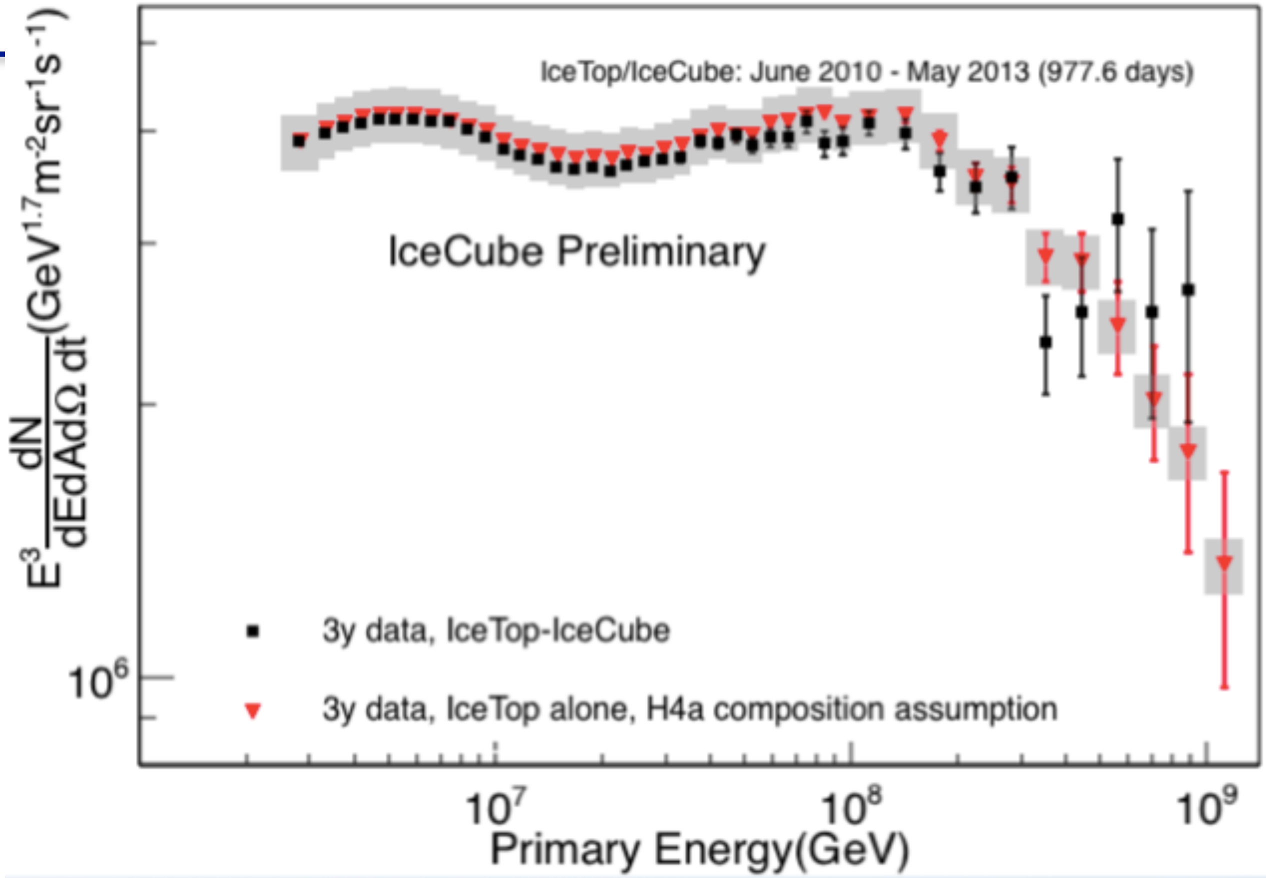

Flux systematic uncertainties

	3.35 PeV	33.5 PeV
VEM calibration/Absolute energy scale	+4.1% -4.4%	+7.0% -4.3%
Snow correction	+5.0% -4.3%	+7.9% -4.7%
QGSJet-II-03	+2.1%	+1.4%
Light yield	+3.1% - 3.0%	+1.1%
Total	+7.5% -6.5%	+10.8% -6.4%

	Systematics Uncertainty
DOM efficiency	±3%
Hole Ice 30cm	+4.5%
Hole Ice 100cm	-2.9%
+10% scattering	+3.6%
+10% absorption	-11.8%
−7% scattering AND absorption	+7%
Total	+9.6% −12.5%

IceTop : composition

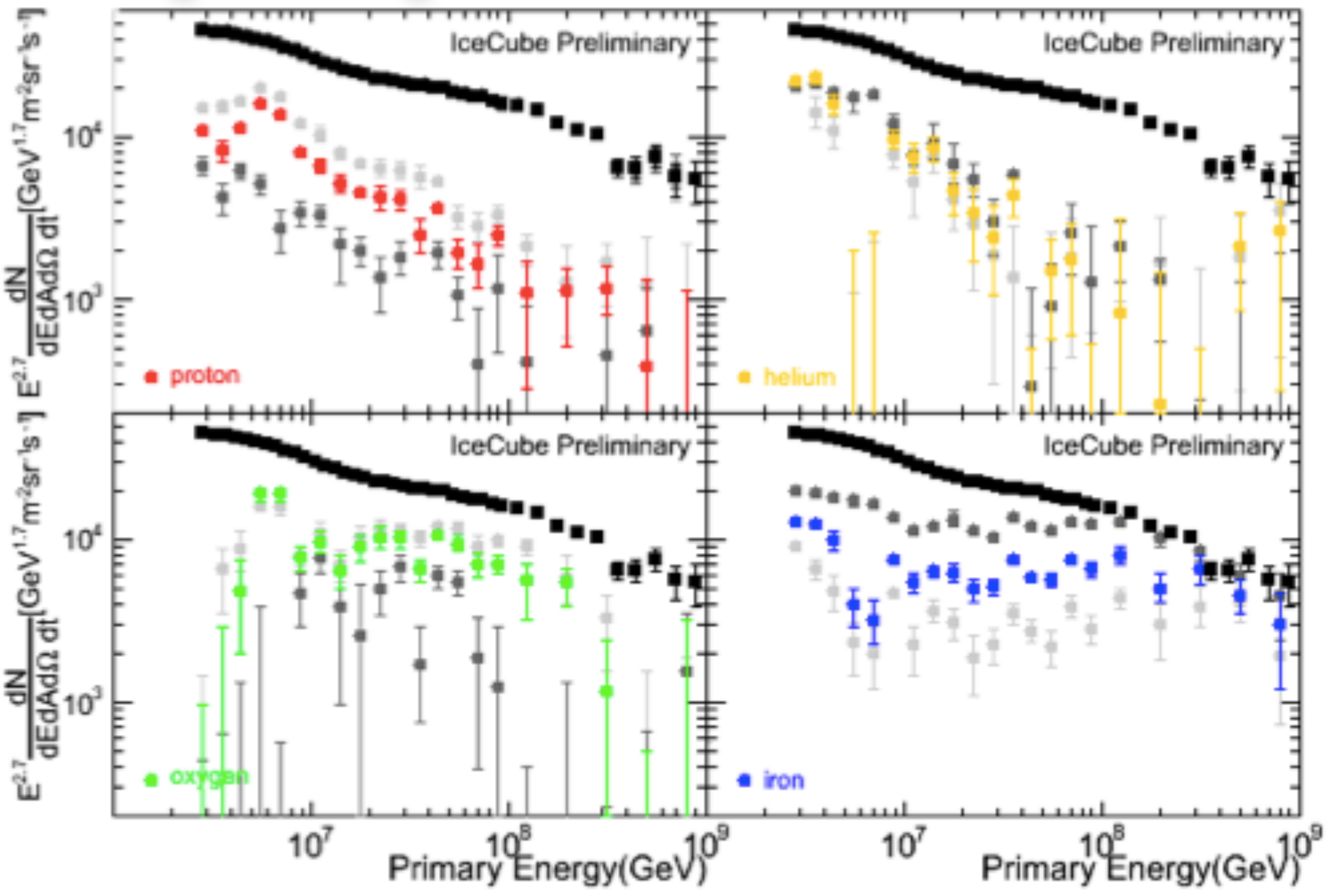

Elemental spectra= all-particle x NN fractions

Systematic uncertainty: +9.6% -12.5% (dominant effect light yield in the in-ice detectors)

- p, He steeper, medium and heavy harder
- composition increases up to ~ 10^{17} eV, then go a lighter one again

IceTop : composition

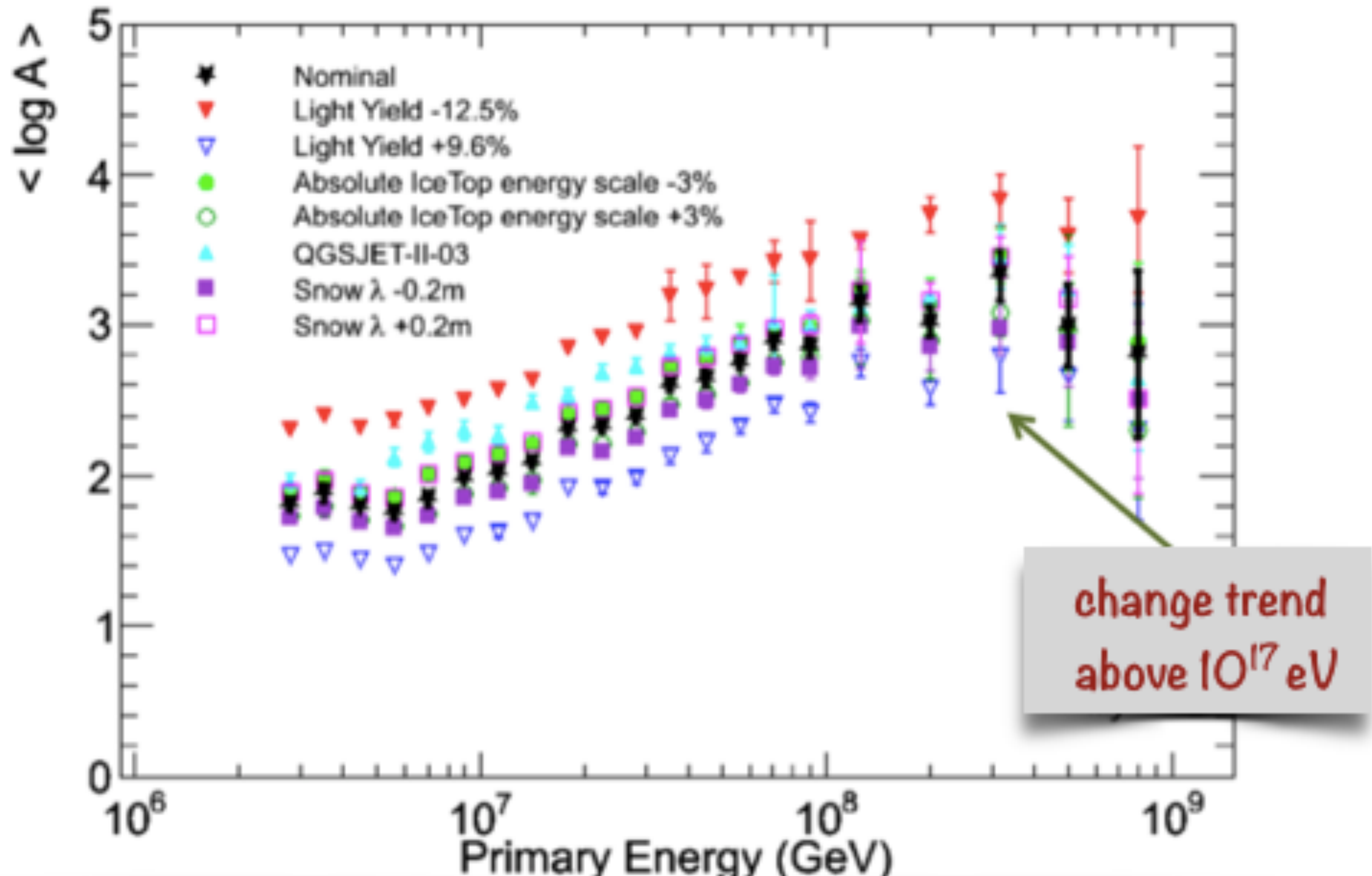

- composition measured from 4 10^{15} to 10^{18} eV
- composition increases up to ~ 10^{17} eV, then go to a lighter one again
- main systematic uncertainty light yield

Above the knee : Tunka

675 m a.s.l.
A ~ 3 km^2, 85 m grid
175 unshielded optical detectors

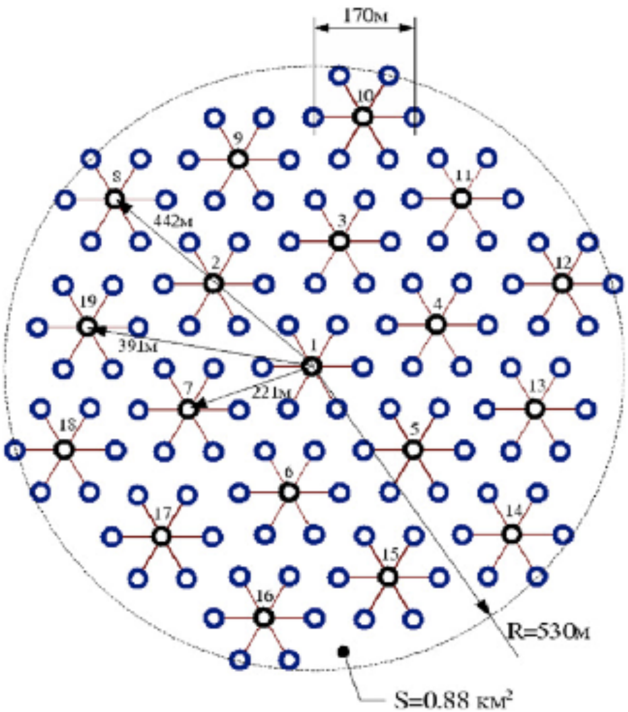

TUNKA-133
175 optical detectors

+TUNKA-Grande

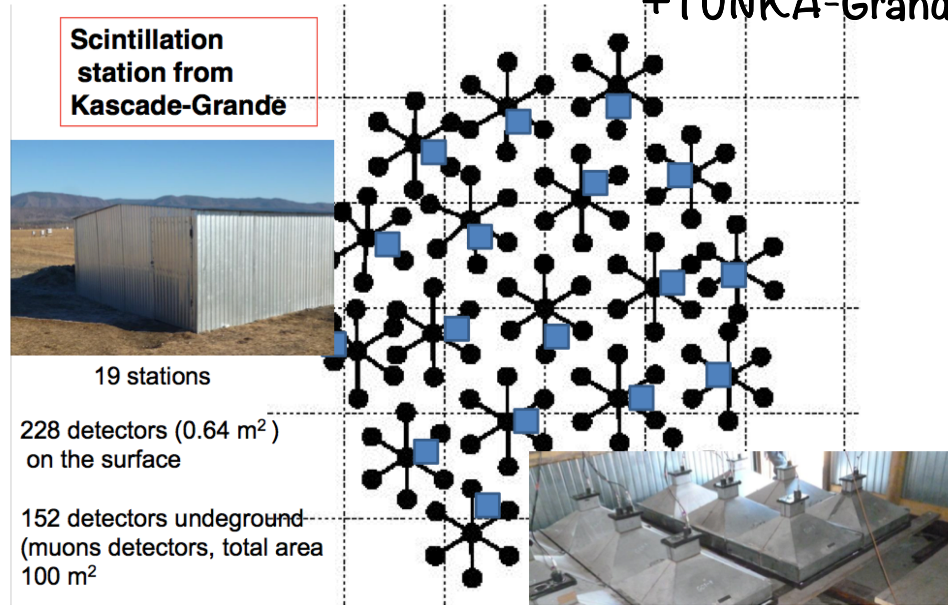

- +Tunka-HISCORE : 9(+33) stations each with 4 PMT (Winston cones)
- +Tunka-REX : 20 radio antennas
- +5 IACT
- +muon detectors (2000 m^2)

Tunka : Analysis technique

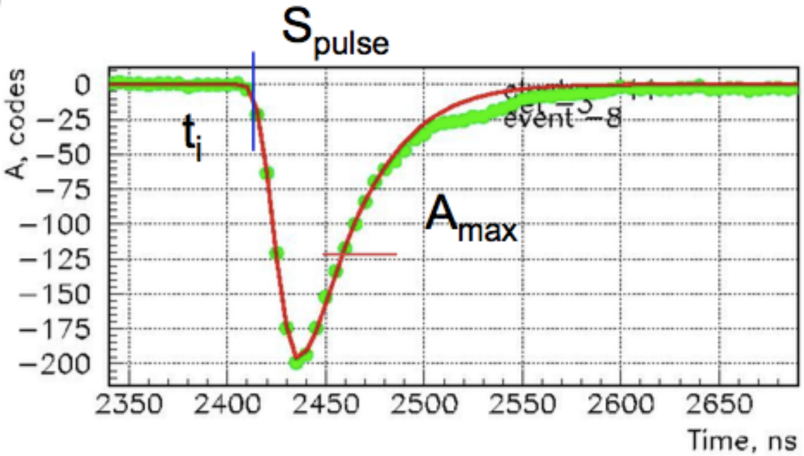

$$A(R) = A(200) \cdot f(R) \rightarrow b_A$$

Energy

$$E_0 = C \cdot Q(200)^g \quad [10^{16}\text{-}10^{18}\ \text{eV}]$$

Energy resolution ~ 8 - 12 %

X_{max}

$\sigma_{exp}(X_{max})=$ $(28 \pm 1)\ g\ cm^{-2}$

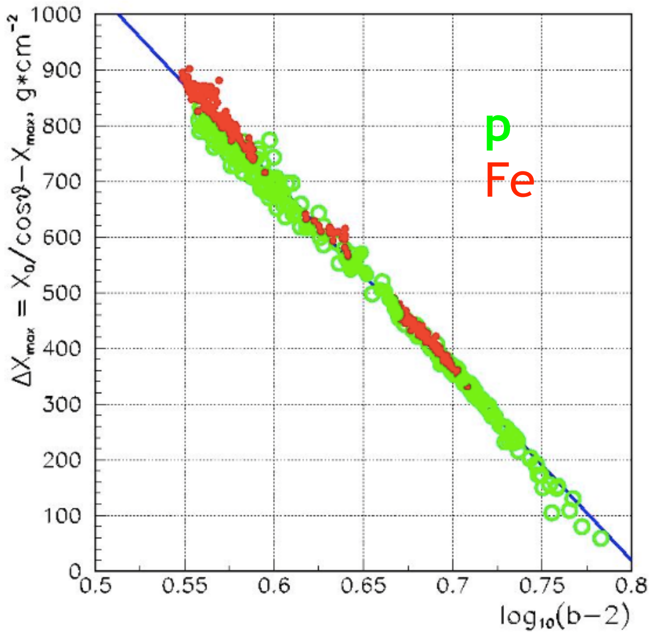

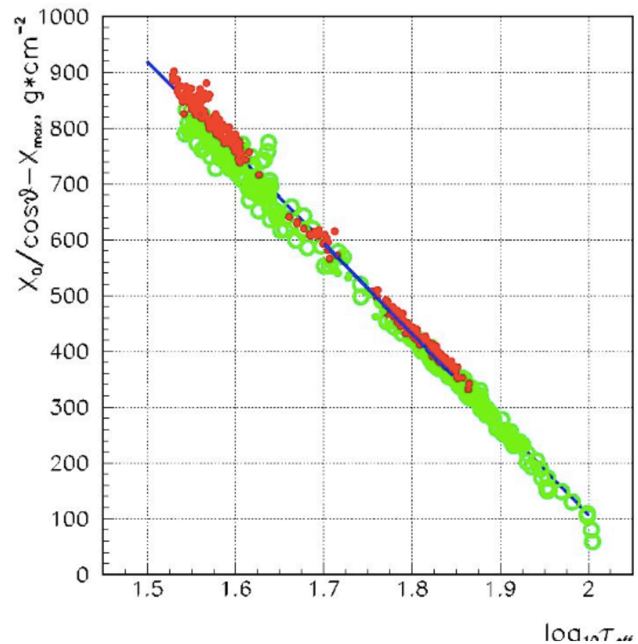

$$\Delta X_{max} = X_0/\cos\theta - X_{max} = A - B \cdot \log(b_A - 2) = C - D \cdot \log\ \tau_{eff}(400)$$

Tunka

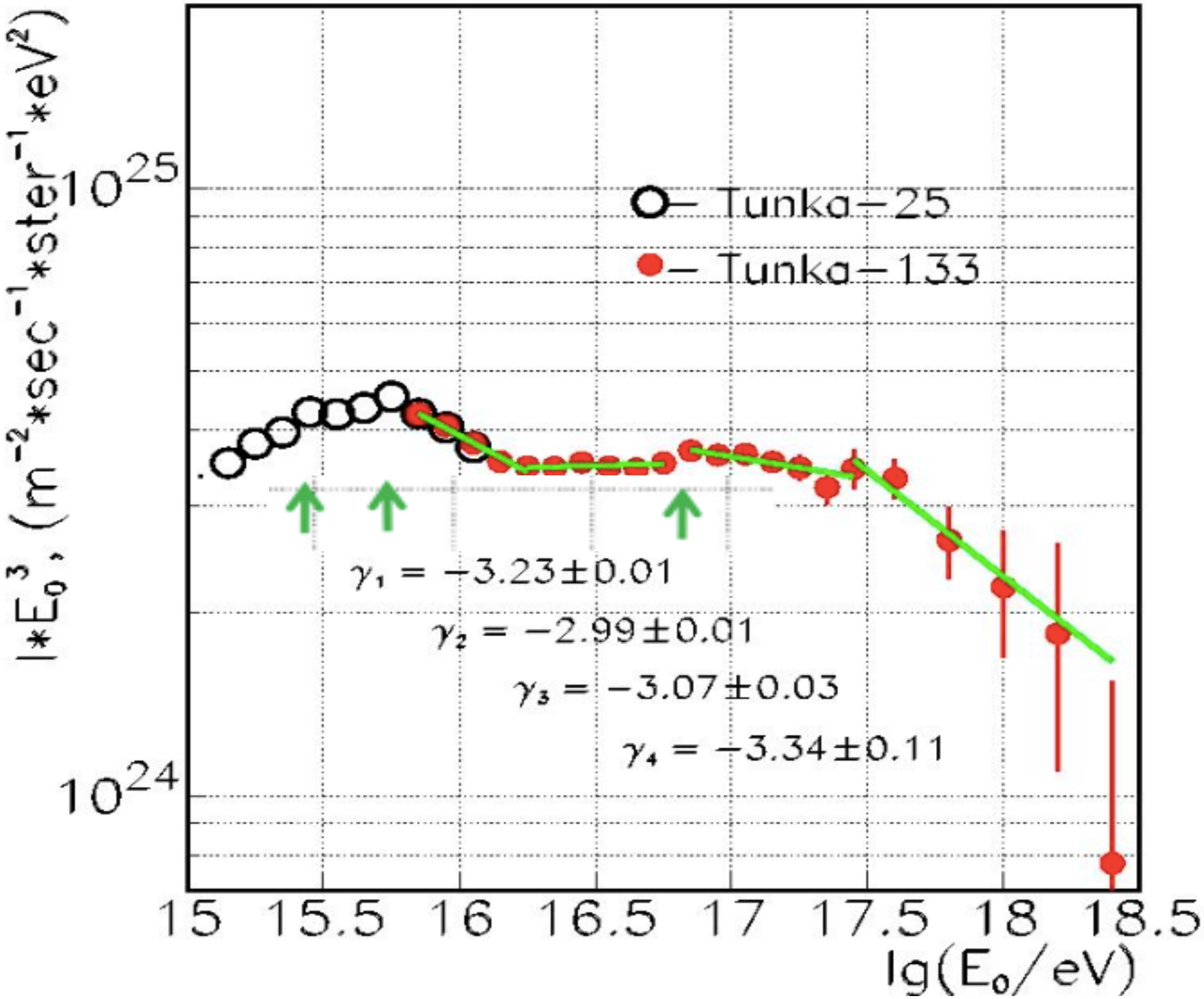

- hardening around $2\ 10^{16}$ eV and steepening at ~ $3\ 10^{17}$ eV in agreement with other experimental results
- agreement with TALE spectrum between $2\ 10^{17}$ and 10^{18} eV

Tunka Composition

light: p+He

heavy: N+Fe

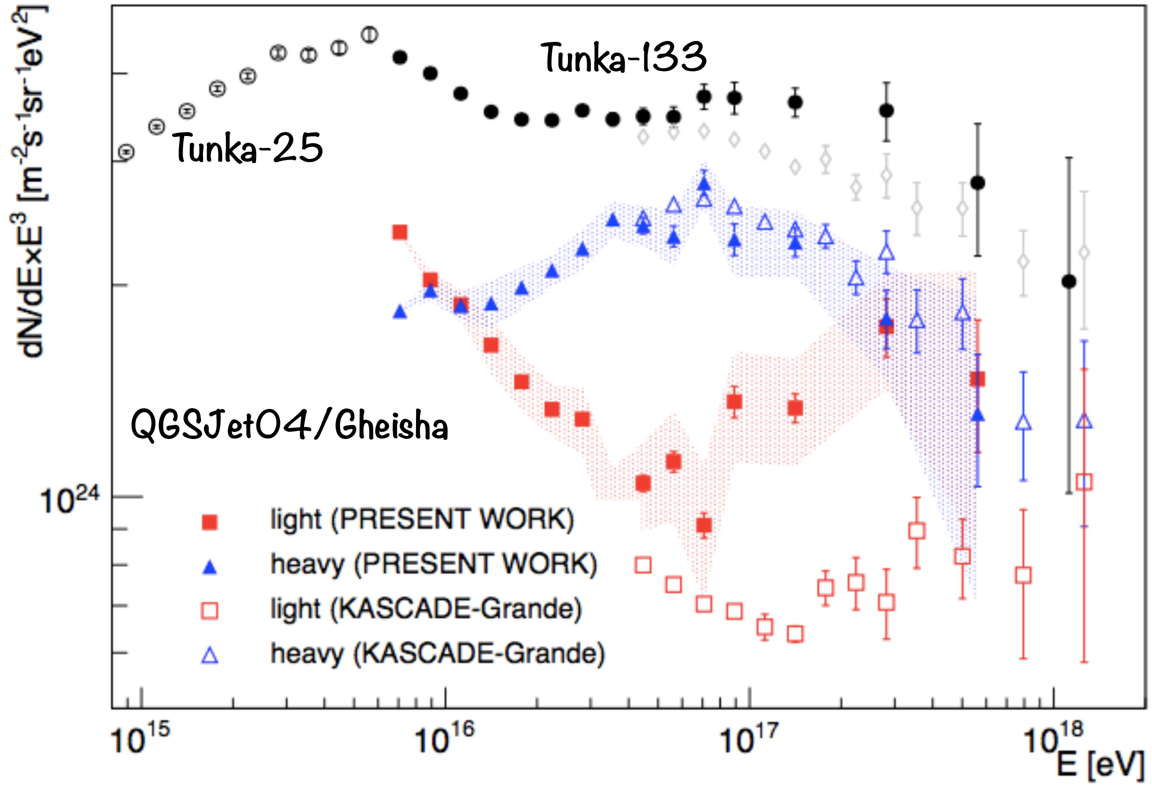

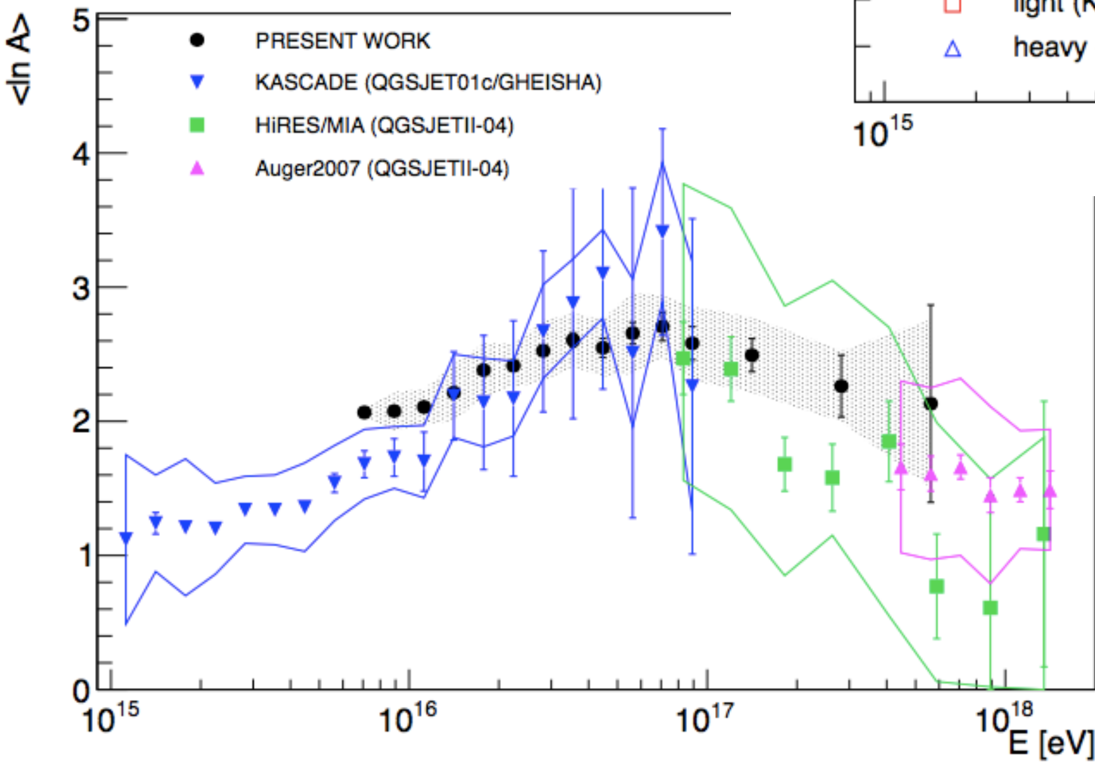

- knee : p, He
- heavy knee at ~ 7 10^{16} eV
- light component growing above 4-5 10^{16} eV
- mean mass getting heavier up to ~ 10^{17} eV, then lighter again

Yakutsk

100 m a.s.l. [1020 g cm^{-2}]
A ~ 40 km^2, 1000 m grid
10^{15}-10^{19} eV

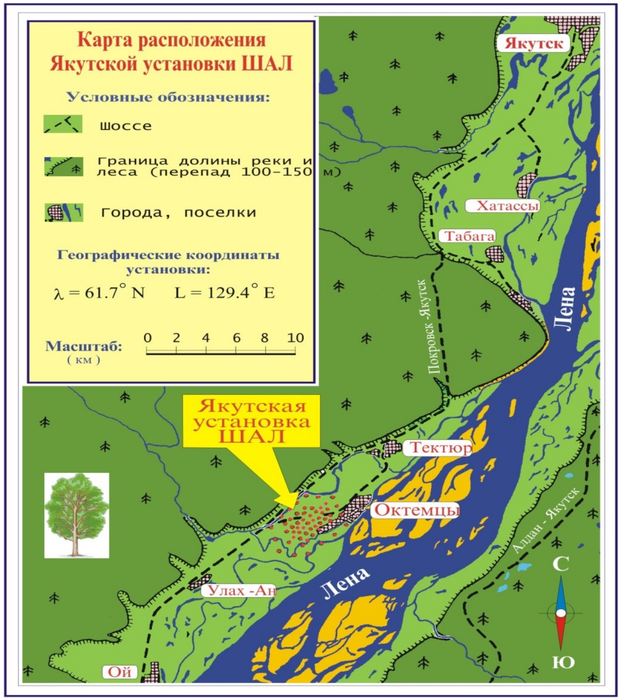

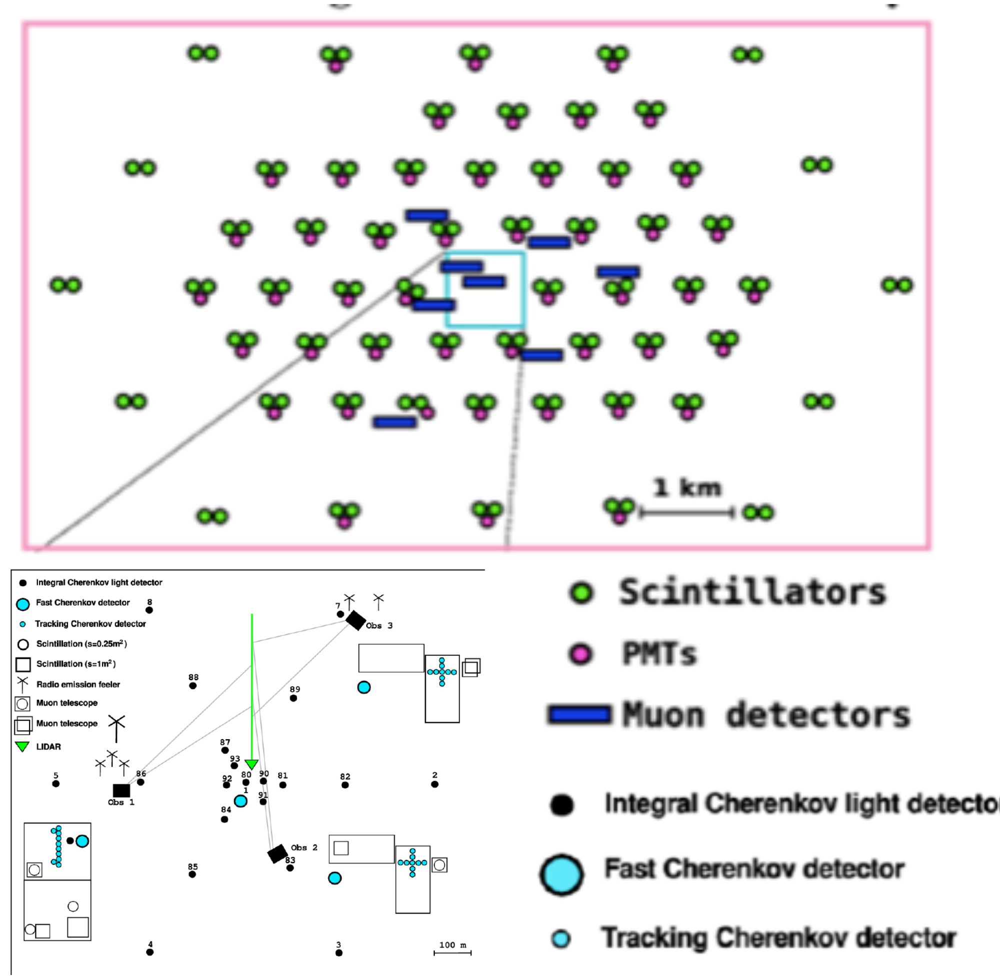

40 years data taking: many reconfigurations

Small Cherenkov array: measure of the 10^{15}-10^{18} eV range with hybrid technique: electrons, muons, Cherenkov light

20 years of data

Yakutsk

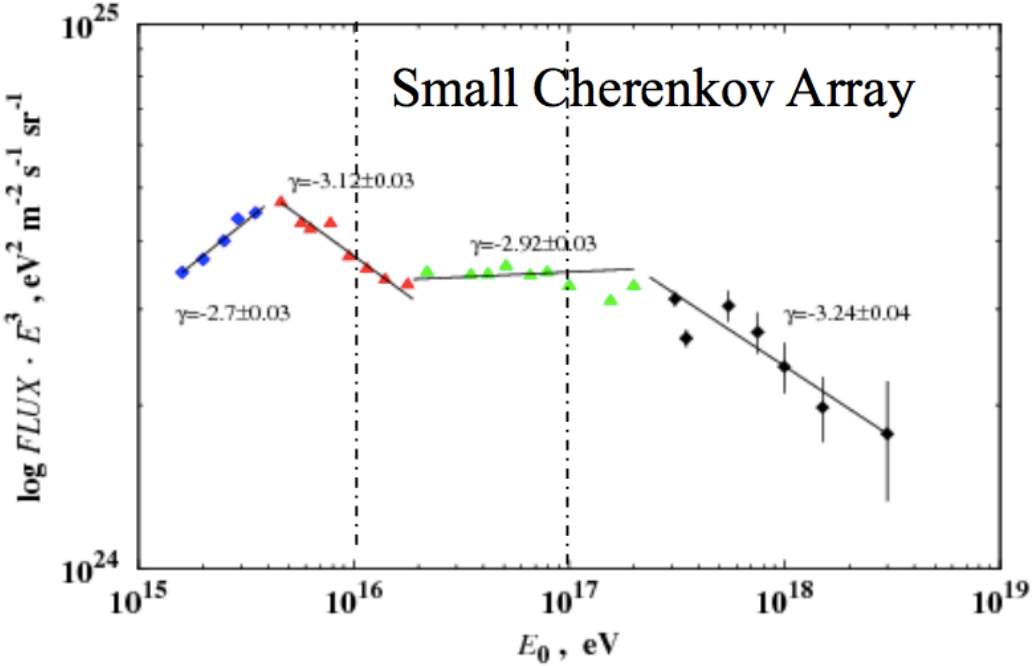

- knee ~ 4 10^{15} eV, Δγ~0.42
- second knee ~ 2 10^{17} eV, Δγ~0.32 lower than that of 1st knee (metagalactic component?)

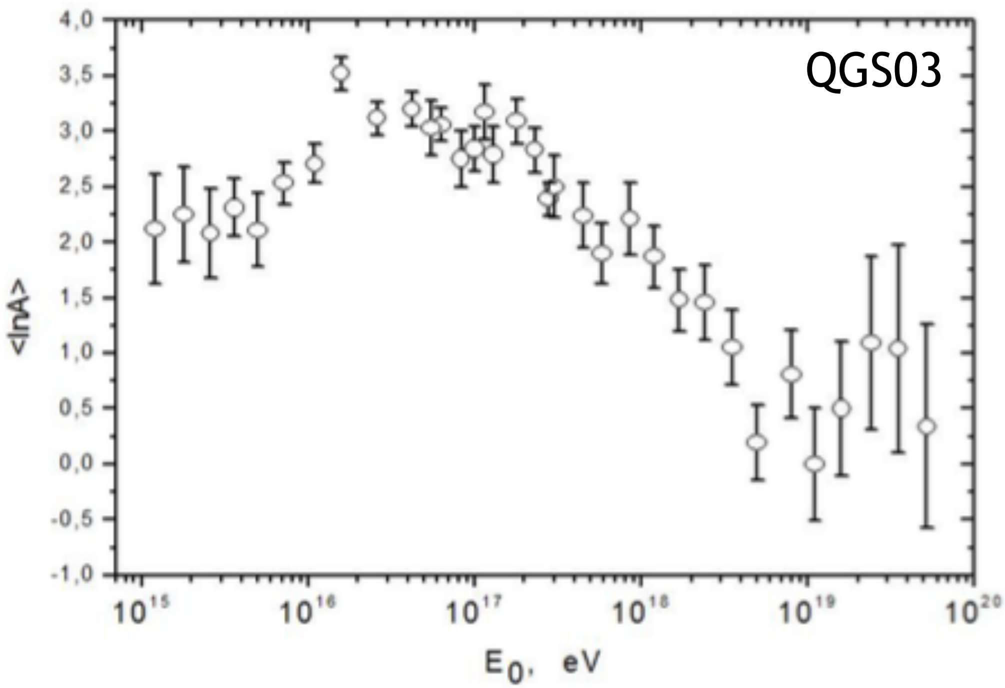

- changing mass across the range
- peak ~ 0.8-2 10^{17} eV
- agreement among different analysis methods (X_{max}, $\sigma(X_{max})$, muons, etc.)

Telescope Array

1400 m a.s.l. [880 g cm^{-2}]
507 SD, 1.2 km grid, 700 km^{2}
16 TALE counters, 400 m grid
3 FD (BR,LR,MD/TALE)

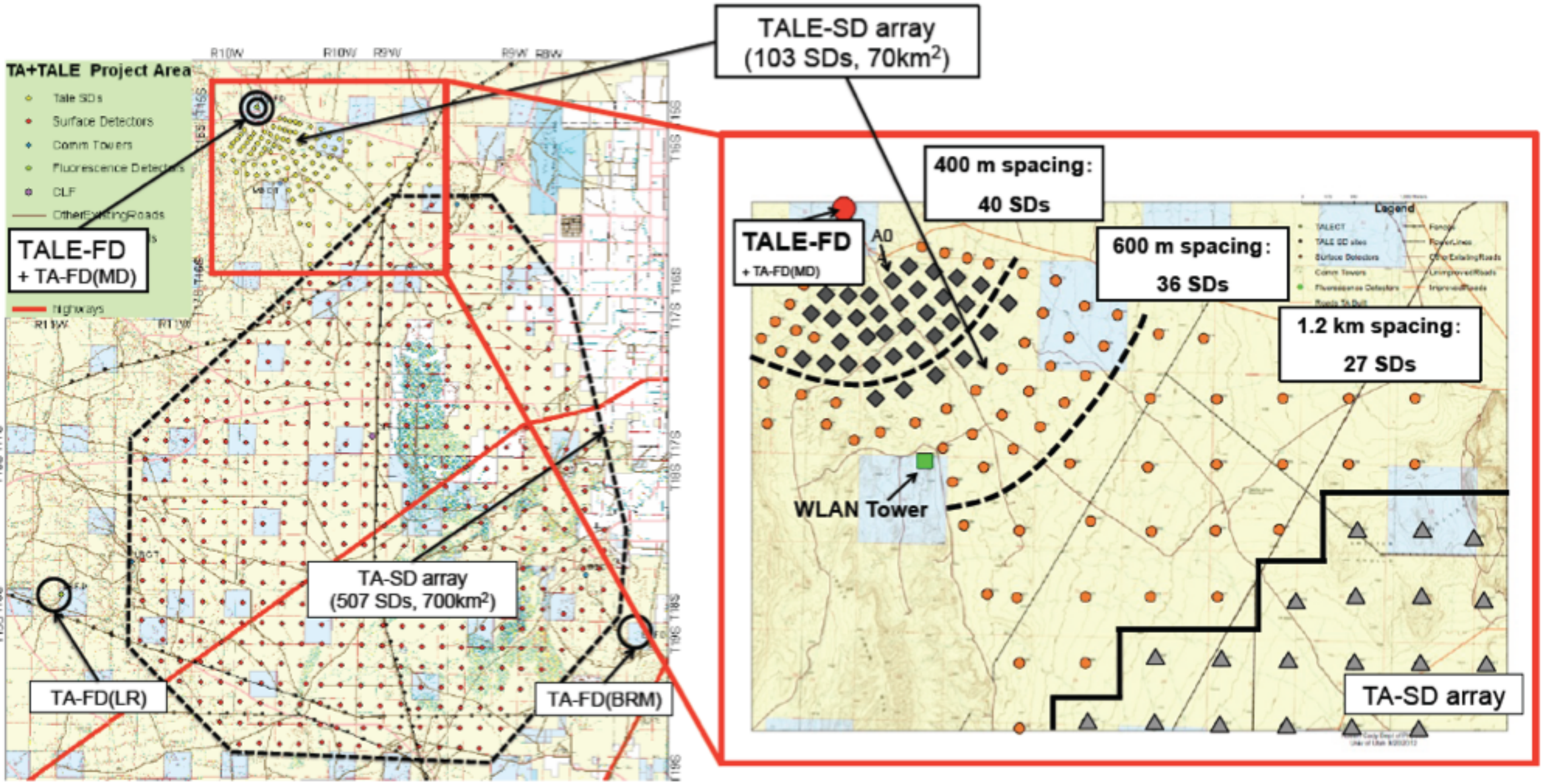

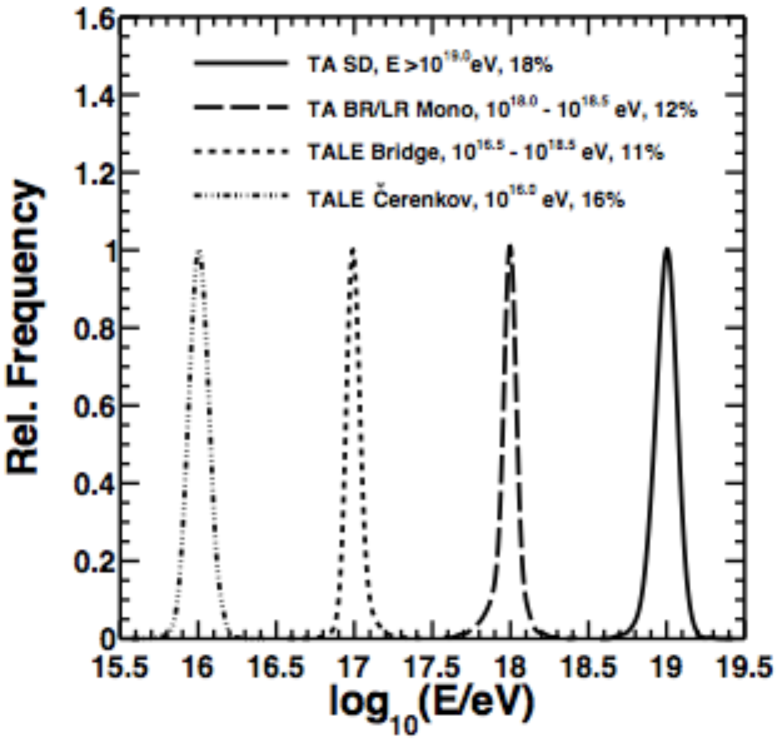

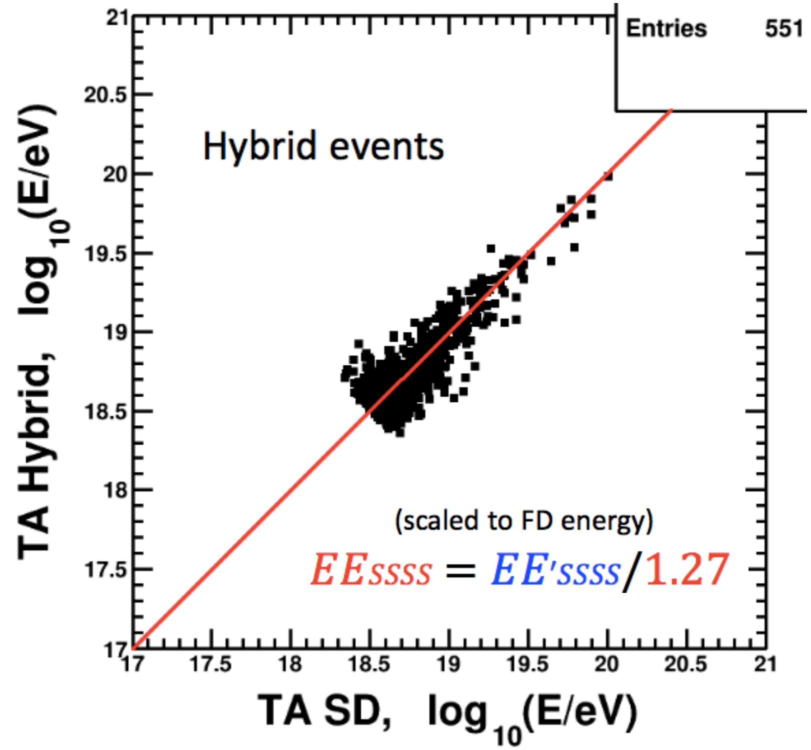

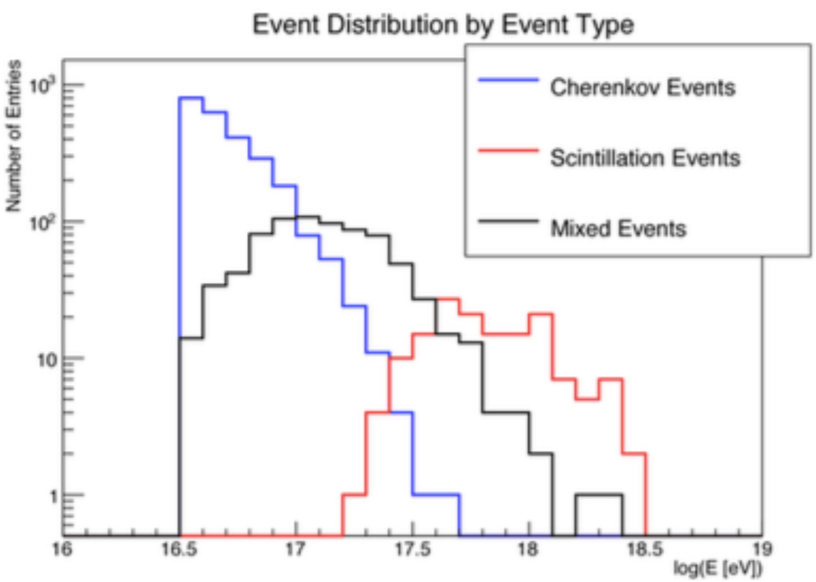

4 different data sets

SD alone $>10^{19}$ eV

FD-Mono $>10^{17.2}$ eV

TALE-FD $10^{16.5}$-10^{19} eV

TALE-Ch $10^{15.6}$-$10^{17.7}$ eV

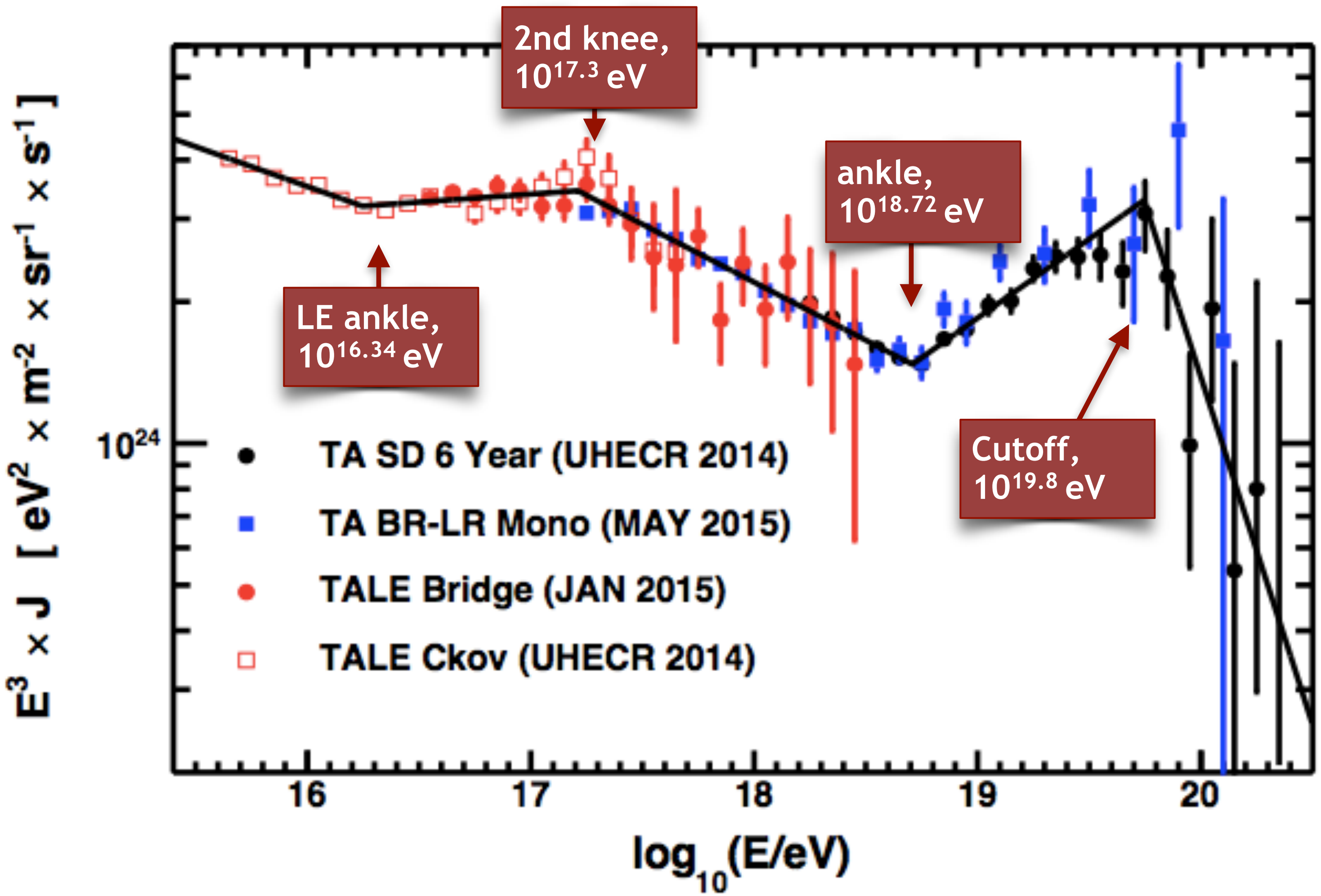

- 4.8 orders of magnitude spectrum, 4 spectral features
- thanks to TALE, a clear 2nd knee is visible at ~1.5 10^{17} eV and a low energy ankle appears at 1.8 10^{16} eV
- ankle at 5.2 10^{18} eV cutoff at 6.3 10^{19} eV (6.5σ)

Telescope Array - composition

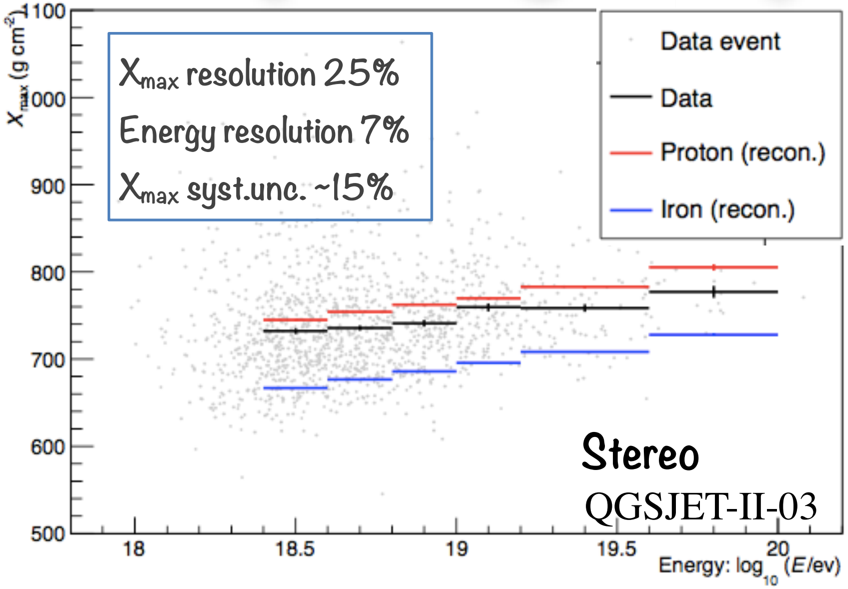

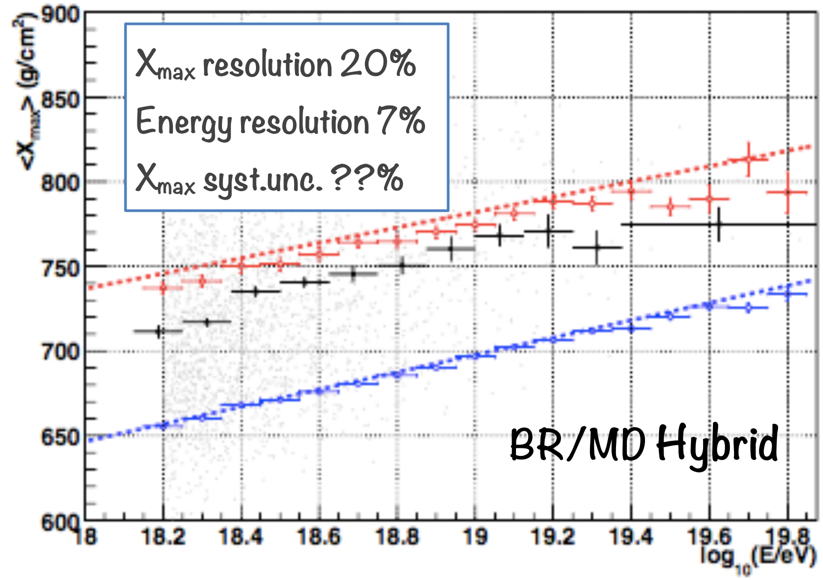

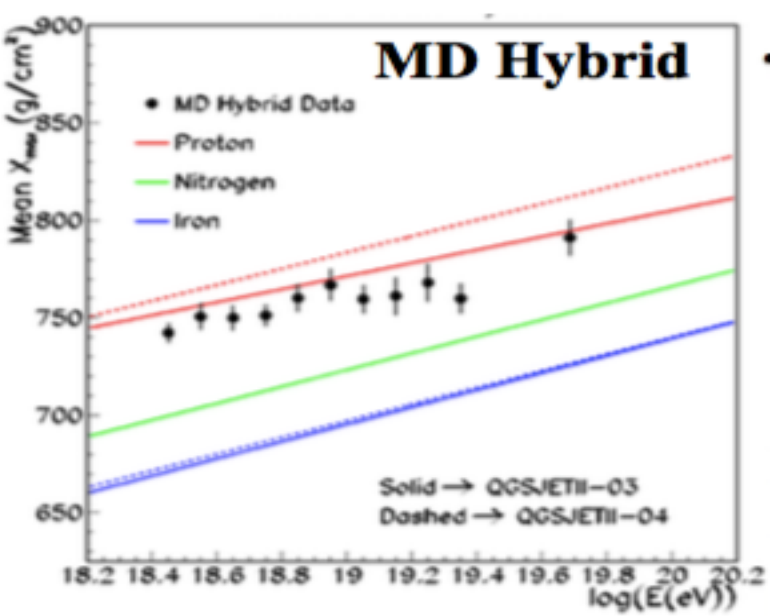

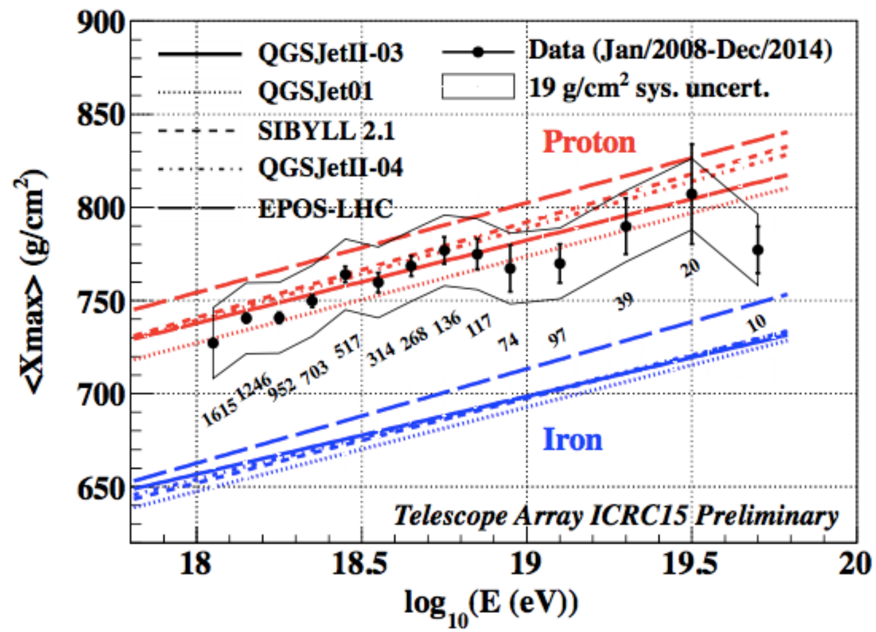

Telescope Array - interpreting the energy spectrum

Hypotheses

- Pure proton, $E > 10^{18.2}$ eV
- Injection spectrum $E^{-\gamma}$, $E_{max} = 10^{21}$ eV
- Source density $(1 + z)^{m}$ (per comoving unit volume)
- Energy losses with CMB and IRB.
- Propagation code: TransportCR [checked by CRPropa]
- Propagation without considering magnetic fields ($B_{IGMF} < \sim 0.1$ nG)

→ Source distance: $Z < \sim 0.7$

- data compatible with pure proton model
- constraints on fit parameters

  $\gamma = 2.18 - 0.14 + 0.08$ (stat.+sys.)

  $m = 6.8 - 1.1 + 1.6$

  $\Delta \log_{10} E = -0.04$ (-9%) $- 0.03 + 0.04$

  X^2_{min}/d.o.f.= 18.0/17
- z_{min} upper limit (no sources with $z < z_{min}$)

  $z_{min} = 0.01$ (~40 Mpc) 99.7% C.L.

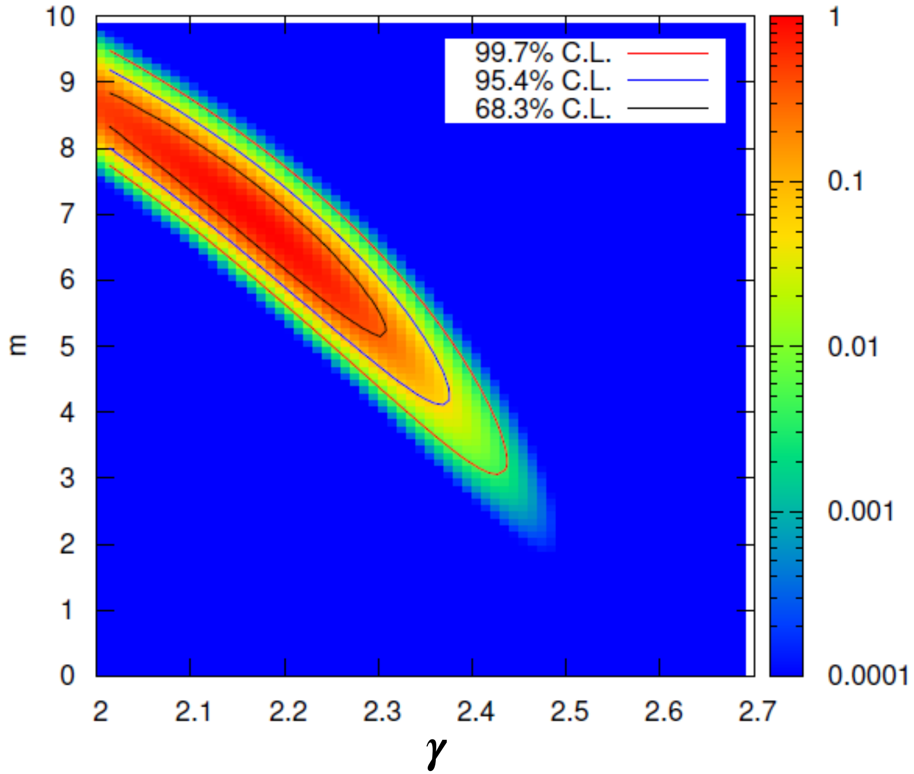

The Pierre Auger Observatory

1400 m a.s.l. [820 g cm^{-2}]
A ~ 3000 km^2, 1500 m grid
1660 water Cherenkov SD + 24 FD

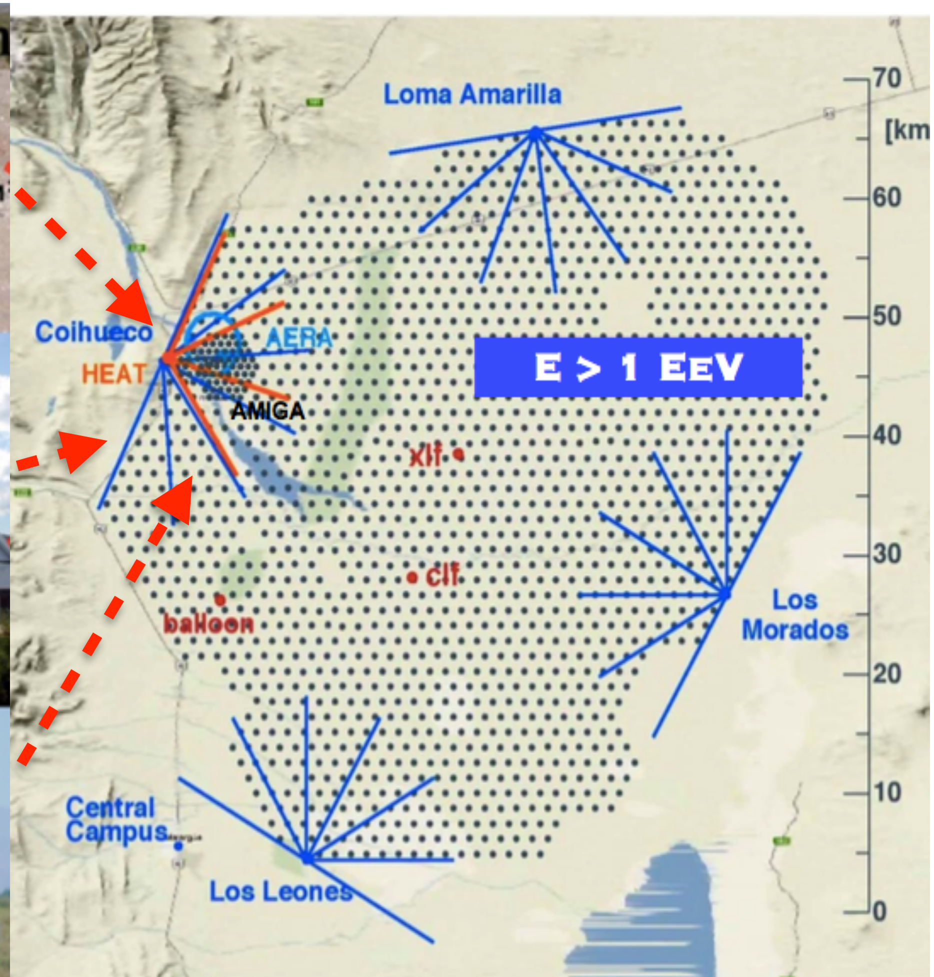

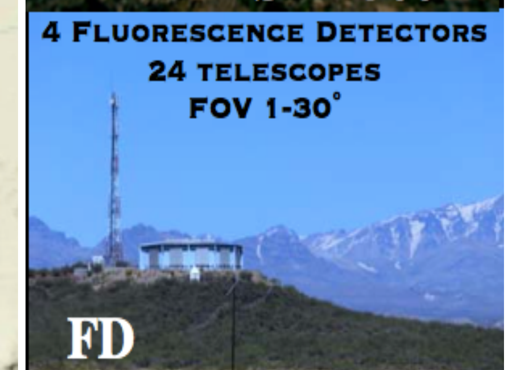

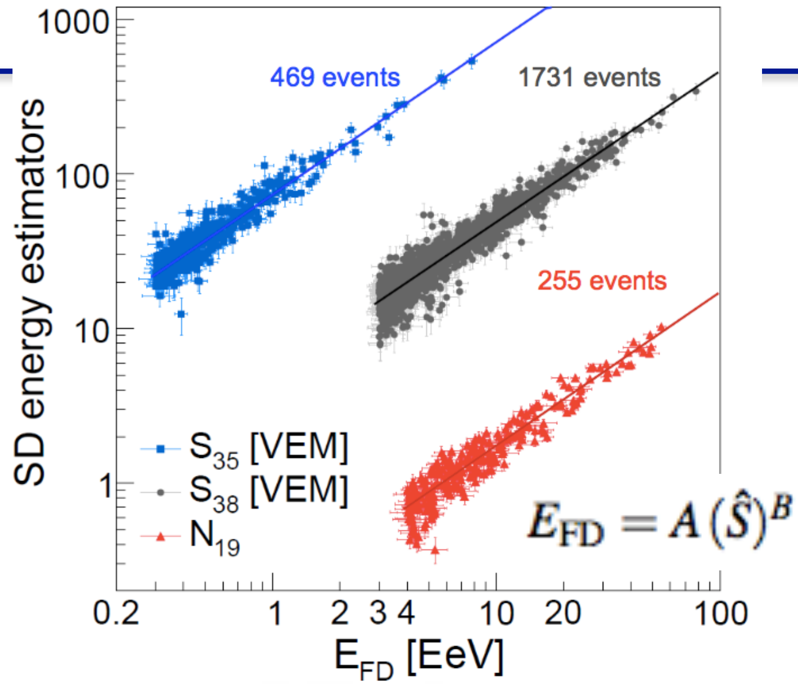

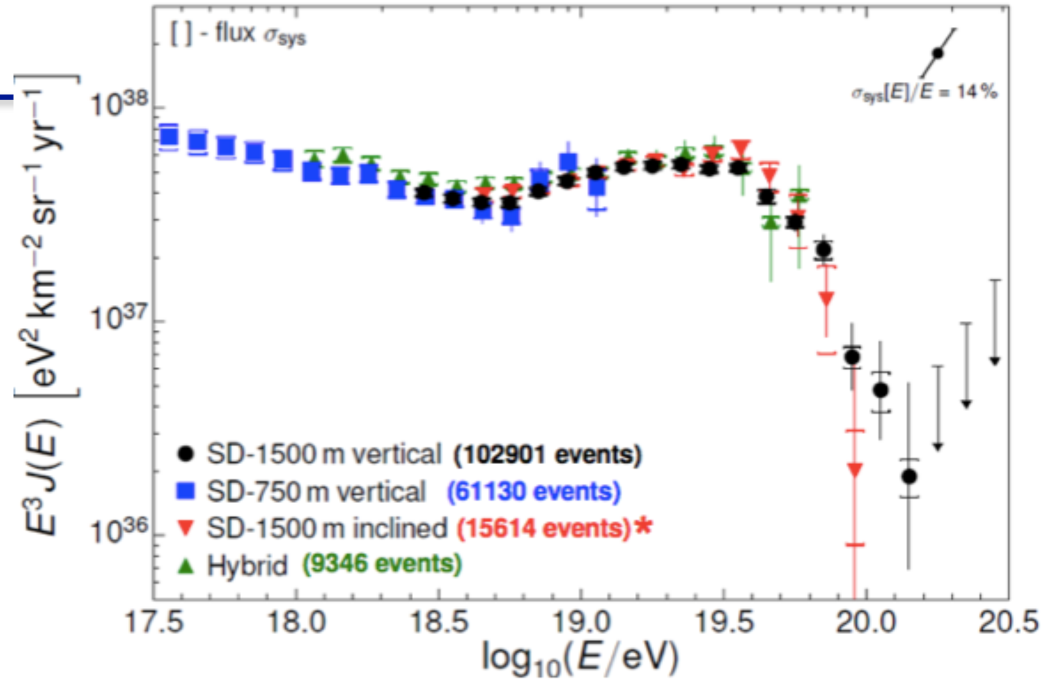

- FD used to set the energy scale of all data sets
- E_{FD} systematic uncertainty 14%, shared by SD
- the 4 independent spectra agree within systematics

	SD-1500 (θ<60⁰)	SD-1500 (θ>60⁰)	SD-750 (θ<60⁰)
Energy resolution	*(15.3 ± 0.4)%*	*(19 ± 1)%*	*(13 ± 1)%*
Flux syst. uncertainties	*5.8%*	*5%*	*14% (<7%) at 0.3 (3) EeV*

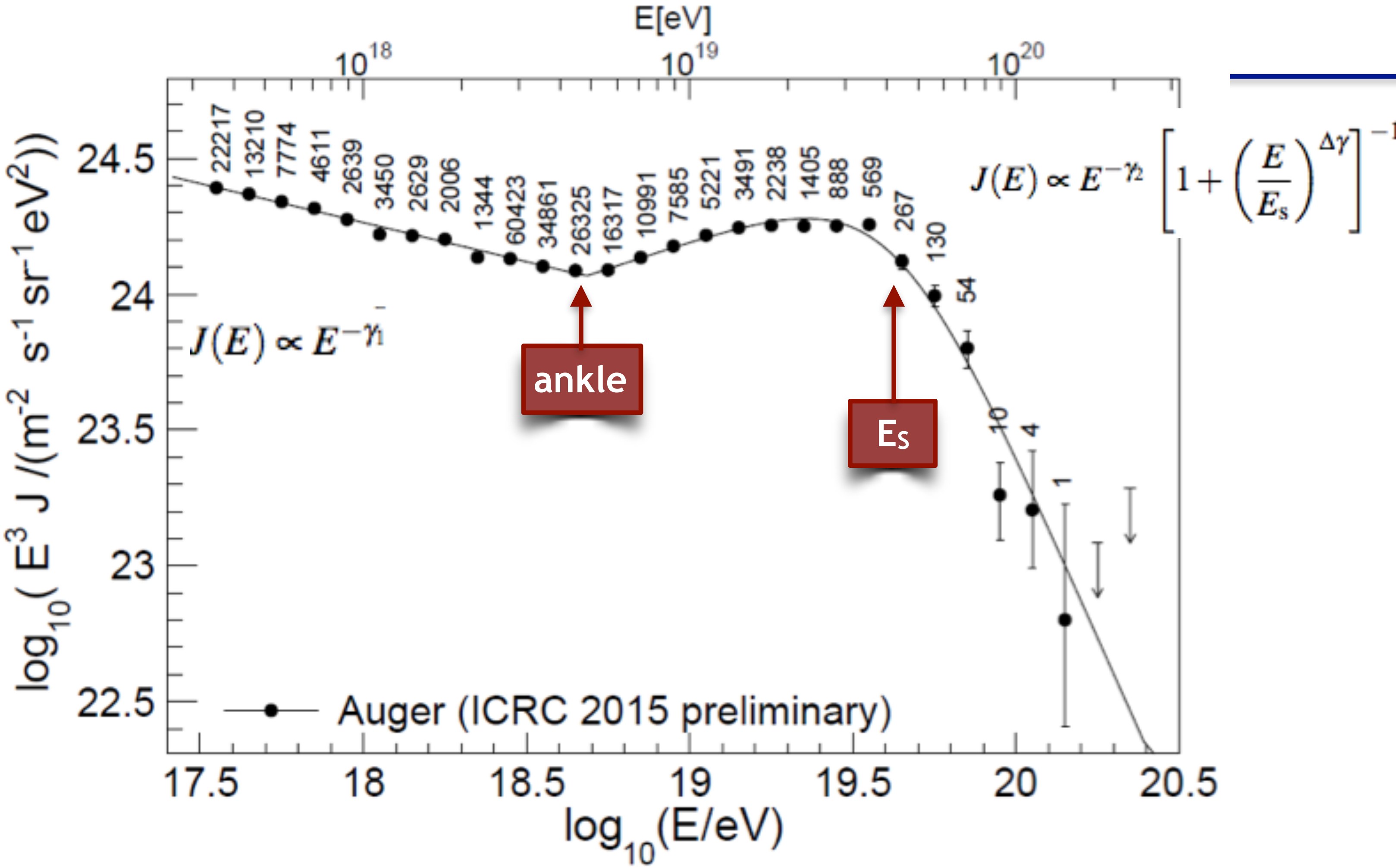

- ankle observed at E_{ankle}= 4.8 10^{18} eV
- cut-off clearly observed (>20σ significance)
- fitting model: power law below the ankle+power law with smooth suppression above
- Es=4.2 10^{19} eV, $E_{1/2} = (2.48 \pm 0.01)\times10^{19}$ eV

Auger - composition

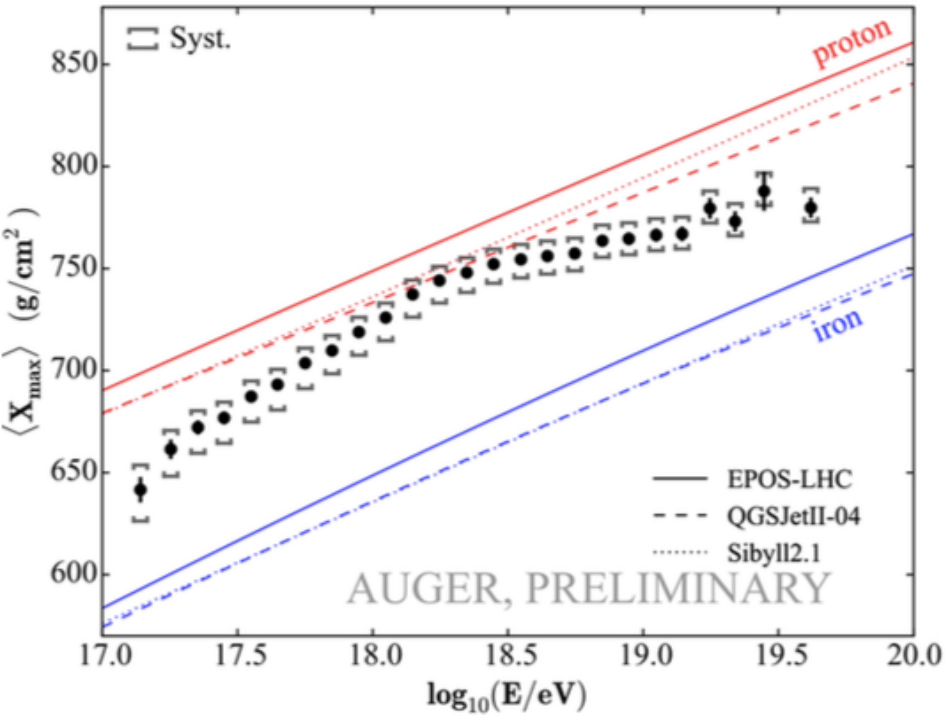

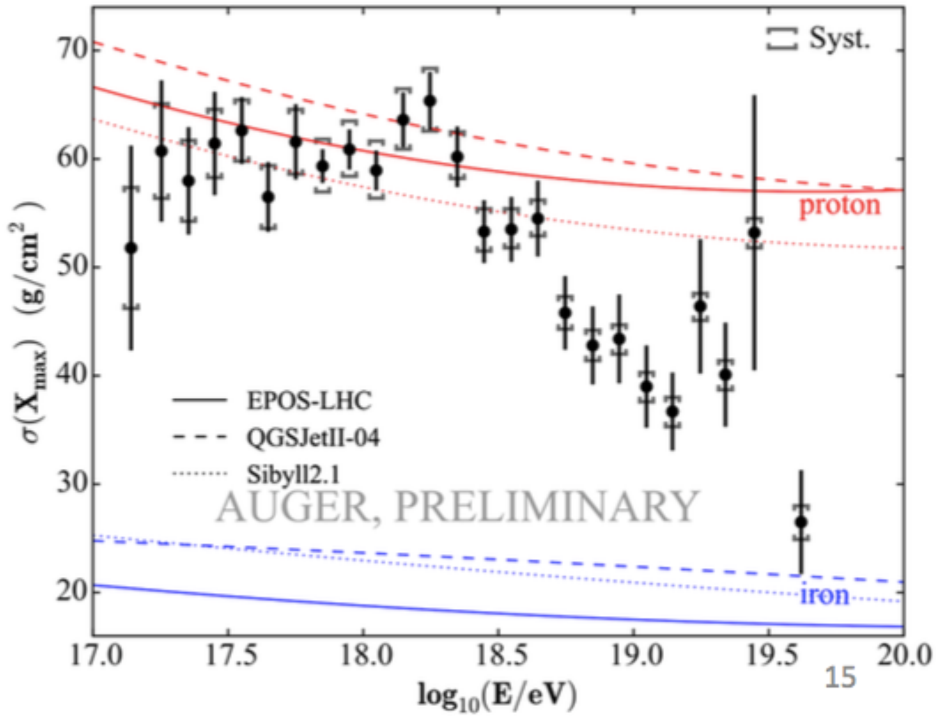

- measurement extended down to 3 10^{17} eV thanks to HEAT
- $E_{1/2} = (2.48 \pm 0.01) \times 10^{19}$ eV

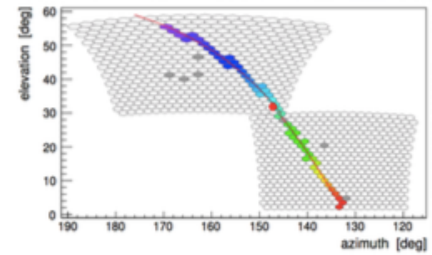

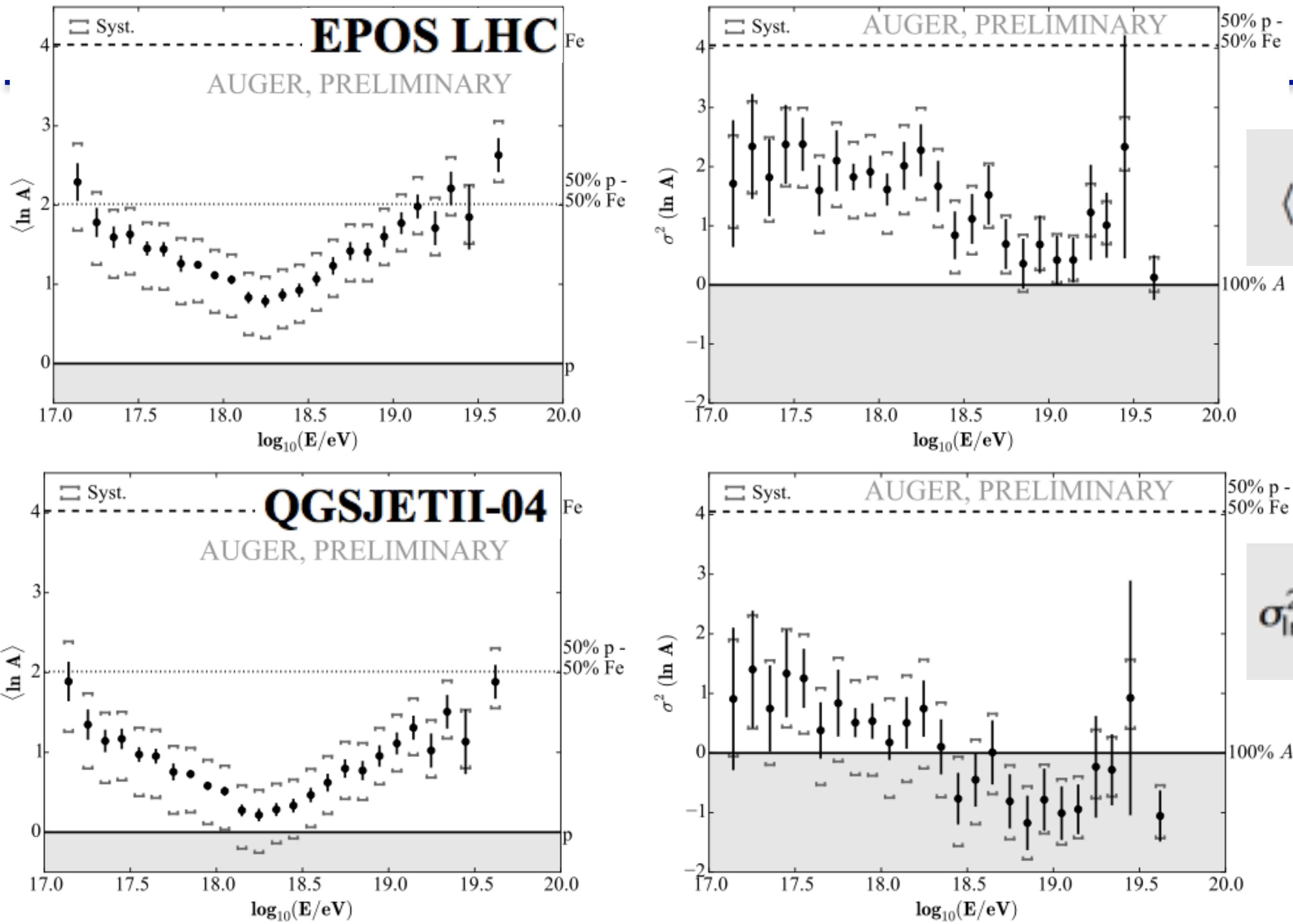

$$\langle \ln A \rangle = \frac{\langle X_{max} \rangle - \langle X_{max} \rangle_p}{f_E}$$

info on average composition

$$\sigma^2_{\ln A} = \frac{\sigma^2(X_{max}) - \sigma^2_{sh}(\langle \ln A \rangle)}{b\sigma^2_p + f^2_E}$$

dispersion of masses at Earth: spread at the sources AND propagation effects

- both post-LHC models suggest heavier composition at lower energies , lightest around 2 10^{18} eV, heavier again towards highest energies
- unphysical results with QGSJet-04 for the second moment of lnA

Auger : muon production depth

$$\langle \ln A \rangle = \ln 56 \frac{X^p_{max} - \langle X_{max} \rangle}{X^p_{max} - X^{Fe}_{max}}$$

$$\langle \ln A \rangle^\mu = \ln 56 \frac{X^{\mu p}{}_{max} - \langle X^\mu{}_{max} \rangle}{X^{\mu p}{}_{max} - X^{\mu Fe}{}_{max}}$$

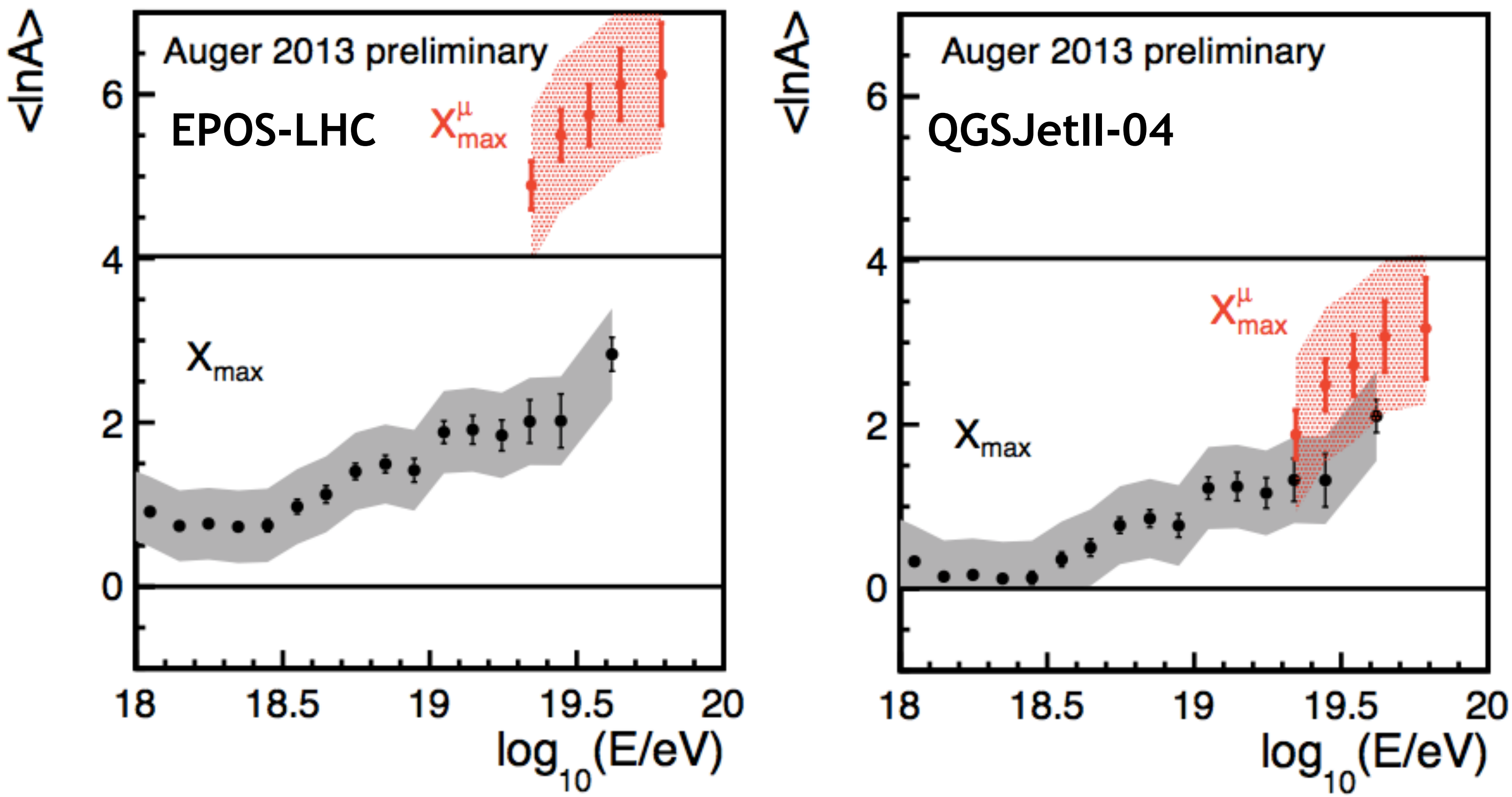

the consistency between the two Xmax can help to constrain hadronic interaction model

Auger

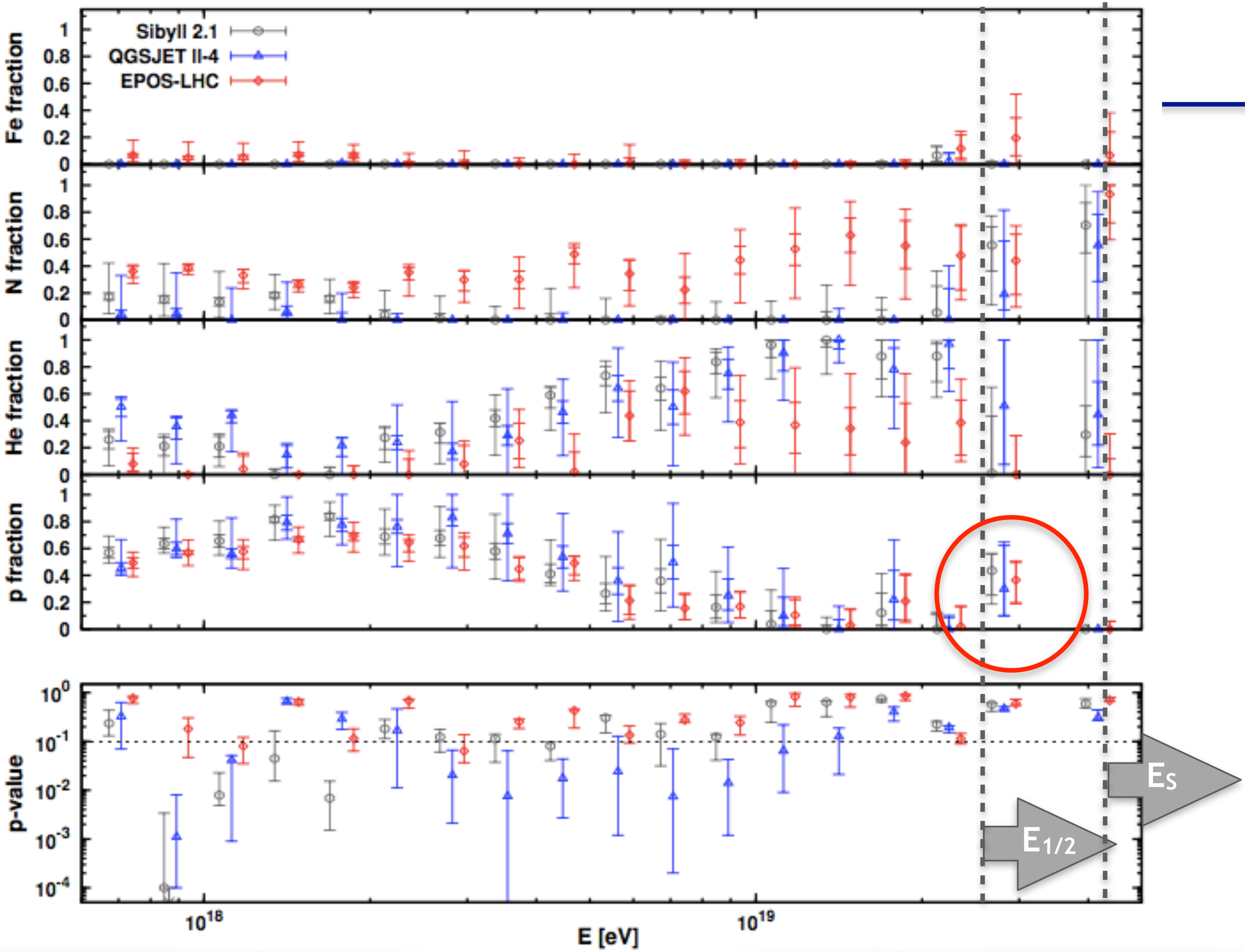

- data better reproduced with a mixture of p+He+N+Fe
- p fraction increases to >60% at the ankle, drops near 10^{19} eV, maybe rising again at higher energies
  —> EG according to anisotropy limits !
- no significant contribution of Fe

Auger - interpreting the energy spectrum

Hypotheses

- identical sources homogeneously distributed
- Injection of H,He,N,Fe, injection spectrum
- Photodis.cross section + EBL (far IR)
- Propagation code: CRPropa,SimProp - no magnetic fields

$$\frac{dN_{inj,i}}{dE} = \begin{cases} J_0 p_i \left(\frac{E}{E_0}\right)^{-\gamma}, & E/Z_i < R_{cut} \\ J_0 p_i \left(\frac{E}{E_0}\right)^{-\gamma} \exp\left(1 - \frac{E}{Z_i R_{cut}}\right), & E/Z_i > R_{cut} \end{cases}$$

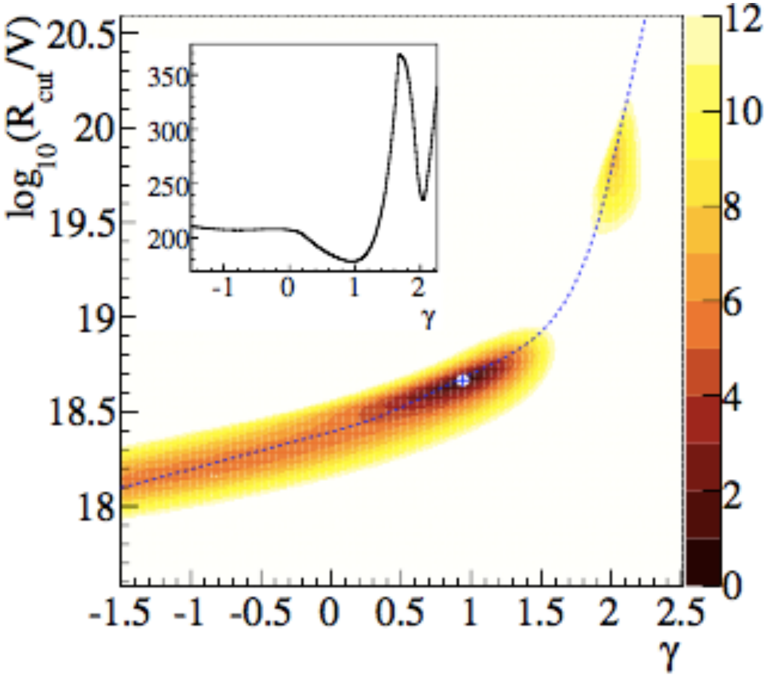

- hard injection (γ~1) and low cutoff (R_{cut}<$10^{18.7}$ eV) favored
- γ~2 strongly disfavoured by X_{max} distribution width
- EPOS-LHC favoured over Sibyll2.1 and QGSJet04

- result mainly due to narrow X_{max} distributions
- 1st minimum very sensitive to propagation models
- better fit for lower photodisintegration rates and/or lower E,X_{max} in data (within syst.unc.)

X_{max} distributions at best fit

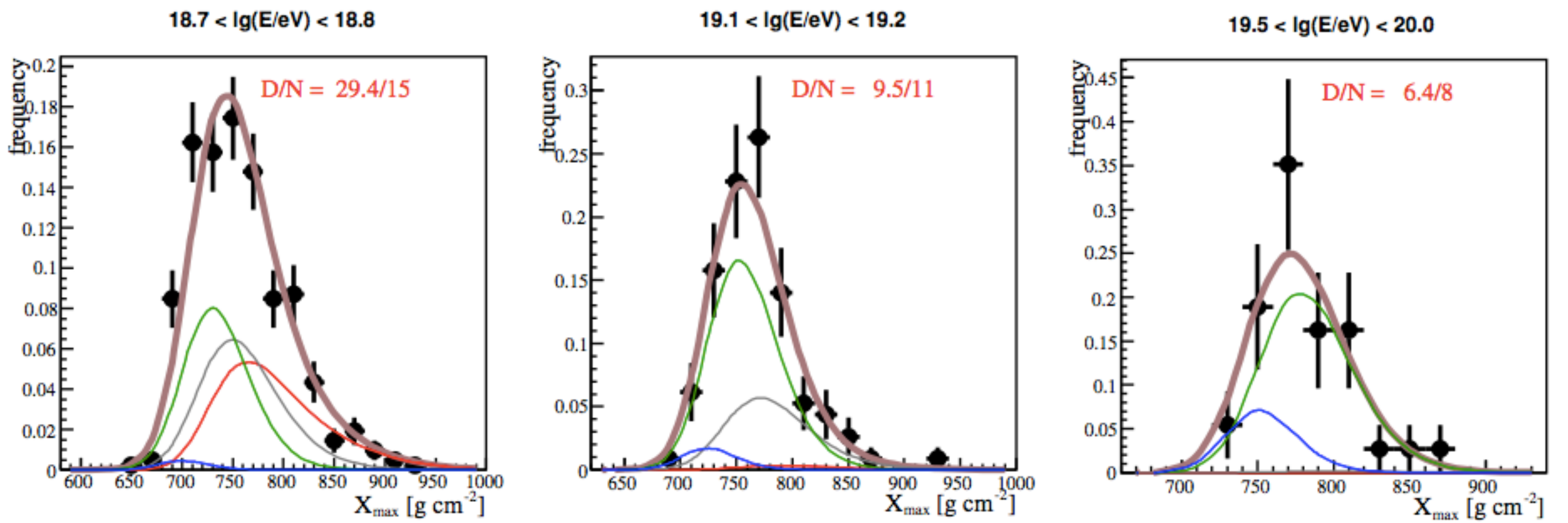

- red: $A = 1$
- gray: $2 \leq A \leq 4$
- green: $5 \leq A \leq 22$
- blue: $A \geq 23$
- **thick brown**: total
- **black dots**: Auger data

Auger / Telescope Array comparison

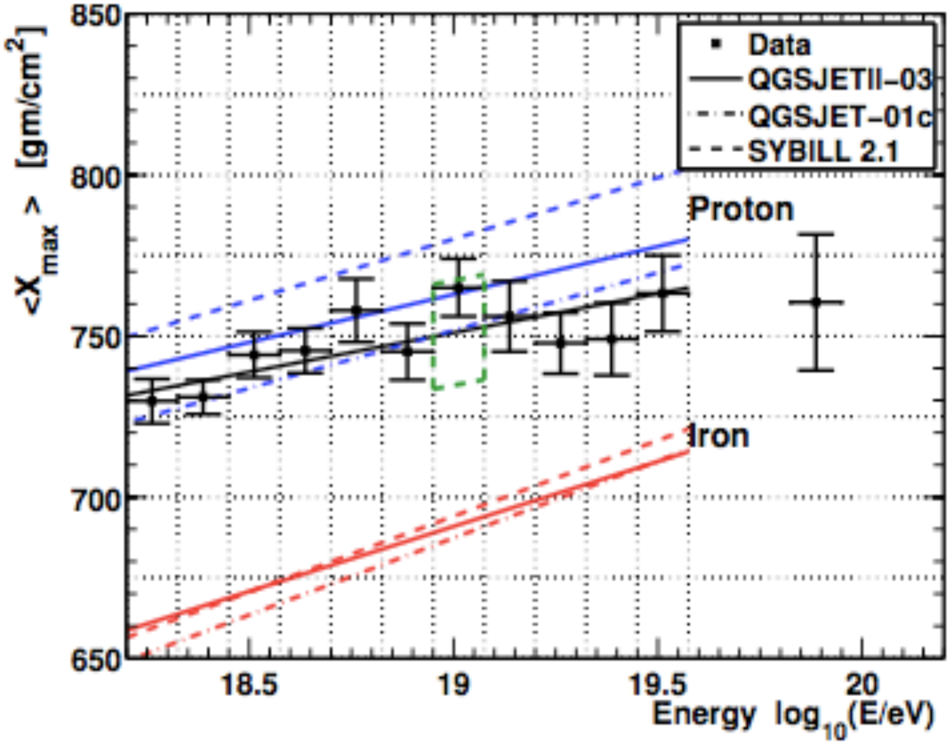

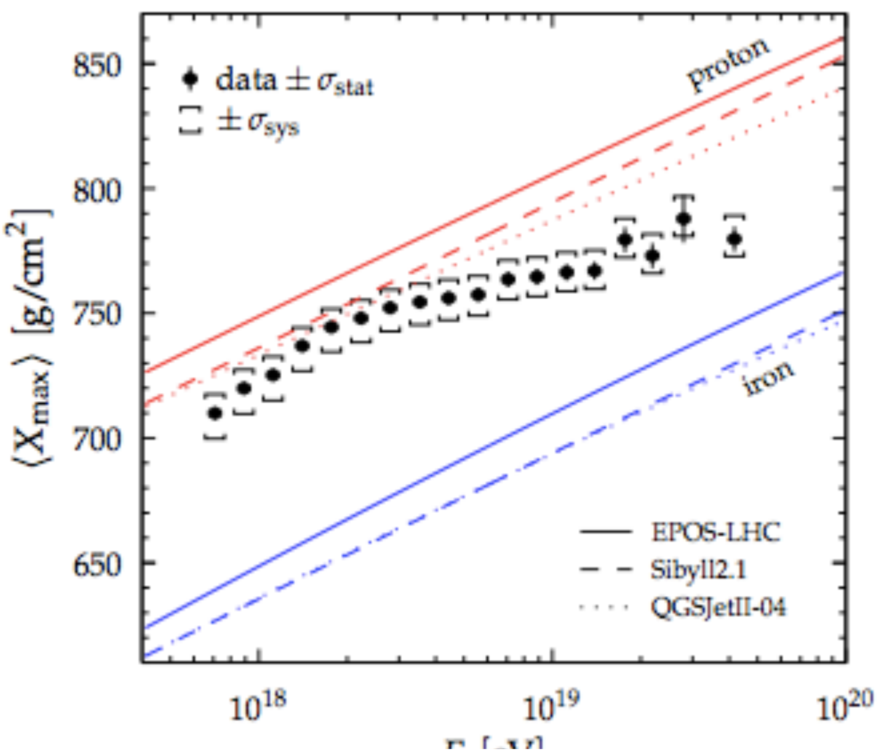

TA:

- maximize statistics
- result: "$\langle X_{\max}\rangle$ in detector"
- compare to: simulations including detector effects

Auger:

- minimize measurement bias
- result: "$\langle X_{\max}\rangle$ in atmosphere"
- compare to: simulations at generator level

Auger / Telescope Array comparison

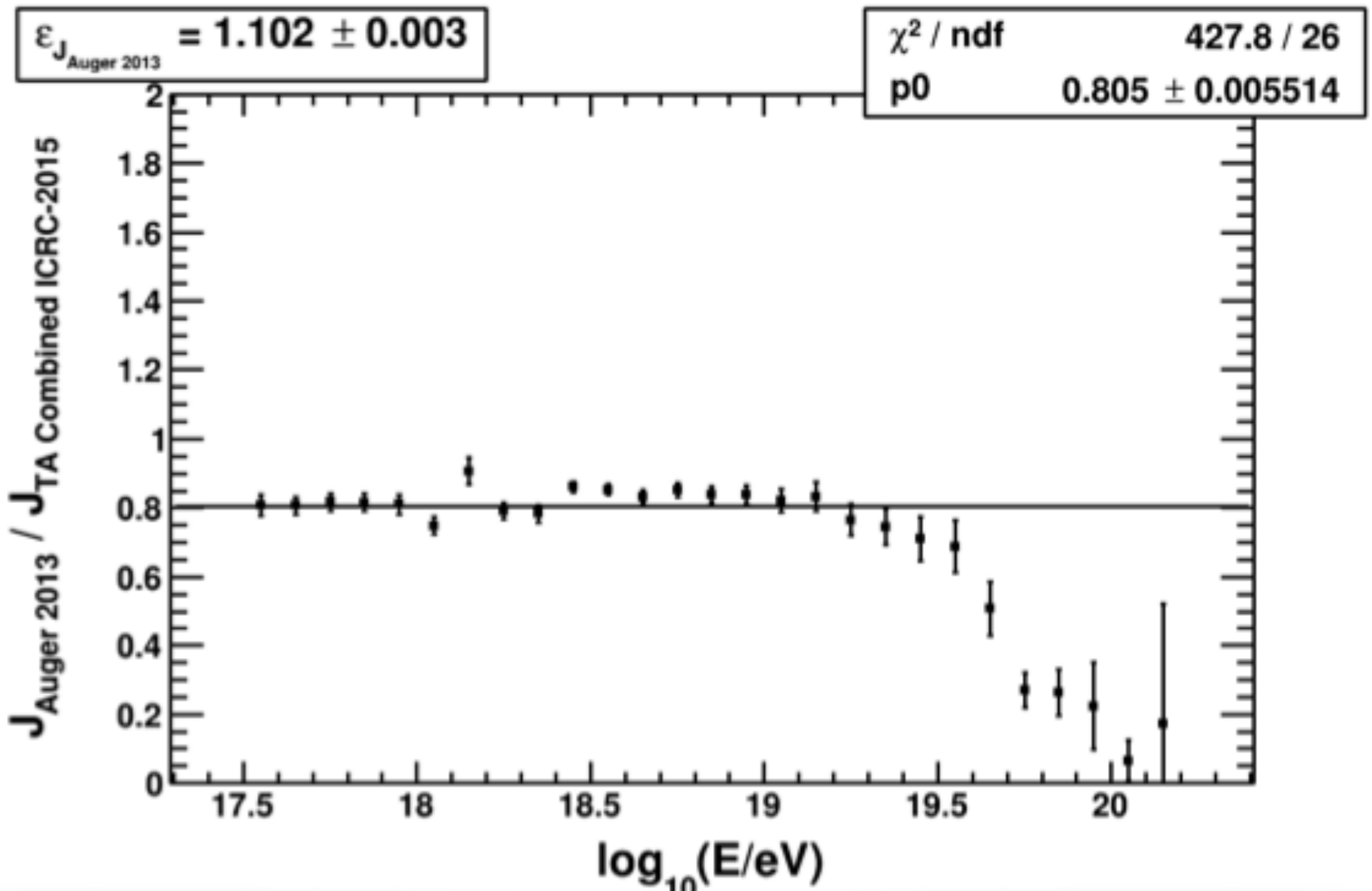

- 10% shift in energy would bring the two in agreement up to $10^{19.3}$ eV
- large discrepancy above

Auger : declination dependence of energy flux

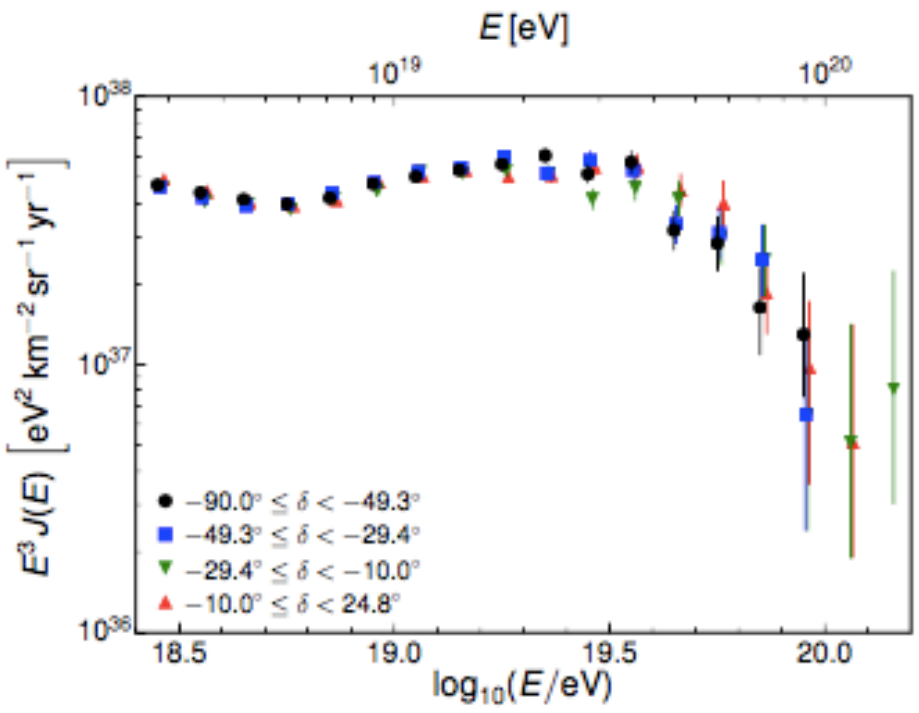

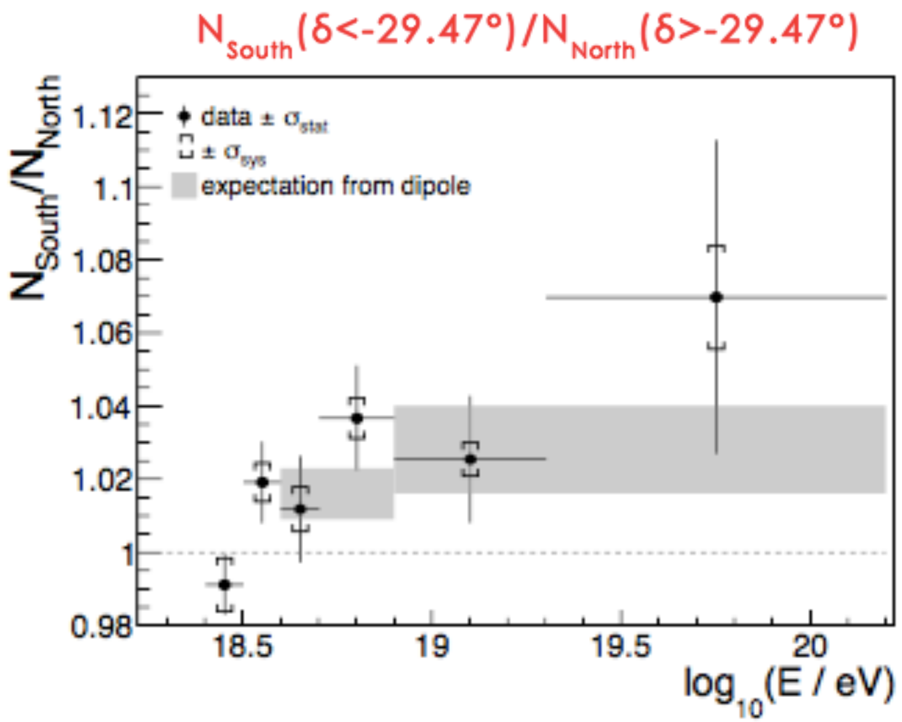

- no indication of a declination-dependent flux (<5%below E_s, <13% above)
- differencies between Auger and TA in the suppression region not explained
- the differences found between the measurements in two separate declination bands are compatible with the variations expected from a dipolar modulation of the flux.

Auger / Telescope Array comparison

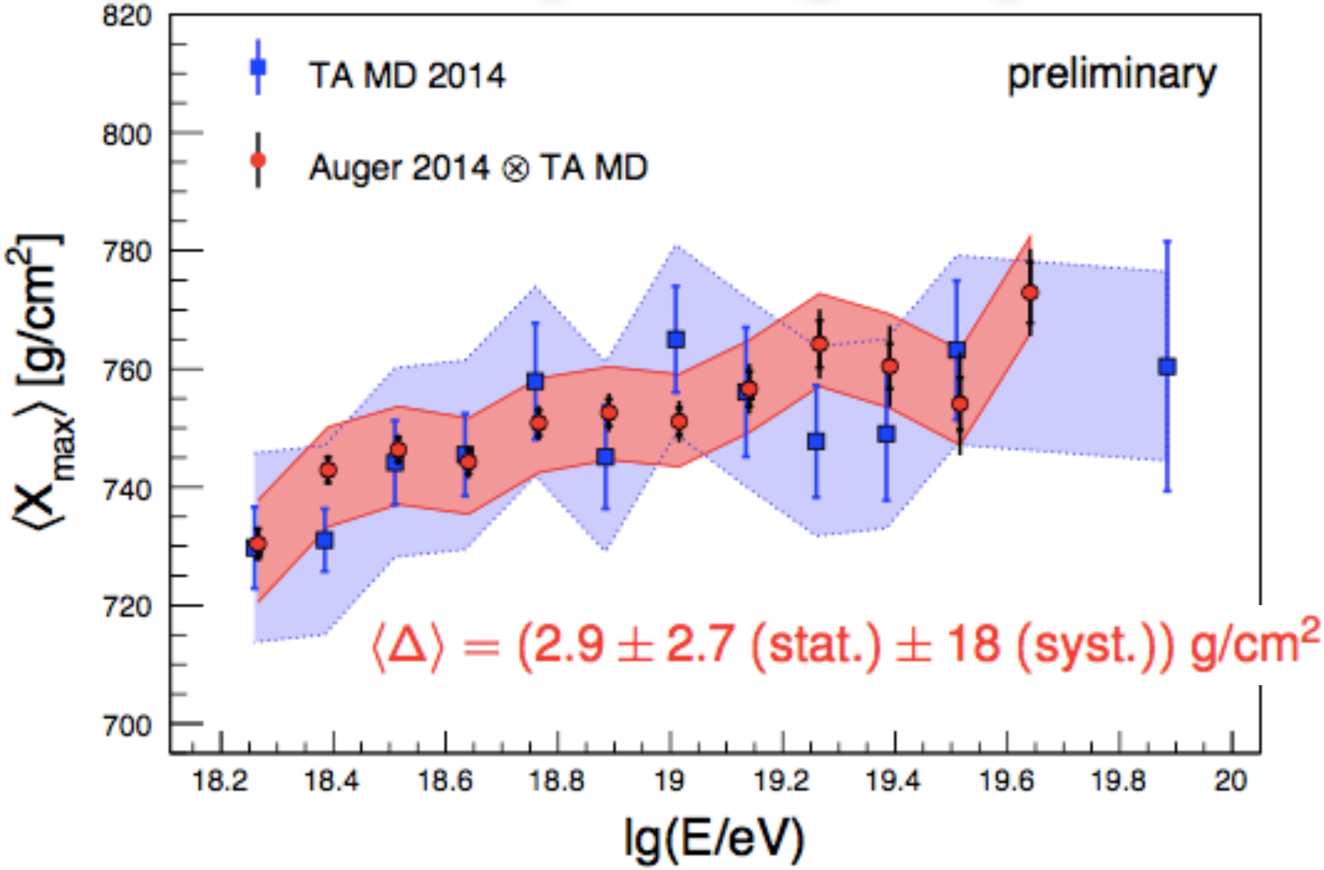

Simulated composition according to Auger result fed to the TA MC simulation and analysis

- the two data sets are in excellent agreement even without accounting for systematics on X_{max}
- TA cannot distinguish between proton or "Auger mixed" composition with the current level of uncertainties
- inclusion of difference in energy scale still to be included (foreseen effect only few g cm^{-2})

Large Scale Anisotropy above PeV

Sky map of the CR flux **E > 8 EeV**

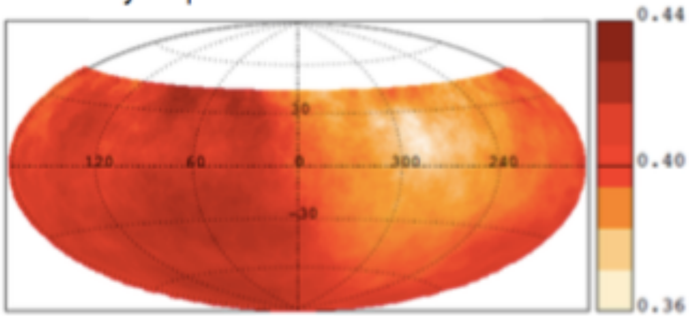

Auger (7.3 ± 1.5)% (p=6.4 10^{-5})

Sky map of the CR flux **E > 10 EeV**

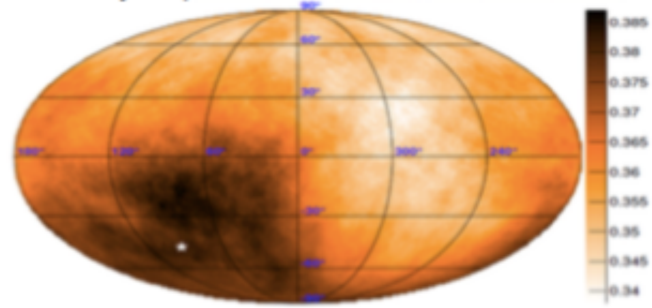

Auger and TA (6.5 ± 1.9)% (p=5 10^{-3})

Dipole Amplitude

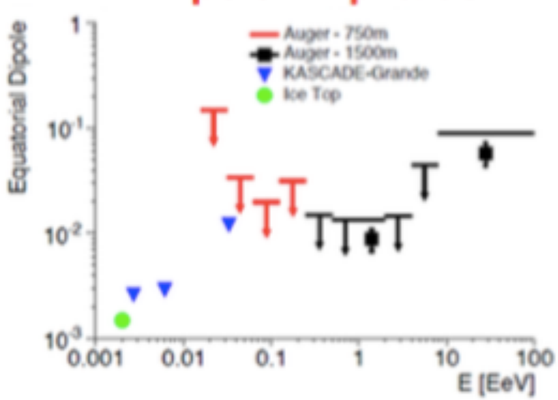

Phase

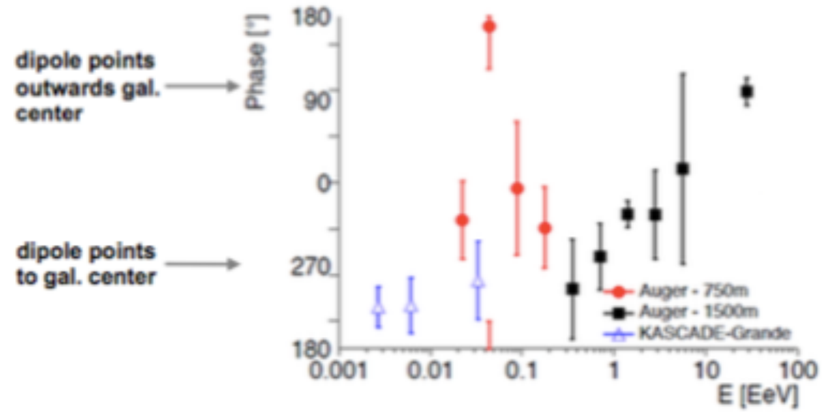

- upper limits on amplitudes are at the % level over a wide energy range
- 5.7% equatorial dipole amplitude above 8 EeV from Auger analysis
- phase transition : increasing contribution of EG cosmic rays

Anisotropy... compilation

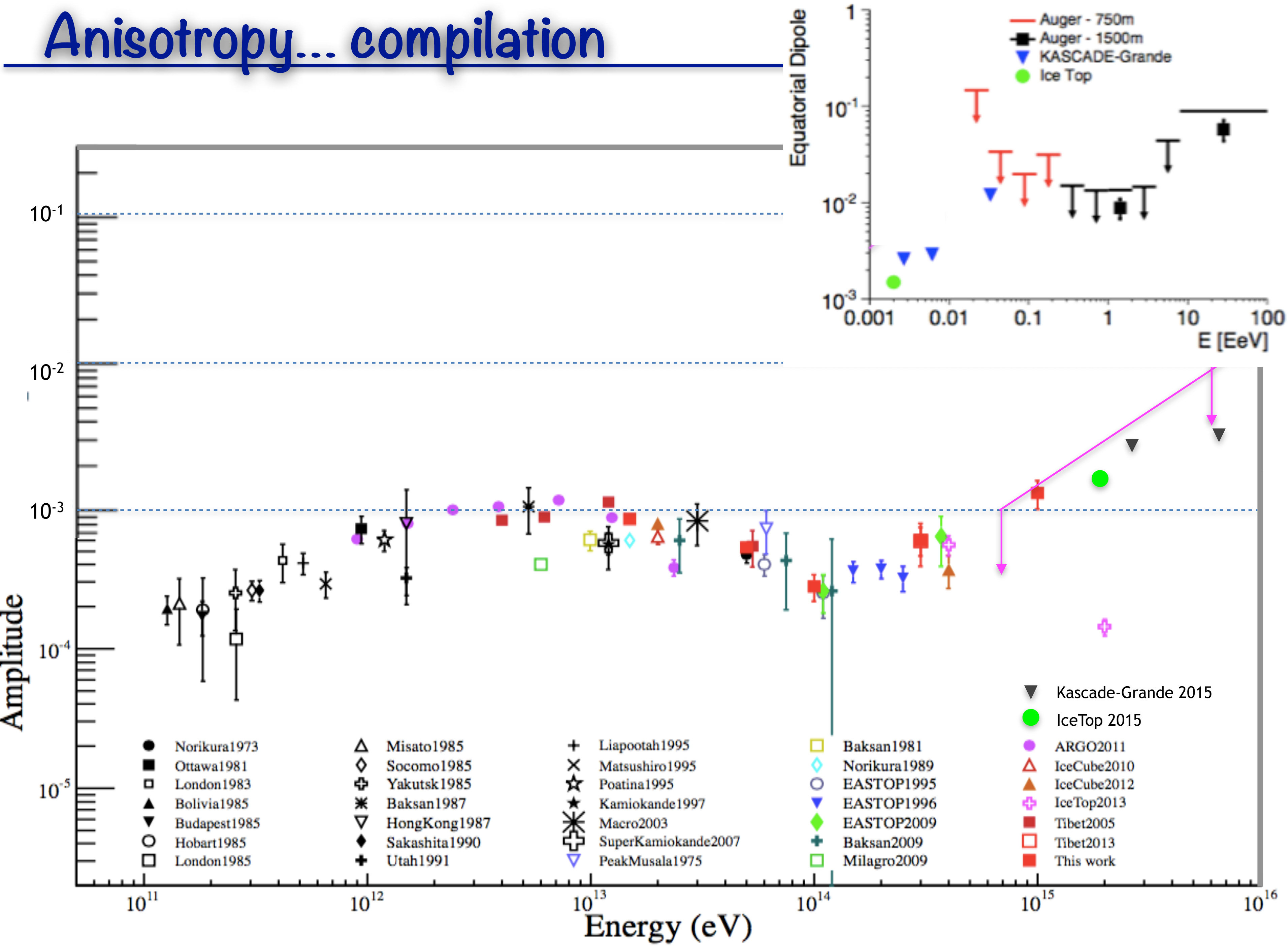

Point source searches

- astrophysical origin of UHE sources (top-down models strongly disfavoured)
- look at highest energies (as deflections proportional to Z/E)
- look close (as cutoff is seen for E> 40 EeV)

  - No significant excesses were found
  - Two medium scale spots

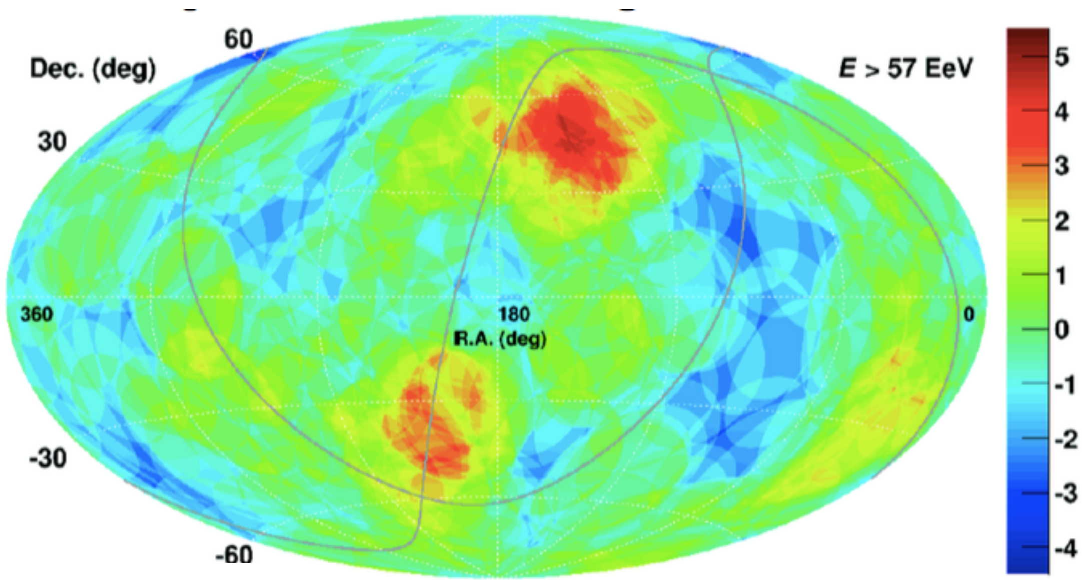

TA

7 years, 109 Events (> 57 EeV)

Northern Hemisphere: hot spot seen by TA (3.4 σ) near the Ursa Major cluster

Auger

10 years 157 events (> 57 EeV)

Southern Hemisphere: hot spot seen by Auger (post-trial prob 1.4%) near to Cen A

Some conclusion from experimental data

1 knee region

- ✓ all particle knee ~4 10^{15} eV
- ✓ light component knee < PeV (Tibet), ~700 TeV, (Argo) a factor ~4 lower than Kascade

- ✓ 10^{-3}-10^{-4} LSA amplitudes found around TeV energies
- ✓ change of trend, already pointed out by EasTop and others, above 10^{14} eV

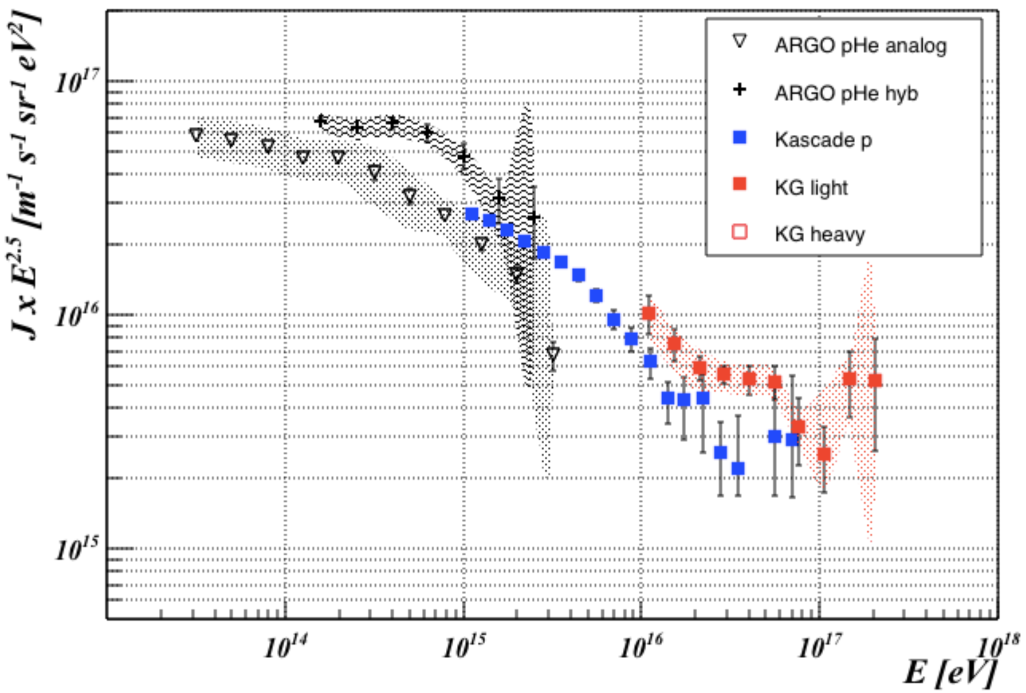

- different analysis, at different altitude
- comparison of systematics

Some conclusion from experimental data

2 **transition region : 10^{16}-10^{18} eV**

- ✓ good agreement of all experiments within systematics
- ✓ good superposition with UHE arrays
- ✓ concave region above 2 10^{16} eV
- ✓ steepening ~ 10^{17} eV

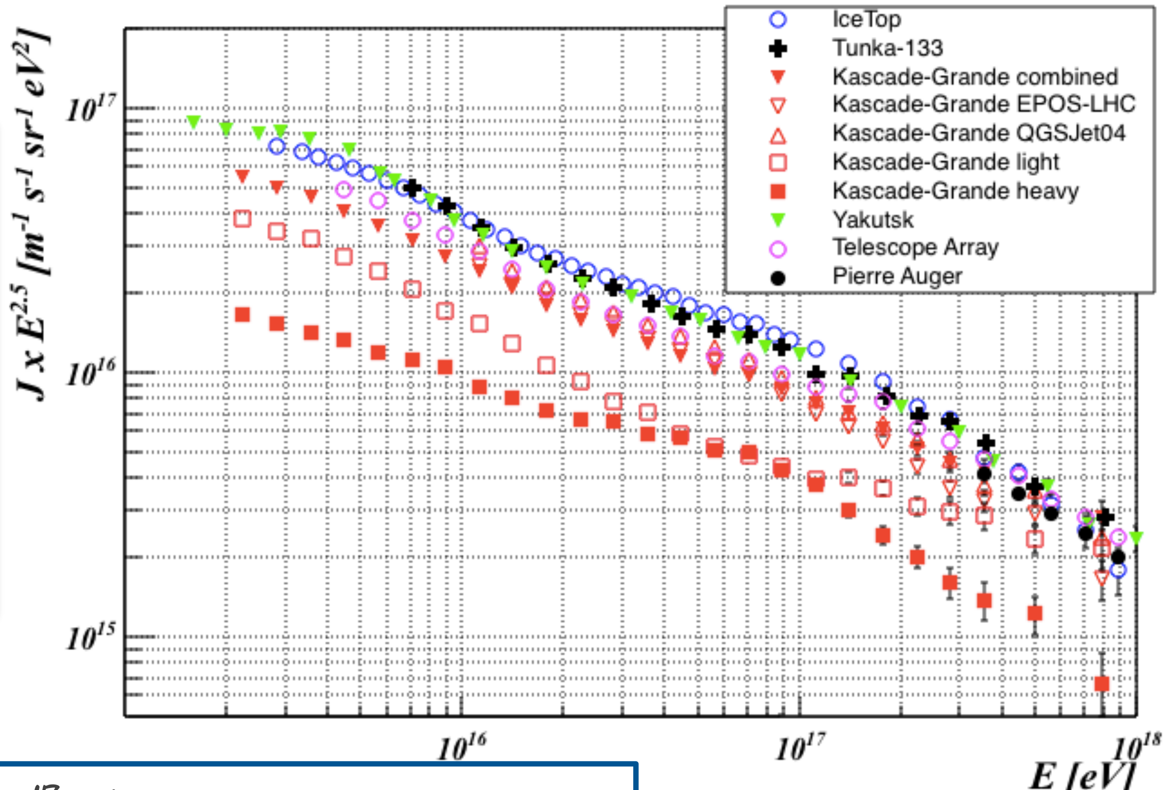

- ✓ evidence for a knee at ~ 8 10^{16}-10^{17} eV due to the heavy component
- ✓ ankle-like feature of the light component above 10^{17} eV

- ✓ between 10^{16} and 10^{18} eV, the equatorial dipole does not exceed ~ 10^{-2}

Some conclusion from experimental data

3 UHE region

- ✓ TA and Auger data agree in composition, but different interpretation is given
- ✓ Auger shows p-fraction ~60% ~$10^{18.2}$ eV, almost zero ~10^{19} eV
- ✓ Fe fraction always negligible, p fraction compatible with 10% at highest energies
- ✓ strong upper limits to primary photons
- ✓ absence of cosmogenic neutrinos disfavours pure p composition

- ✓ flux suppression and ankle clearly established
- ✓ difference in UHE flux between TA and Auger, not explained by declination dependence

- ✓ isotropic sky around 10 EeV
- ✓ no significant point source anisotropy
- ✓ hot spot in TA sky at 57 EeV, warm spot in Auger sky at 57 EeV

- poor statistics >3 10^{19} eV, need composition measurement above (TAx4, AugerPrime)
- importance of joint working groups, study of systematics

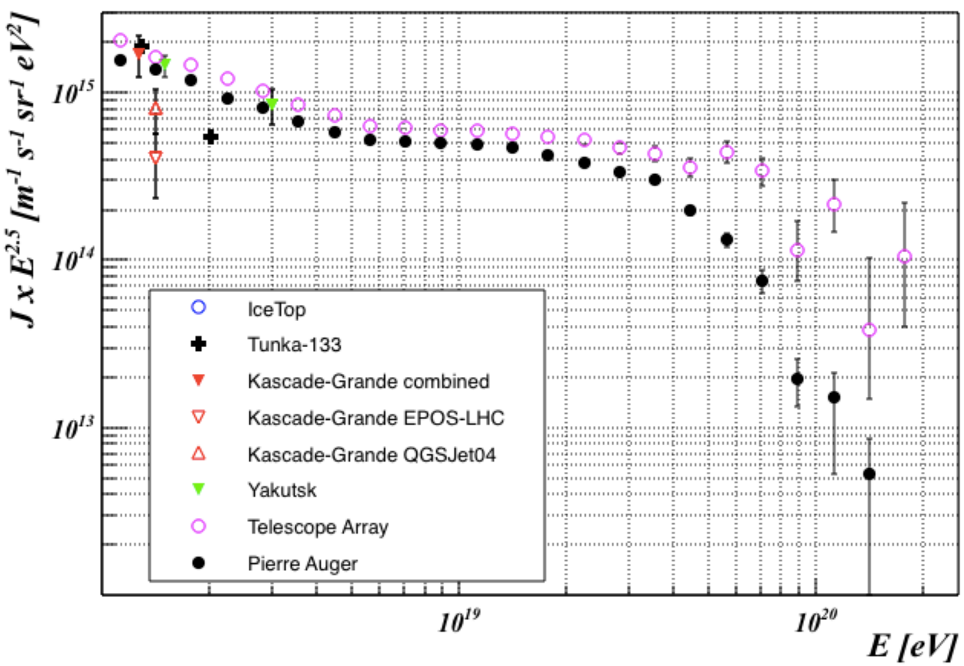

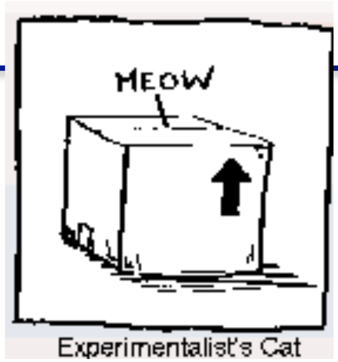

We need
...more data
...better control of systematics
... upgrades !

Joint effort among different collaborations is now a most welcomed reality
(...hopefully more to come) !

Backup slides

UHE: future upgrades

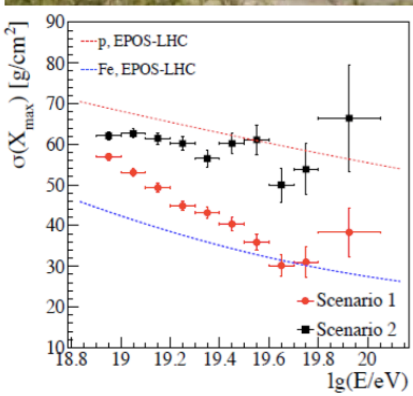

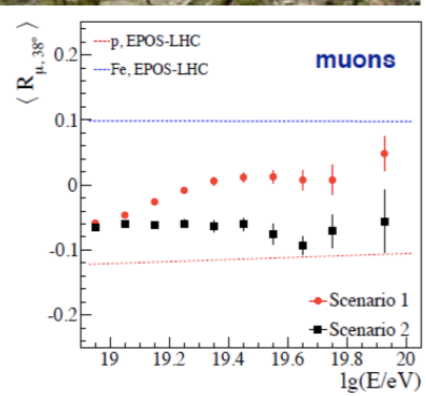

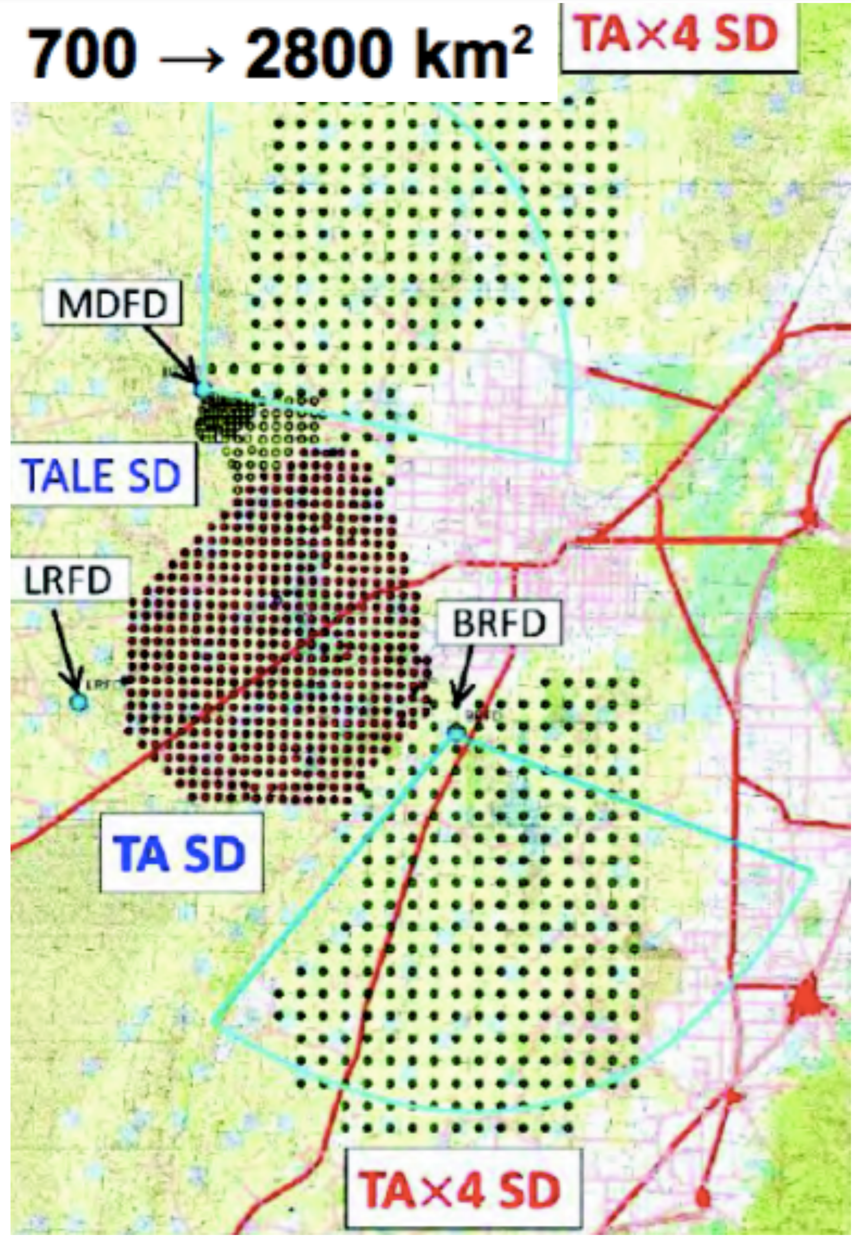

Photons

- to set limits on top-down mechanisms
- to search for GZK photons
- to fix the maximum photon fraction in the primary flux

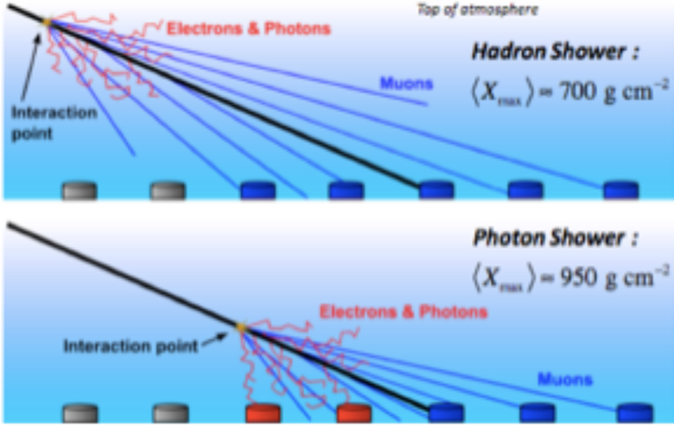

Exploit observable differencies between γ and hadrons

- γ EAS develop deeper in atmosphere: larger Xmax
- γ EAS look young: larger rise time, smaller radius of curvature

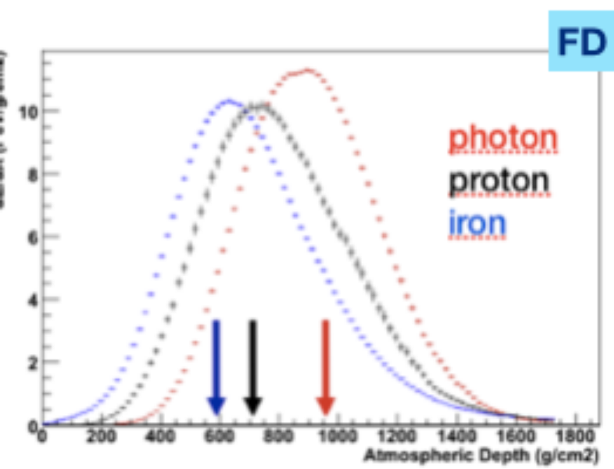

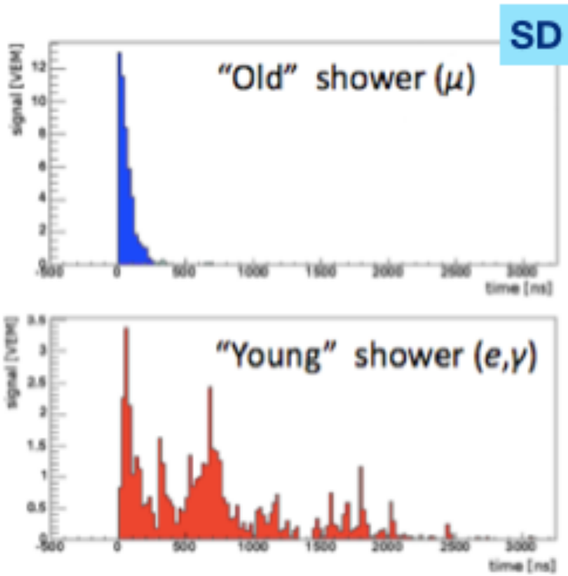

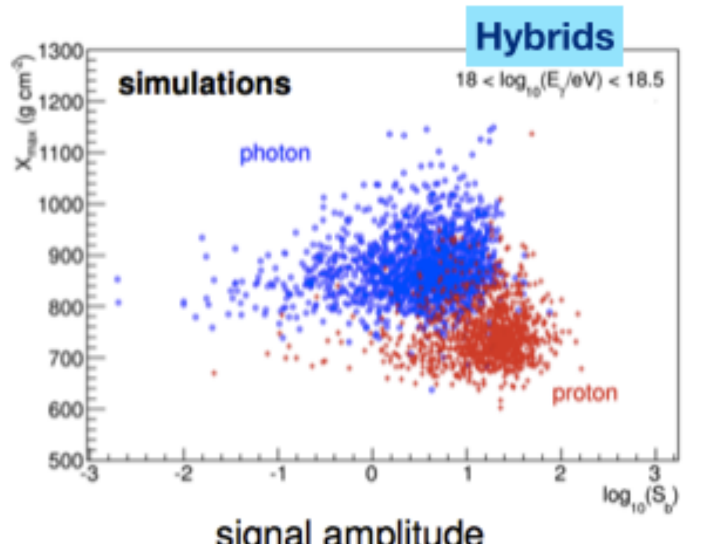

Photons

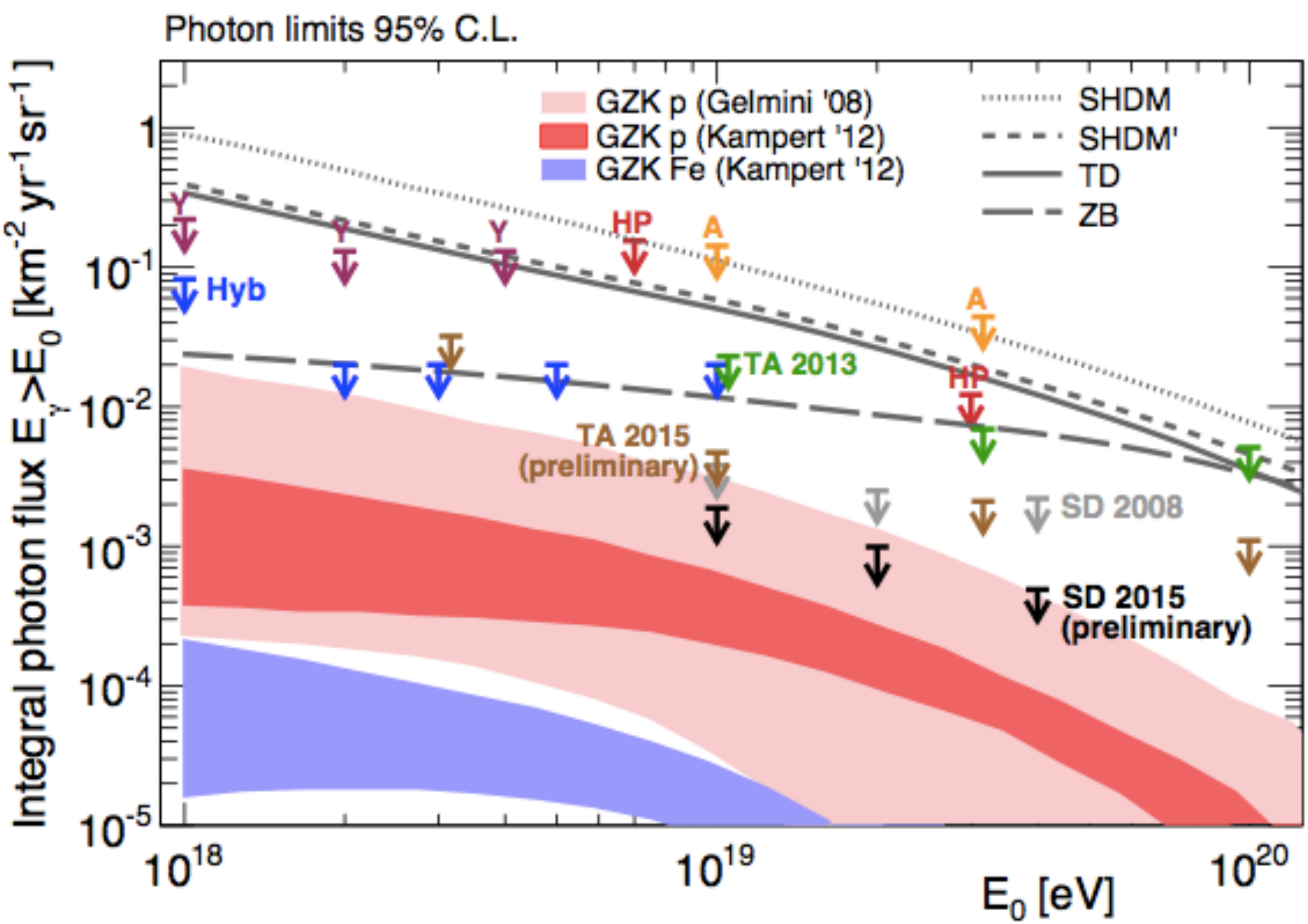

Photon limits 95% C.L.
GZK p (Gelmini '08)
GZK p (Kampert '12)
GZK Fe (Kampert '12)
SHDM
SHDM'
TD
ZB
Y
HP
A
Hyb
TA 2013
TA 2015
(preliminary)
SD 2008
SD 2015
(preliminary)
Integral photon flux $E_\gamma > E_0$ [$km^{-2} yr^{-1} sr^{-1}$]
E_0 [eV]
1
10^{-1}
10^{-2}
10^{-3}
10^{-4}
10^{-5}
10^{18}
10^{19}
10^{20}

Photon point sources

- Protons near the ankle produce photons ~ 1 EeV : can we find them?
- as the energy flux in TeV γ rays exceeds 1 eV cm^{-2} s^{-1} for some sources (CenA, Galactic center) with this energy spectrum, we expect similar flux at EeV (as sources with spectrum ~ E^{-2}, put the same energy flux/decade)

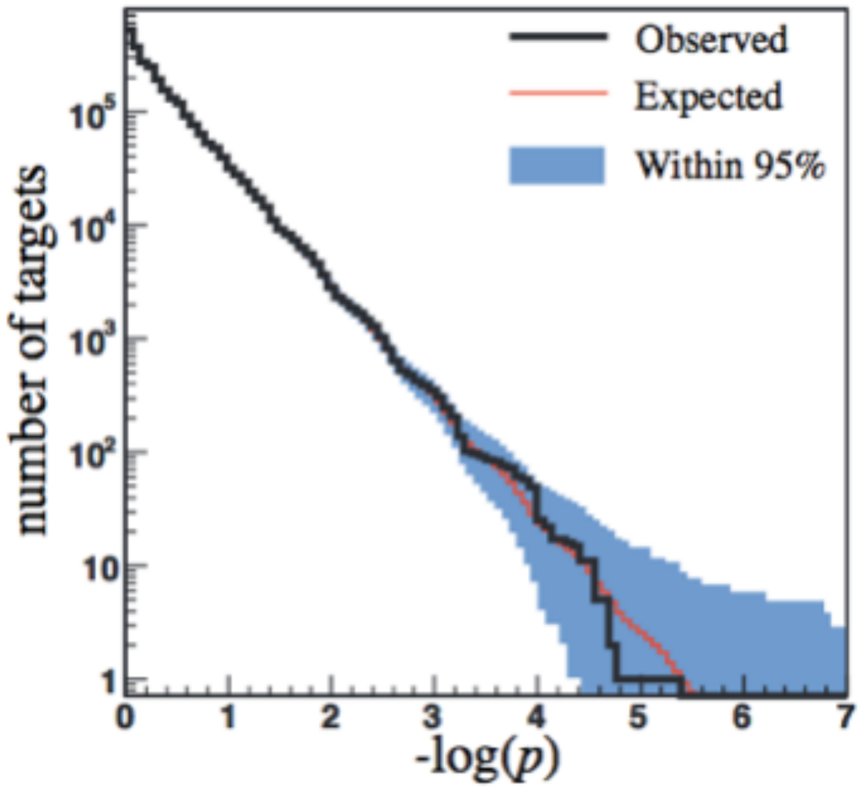

No point sources of EeV photons is found.

For $d\phi/dE \sim E^{-2}$

$\phi_\gamma < 0.25$ eV cm^{-2} s^{-1}

well below expectations

No Galactic sources of protons IF

—> they are not transient

—> they do not emit in jets towards Earth

—> they are too faint

Neutrinos

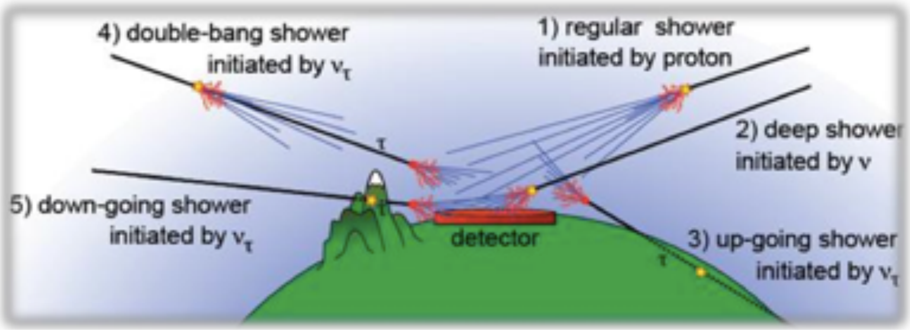

(1) inclined hadronic shower

(2-5) neutrino induced showers

Neutrinos in Auger:

- Earth-skimming: ν_τ CC (90-95^0)
- down-going : all flavours CC&NC

Neutrinos

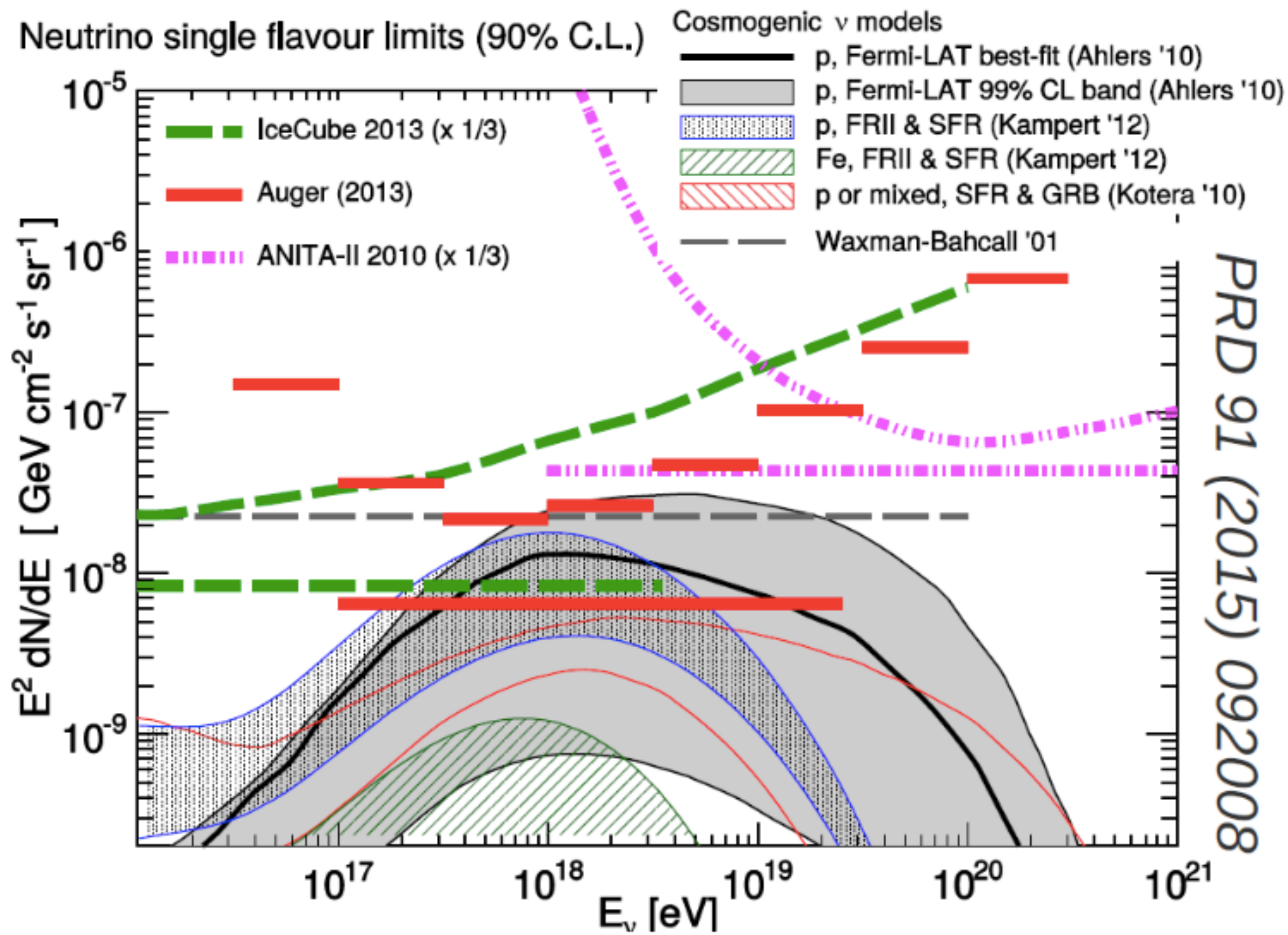

$dN/dE = k\,E^{-2}$

→ $k \sim$ 6.4 x 10^{-9} GeV $cm^{-2} s^{-1} sr^{-1}$ [0.1 – 25] EeV

Auger limits constrains models with pure proton primaries

Correlation with UHE neutrinos

Telescope Array, Auger, IceCube Collaborations @ **ICRC 2015**

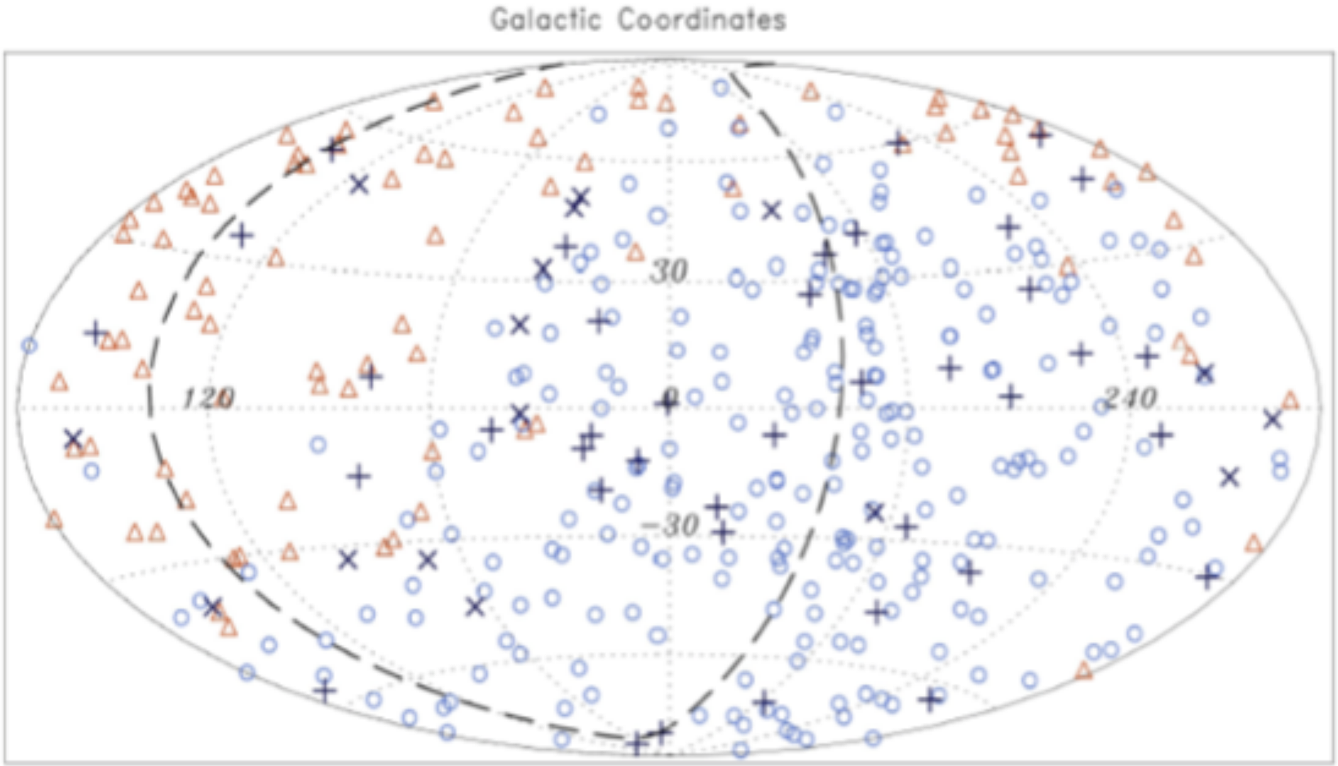

ΔTA > 57 EeV O Auger > 52 EeV + IC cascade X IC tracks

Joint analysis of 3 Collaborations!

All correlations less than 3.3 sigma significance
To be monitored with larger data set
(in particular the analysis with cascades)

Systematic uncertainties on the energy scale	
Absolute fluorescence yield	3.4%
Fluor. spectrum and quenching param.	1.1%
Sub total (Fluorescence yield - sec. 2)	**3.6%**
Aerosol optical depth	3%÷6%
Aerosol phase function	1%
Wavelength depend. of aerosol scatt.	0.5%
Atmospheric density profile	1%
Sub total (Atmosphere - sec. 3)	**3.4%÷6.2%**
Absolute FD calibration	9%
Nightly relative calibration	2%
Optical efficiency	3.5%
Sub total (FD calibration - sec. 4)	**9.9%**
Folding with point spread function	5%
Multiple scattering model	1%
Simulation bias	2%
Constraints in the Gaisser-Hillas fit	3.5% ÷ 1%
Sub total (FD profile rec. - sec. 5)	**6.5% ÷5.6%**
Invisible energy (sec. 6)	**3%÷1.5%**
Stat. error of the SD calib. fit (sec. 7)	**0.7%÷1.8%**
Stability of the energy scale (sec. 7)	**5%**
Total	**14%**

Uncertainties entering into the SD calibration fit	
Aerosol optical depth	3%÷6%
Horizontal uniformity	1%
Atmosphere variability	1%
Nightly relative calibration	3%
Statistical error of the profile fit	5%÷3%
Uncertainty in shower geometry	1.5%
Invis. energy (shower-to-shower fluc.)	1.5%
Sub total FD energy resolution	**7%÷8%**
Statistical error of the $S(1000)$ fit [3]	12%÷3%
Uncert. in lateral distrib. function [3]	5%
shower-to-shower fluctuations [3]	10%
Sub total SD energy resolution	**17%÷12%**

Example scenario

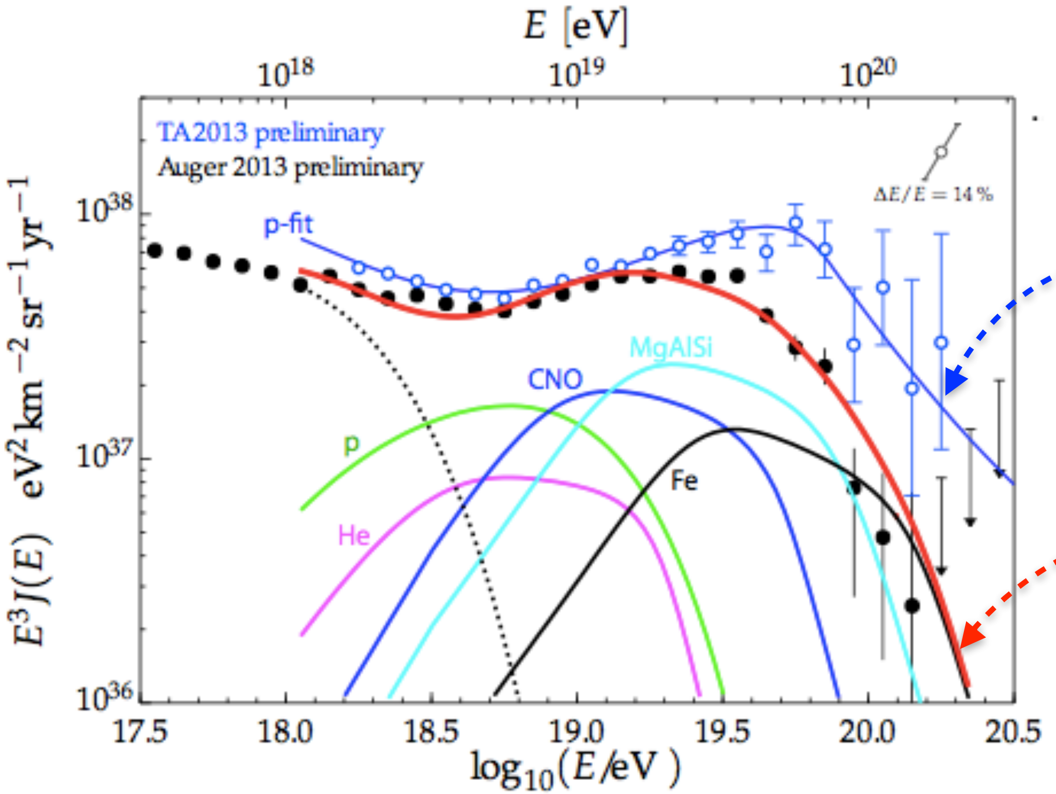

- extragalactic proton sources
- sources distribution $(1+z)^{4.4}$
- injection spectrum $E^{-2.36}$

- Emax ~ $2 \times 10^{18.7}$ eV
- very hard injection spectrum E^{-1}
- enhanced Galactic component

(from arXiv:1312.7459)

- hard spectra: acceleration in rapidly rotating neutron stars, accretion disks with unipolar induction, etc. (high metallicity)
- good fit to Auger only above 5 EeV. Below
  - ✓ Galactic spectrum extending up to 5 EeV
    BUT if light, disfavoured by anisotropy results, if heavy by X_{max}
  - ✓ extraGal. (ad-hoc) sources injecting p, He. In agreement with Kascade-Grande and IceTop results
    BUT too much Fe at 1 EeV wrt Xmax result

The energy estimation with SD

✓ use an **energy estimator** at a given optimal distance [Haverah Park: ρ(600), AGASA : S(600), PAO: S(1000)

✓ the estimator depends on the zenith angle : to combine observations from all angles

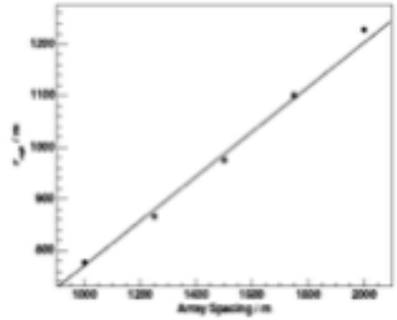

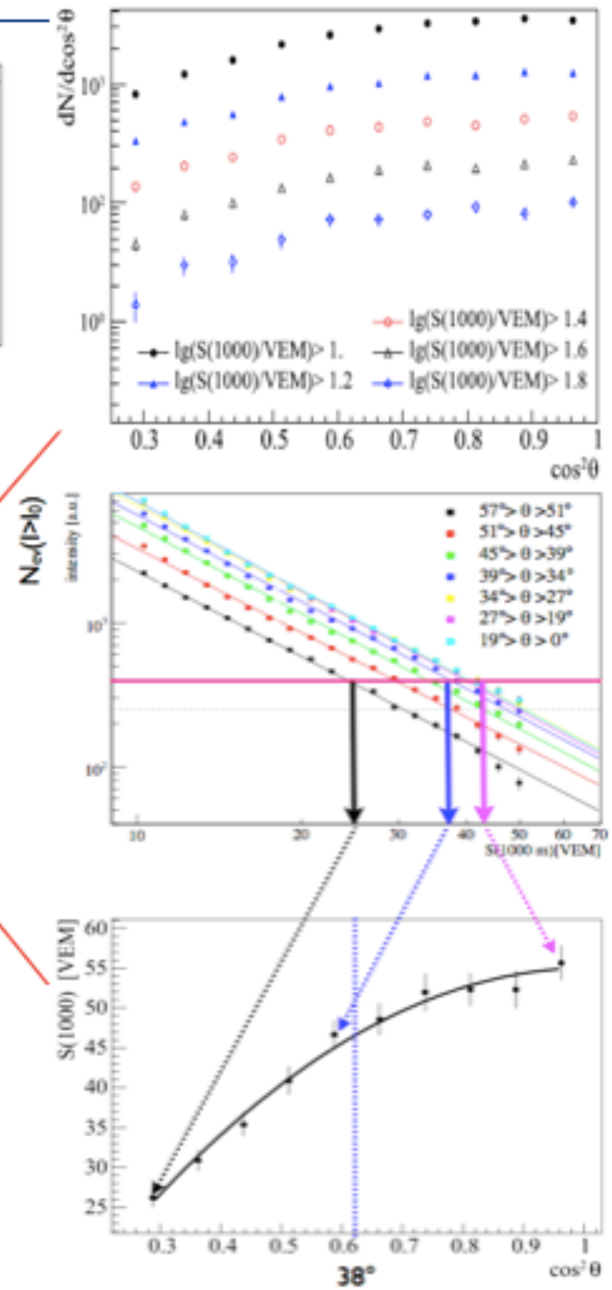

Attenuation curve S vs θ = CIC(θ)
extracted from data using the so-called Constant Intensity Cut

if the CR flux is isotropic
if acceptance(θ) is known → $\frac{dN}{d\,sin^2\theta} = const$

For a shower from direction θ and measured $S(r_{opt})$ → $S(\theta^{est}) = \frac{S(r_{opt})}{CIC(\theta)}$

The estimator is then correlated with energy

- by means of simulations
- by using an independent measure of energy (FD)

Composition issues from technical point of view

1) FD [HiRes]

$$E_{tot} \propto \int_0^{\infty} dX \frac{dE}{dX}$$

Measure the longitudinal development of EAS
Mass dependence: If the primaries are heavy, the energy is higher

[© Song et al, Astrop.Phys. (2000)]

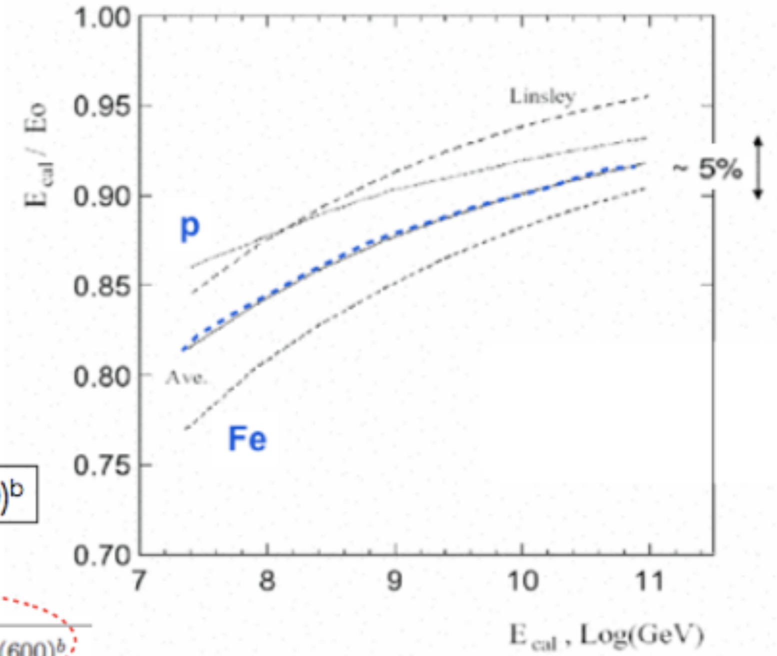

2) SD [AGASA]

Measure the lateral development of EAS

$E = a \times 10^{17}\, S(600)^b$

[© Takeda et al, Astrop.Phys.19 (2003) 447]

Simulation Code	Single Particle	Altitude	Interaction Model	Primary Composition	$E = a \times 10^{17} \cdot S_0(600)^b$ a	b	Example S0=50 VEM
COSMOS	"electrons"	900m	QCDJET	p	2.03	1.02	
CORSIKA (v5.623)	PH^0_{peak}	900m	QGSJET98	p	2.07	1.03	1.04
				Fe	2.24	1.00	
			SIBYLL1.6	p	2.30	1.03	1.13
				Fe	2.19	1.01	
AIRES (v2.2.1)	PW^θ_{peak}	667m	QGSJET98	p	2.17	1.03	1.09
				Fe	2.15	1.01	
			SIBYLL1.6	p	2.34	1.04	1.13
				Fe	2.24	1.02	

energy is lower by ~4 to 13% (depending on the model used) if primaries are heavy